## C. HYDRAULICS OF CONTROL STRUCTURES

**9.10.** ***Shape for Uncontrolled Ogee Crest.***—As discussed in section 9.8(c), crest shapes that approximate the profile of the undernappe of a jet flowing over a sharp-crested weir provide the ideal form for obtaining optimum discharges. The shape of such a profile depends upon the head, the inclination of the upstream face of the overflow section, and the height of the overflow section above the floor of the entrance channel (which influences the velocity of approach to the crest). Crest shapes have been studied extensively in the Bureau of Reclamation hydraulics laboratories, and data from which profiles for overflow crests can be obtained have been published [18]. For most conditions the data can be summarized according to the form shown on figure 9-21(A), where the profile is defined as it relates to axes at the apex of the crest. That portion upstream from the origin is defined as either a single curve and a tangent or as a compound circular curve. The portion downstream is defined by the equation:

$$\frac{y}{H_o} = -K\left(\frac{x}{H_o}\right)^n \qquad (2)$$

in which $K$ and $n$ are constants whose values depend on the upstream inclination and on the velocity of approach. Figure 9-21 gives values of these constants for different conditions.

The approximate profile shape for a crest with a vertical upstream face and negligible velocity of approach is shown on figure 9-22. The profile is constructed in the form of a compound circular curve with radii expressed in terms of the design head, $H_o$. This definition is simpler than that shown on figure 9-21, because it avoids the need for solving an exponential equation; furthermore, it is represented in a form easily used by a layman for constructing forms or templates. For ordinary design conditions for small spillways where the approach height, $P$, is equal to or greater than one-half the maximum head on the crest, this profile is sufficiently accurate to avoid seriously reduced crest pressures and does not materially alter the hydraulic efficiency of the crest. When the approach height is less than one-half the maximum head on the crest, the profile should be determined from figure 9-21.

**9.11.** ***Discharge Over an Uncontrolled Overflow Ogee Crest.***—(a) *General.*—The discharge over an ogee crest is given by the equation:

$$Q = CLH_e^{3/2} \qquad (3)$$

where:

$Q$ = discharge,
$C$ = variable discharge coefficient,
$L$ = effective length of crest, and
$H_e$ = actual head being considered on the crest, including velocity of approach head, $h_a$.

The discharge coefficient, $C$, is influenced by a number of factors, such as (1) the depth of approach, (2) relation of the actual crest shape to the ideal nappe shape, (3) upstream face slope, (4) downstream apron interference, and (5) downstream submergence. The effect of these various factors is discussed in section 9.12.

The total head on the crest, $H_e$, does not include allowances for approach channel friction losses or other losses caused by the curvature of the upstream channel, entrance loss into the inlet section, and inlet or transition losses. Where the design of the approach channel results in appreciable losses, they must be added to $H_e$ to determine reservoir elevations corresponding to the discharges given by equation (3).

(b) *Pier and Abutment Effects.*—Where crest piers and abutments are shaped to cause side contractions of the overflow, the effective length, $L$, is less than the net length of the crest. The effect of the end contraction may be taken into account by reducing the net crest length as follows:

$$L = L' - 2(NK_p + K_a)H_e \qquad (4)$$

where:

$L$ = effective length of crest,
$L'$ = net length of crest,
$N$ = number of piers,
$K_p$ = pier contraction coefficient
$K_a$ = abutment contraction coefficient, and
$H_e$ = actual head on crest.

The pier contraction coefficient, $K_p$, is affected by the shape and location of the pier nose, the thickness of the pier, the design head, and the approach velocity. For conditions of design head, $H_o$, average pier contraction coefficients may be assumed as follows:

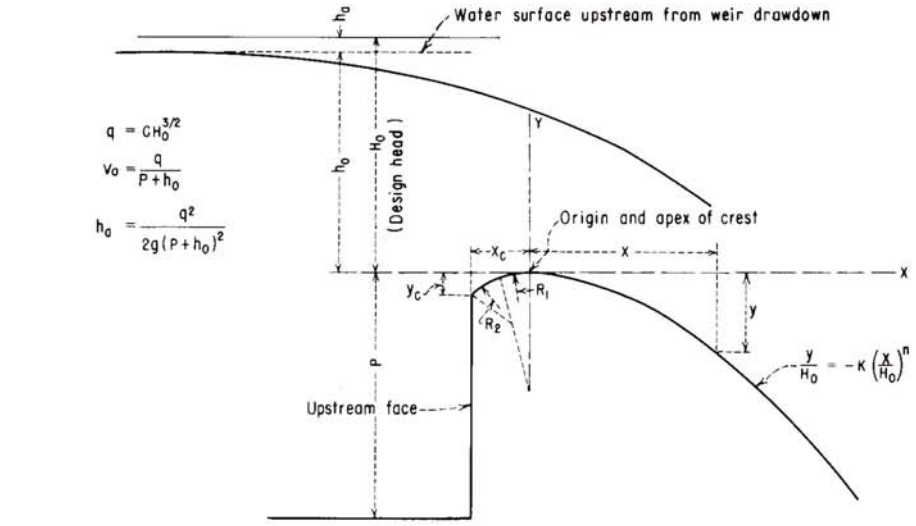


(A) ELEMENTS OF NAPPE-SHAPED CREST PROFILES

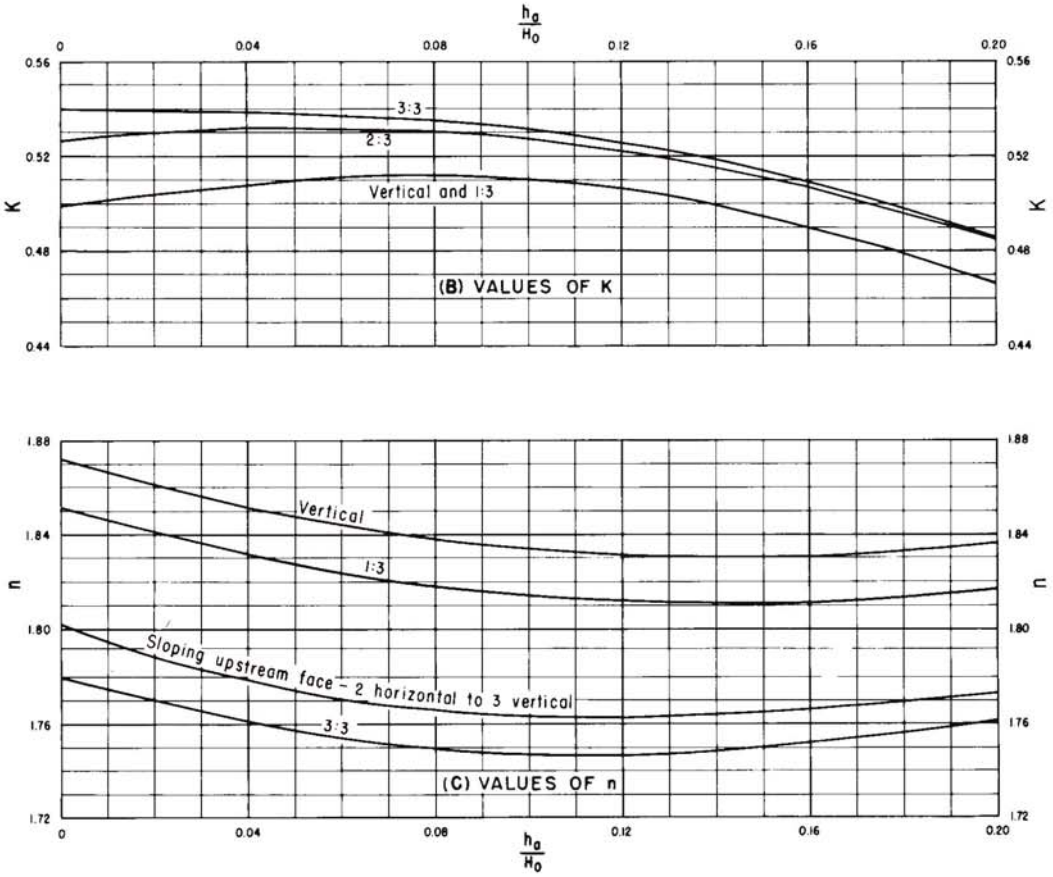


**Figure 9-21.—Factors for definition of nappe-shaped crest profiles. 288–D–2406. (Sheet 1 of 2).**

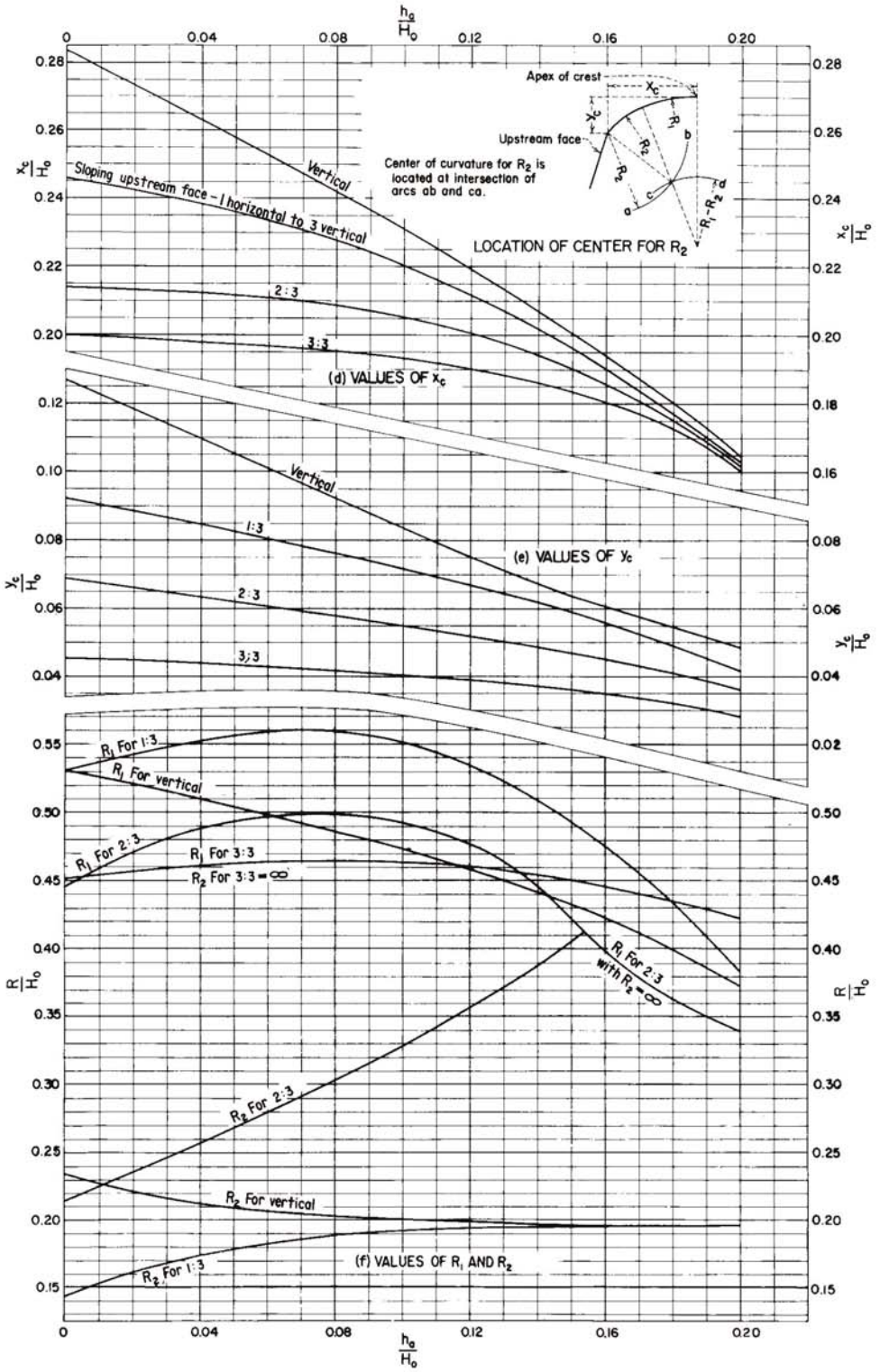


**Figure 9-21.—Factors for definition of nappe-shaped crest profiles. 288–D–2407. (Sheet 2 of 2).**

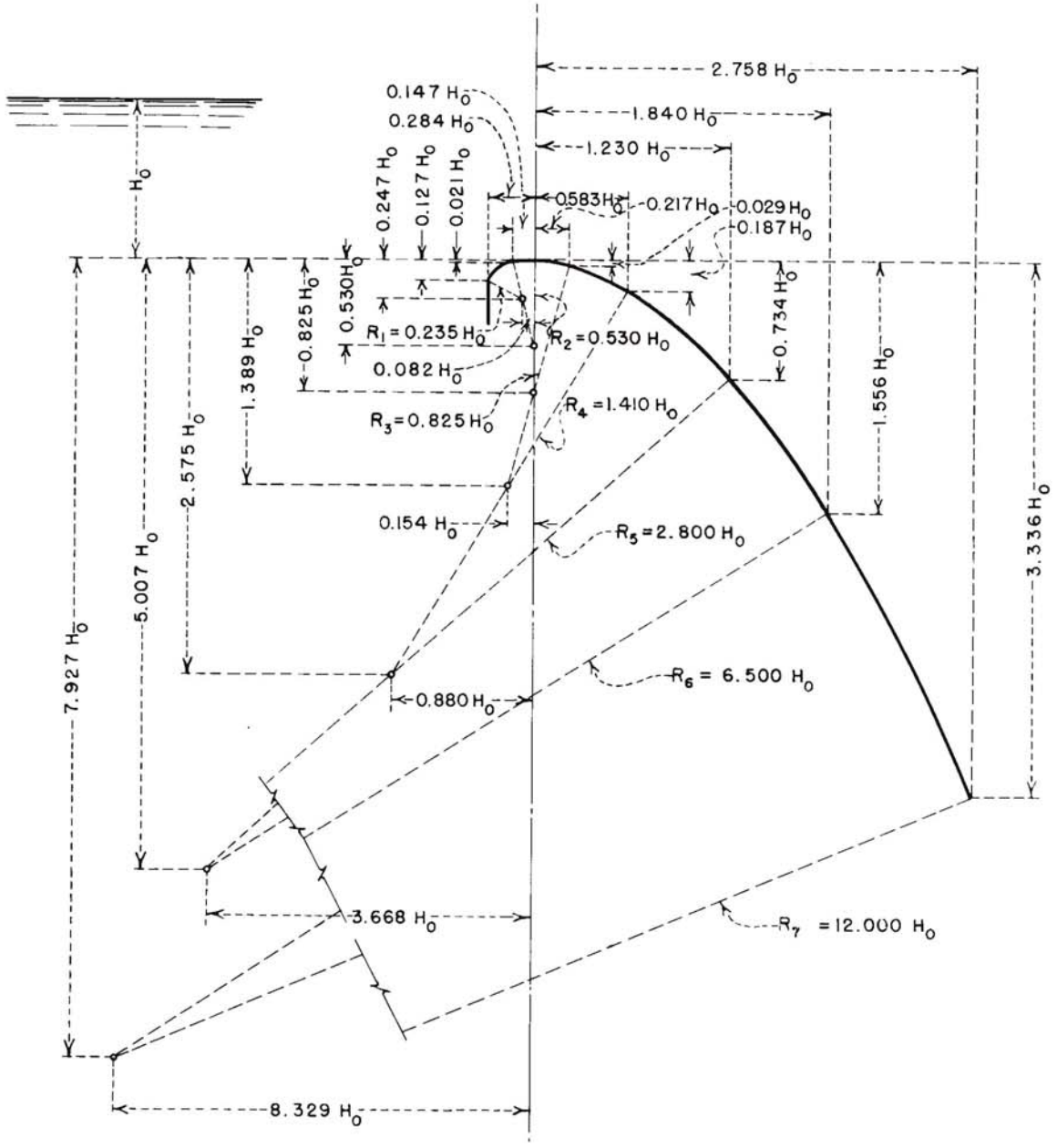


Figure 9-22.—Ogee crest shape defined by compound curves. 288-D-2408.

- For square-nosed piers with corners rounded on a radius equal to about 0.1 of the pier thickness: $K_p = 0.02$
- For round-nosed piers: $K_p = 0.01$
- For pointed-nose piers: $K_p = 0.0$

The abutment contraction coefficient is affected by the shape of the abutment, the angle between the upstream approach wall and the axis of the flow, the head in relation to the design head, and the approach velocity. For conditions of design head, $H_o$, average coefficients may be assumed as follows:

- For square abutments with headwall at 90° to direction of flow: $K_a = 0.20$
- For rounded abutments with headwall at 90°

to direction of flow, when $0.5H_o \leq r \leq 0.15H_o$: $K_a = 0.10$

- For rounded abutments where $r > 0.5H_o$ and headwall is placed not more than 45° to direction of flow: $K_a = 0.0$

where $r$ = radius abutment rounding.

**9.12. *Discharge Coefficient for Uncontrolled Ogee Crests.*—**(a) *Effect of Depth of Approach.*—For a high sharp-crested weir placed in a channel, the velocity of approach is small and the underside of the nappe flowing over the weir attains maximum vertical contraction. As the approach depth is decreased, the velocity of approach increases and the vertical contraction diminishes. For sharp-crested wiers whose heights are not less than about one-fifth the heads producing flow over them, the discharge coefficient remains fairly constant with a value of about 3.3, although the contraction diminishes. For weir heights less than about one-fifth the head, the contraction of the flow becomes increasingly suppressed and the crest coefficient decreases. When the weir height becomes zero, the contraction is entirely suppressed and the overflow weir becomes, in effect, a channel or a broad-crested weir, for which the theoretical discharge coefficient is 3.087. If the sharp-crested weir coefficients are related to the head measured from the point of maximum contraction instead of to the head above the sharp crest, coefficients applicable to ogee crests shaped to profiles of undernappes for various approach velocities can be established. The relationship of the ogee crest coefficient, $C_o$, to various values of $P/H_o$ is shown on figure 9-23. These coefficients are valid only when the ogee is formed to the ideal nappe shape; that is, when $H_e/H_o = 1$.

(b) *Effect of Heads Different from Design Head.*—When the ogee crest shape is different from the ideal shape or when the crest has been shaped for a head larger or smaller than the one under consideration, the discharge coefficient will differ from that shown on figure 9-23. A wider shape will result in positive pressures along the crest contact surface, thereby reducing the discharge. With a narrower crest shape, negative pressures along the contact surface will occur, resulting in an increased discharge. Figure 9-24 shows the variation of the coefficient as related to values of $H_e/H_o$, where $H_e$ is the actual head being considered.

An approximate discharge coefficient for an irregularly shaped crest whose profile has not been formed according to the undernappe of the overflow jet can be estimated by finding the ideal shape that most nearly matches it. The design head, $H_o$, corresponding to the matching shape can then be used as a basis for determining the coefficients [19].

The coefficients for partial heads on the crest, for preparing a discharge-head relationship, can be determined from figure 9-24.

(c) *Effect of Upstream Face Slope.*—For small ratios of the approach depth to the head on the crest, sloping the upstream face of the overflow results in an increase in the discharge coefficient. For large ratios the effect is a decrease in the coefficient. Within the range considered in this text, the discharge coefficient is reduced for large ratios of $P/H_o$ only for relatively flat upstream slopes. Figure 9-25 shows the ratio for the coefficient for an overflow ogee crest with a sloping (inclined) face, $C_i$, to the coefficient for a crest with a vertical upstream face, $C_v$, as obtained from figure 9-23 (and as adjusted by figure 9-24 if appropriate), as related to values of $P/H_o$.

(d) *Effect of Downstream Apron Interference and Downstream Submergence.*—When the water level below an overflow weir is high enough to affect the discharge, the weir is said to be submerged. The vertical distance from the crest of the overflow to the downstream apron and the depth of flow in the downstream channel, as it relates to the head pool level, are factors that alter the discharge coefficient.

Five distinct characteristic flows can occur below an overflow crest, depending on the relative positions of the apron and the downstream water surface: (1) flow can continue at supercritical stage; (2) a partial or incomplete hydraulic jump can occur immediately downstream from the crest; (3) a true hydraulic jump can occur; (4) a drowned jump can occur in which the high-velocity jet will follow the face of the overflow and then continue in an erratic and fluctuating path for a considerable distance under and through the slower water; and (5) no jump may occur—the jet will break away from the face of the overflow and ride along the surface for a short distance and then erratically intermingle with the slow moving water underneath. Figure 9-26 shows the relationship of the floor positions and downstream submergences that produce these distinctive flows.

Where the downstream flow is at supercritical stage or where the hydraulic jump occurs, the decrease in the discharge coefficient is principally caused by the back-pressure effect of the down-

stream apron and is independent of any submergence effect from the tailwater. Figure 9-27 shows the effect of downstream apron conditions on the discharge coefficient. It should be noted that this curve plots, in a slightly different form, the same data represented by the vertical dashed lines on figure 9-26. As the downstream apron level nears the crest of the overflow, $(h_d + d)/H_e$ approaches 1.0, and the discharge coefficient is about 77 percent of the coefficient for unretarded flow. On the basis of a coefficient of 4.0 for unretarded flow over a high weir, the coefficient when the weir is submerged will be about 3.08, which is virtually the coefficient for a broad-crested weir.

From figure 9-26, it can be seen that when $(h_d + d)/H_e$ exceeds about 1.7, the downstream floor position has little effect on the coefficient, but there is a decrease in the coefficient caused by tailwater submergence. Figure 9-28 shows the ratio of the discharge coefficient where affected by tailwater conditions to the coefficient for free flow conditions. This curve plots, in a slightly different form, the data represented by the horizontal dashed lines on figure 9-26. Where the dashed lines on figure 9-26 are curved, the decrease in the coefficient is the result of a combination of tailwater effects and downstream apron position.

**9.13. *Examples of Designs of Uncontrolled Ogee Crests.*** —The two examples cited below illustrate the methods of designing uncontrolled ogee crests, including the computation of approach channel losses and velocity head, the determination of the total length of the crest, and the correction of the discharge coefficient for various effects.

(a) *Example 1.*—Design an uncontrolled overflow ogee crest for a chute spillway that will discharge 2,000 ft³/s at a 5-foot head, and prepare a discharge-head curve. The upstream face of the

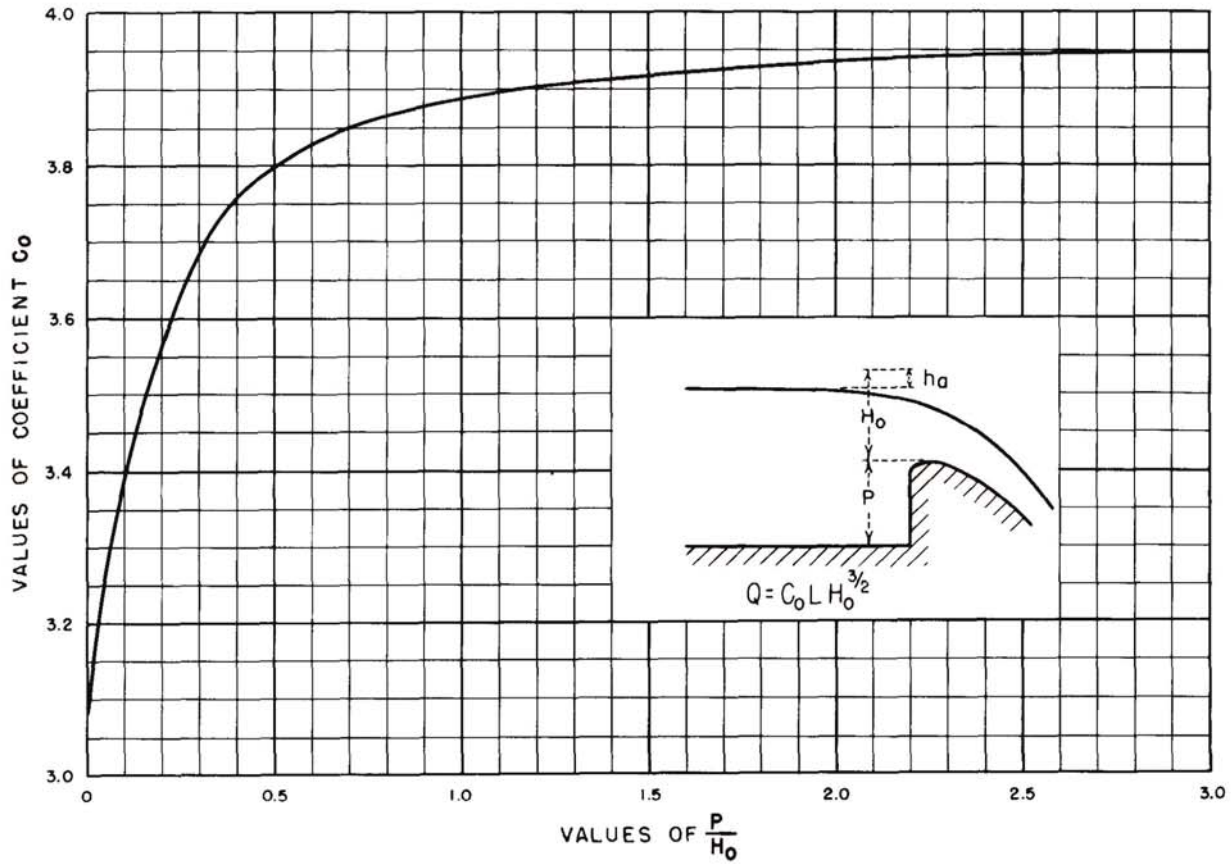


Figure 9-23.—Discharge coefficients for vertical-faced ogee crest. 288–D–2409.

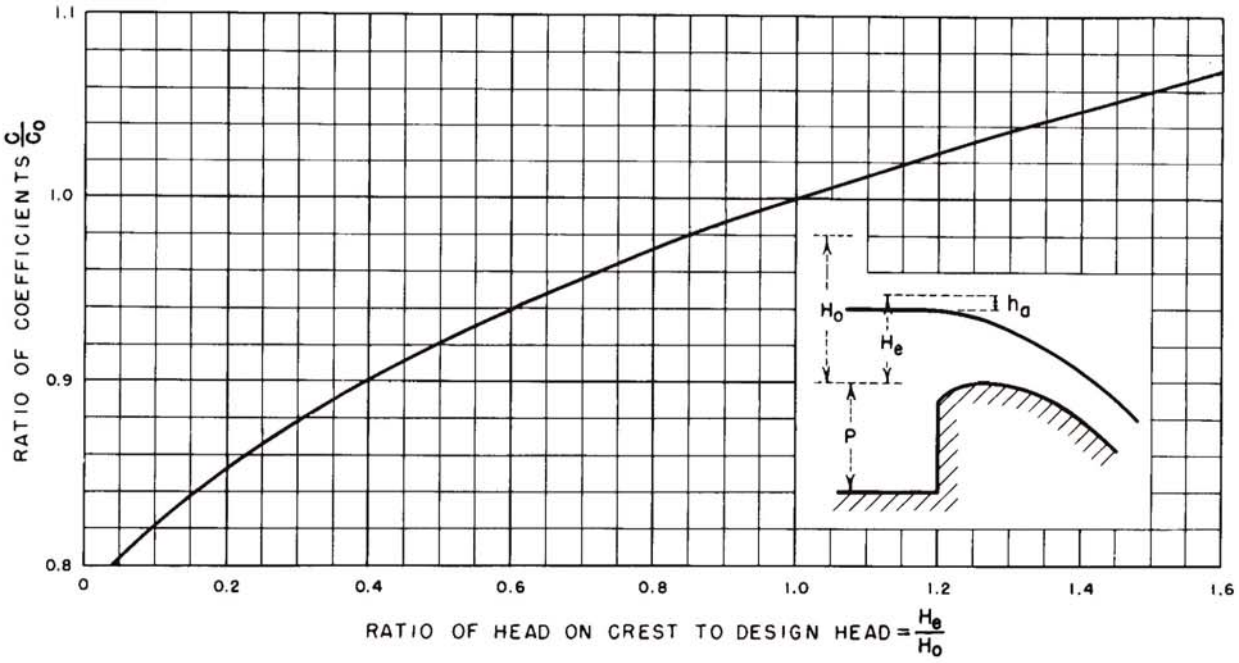


Figure 9-24.—Discharge coefficients for other than the design head. 288–D–2410.

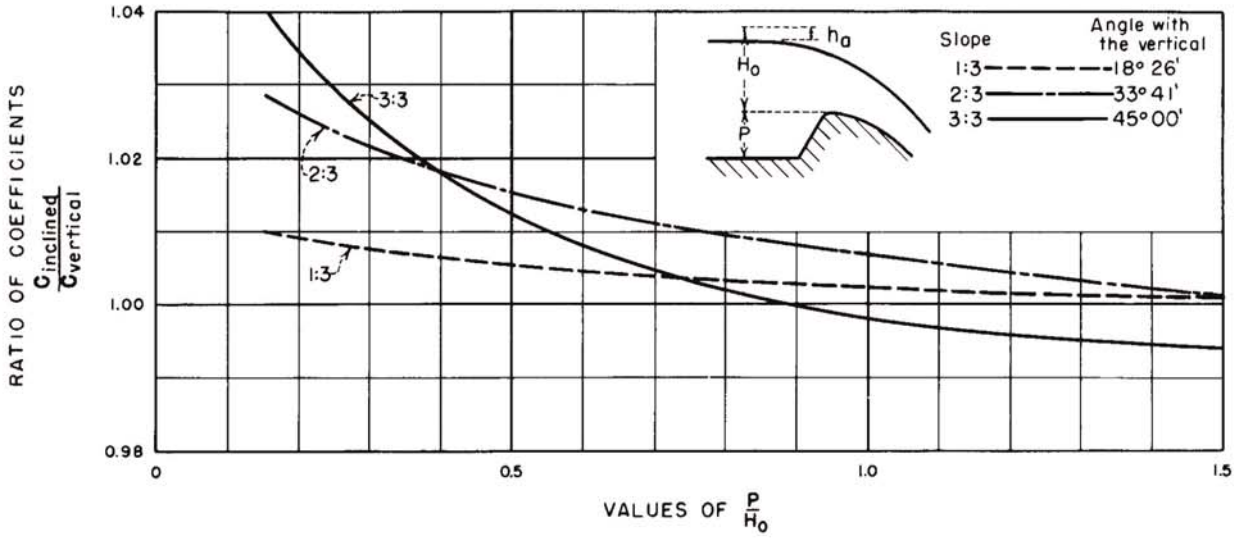


Figure 9-25.—Discharge coefficients for ogee-shaped crest with sloping upstream face. 288–D–2411.

crest is sloped 1:1, and the entrance channel is 100 feet long. A bridge is to span the crest, and 18-inch-wide bridge piers with rounded noses are to be provided. The bridge spans are not to exceed 20 feet. The abutment walls are rounded to a 5-foot radius, and the approach walls are to be placed at 30° with the centerline of the spillway entrance.

To solve the problem, either the approach depth and apron position with respect to the crest must be selected and the appropriate coefficient determined, or an arbitrary coefficient must be selected and the appropriate dimensions determined. The

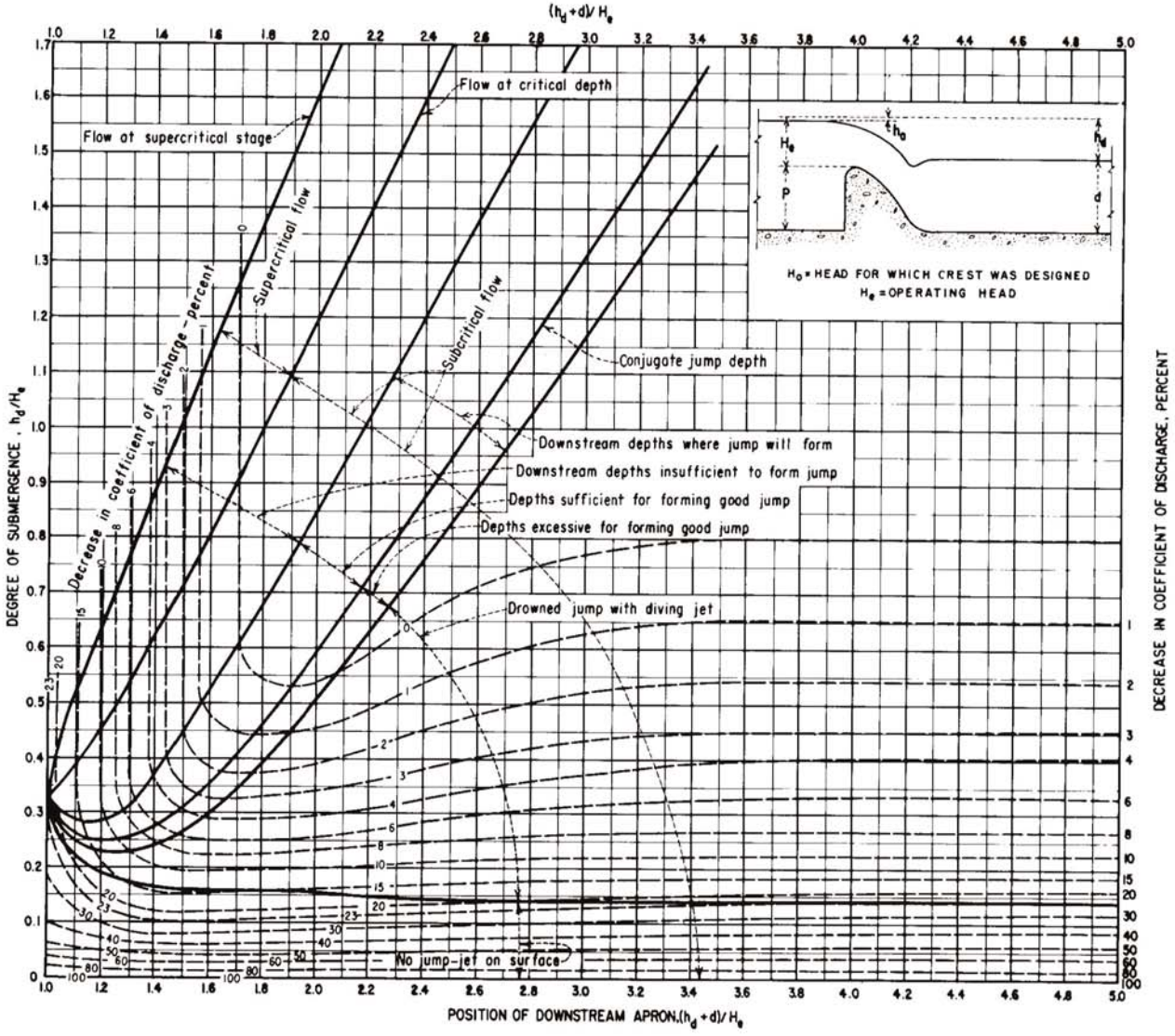


Figure 9-26.—Effects of downstream influences on flow over weir crests. 288–D–2412.

solutions will show both procedures.

(1) *Procedure 1.*—First, assume the position of the approach and downstream apron levels with respect to the crest level, say 2 feet below crest level. Then $H_e + P$ is approximately 7 feet.

To evaluate the approach channel losses, assume a value of $C$ to obtain an approximate approach velocity, say $C = 3.7$. Then the discharge per unit of crest length, $q$, is equal to $CH_e^{3/2} = 3.7 \times 5^{3/2} = 41$ ft$^3$/s. Therefore, the velocity of approach $v_a = q/(H_e + P) = 41/7 = 5.9$ ft/s, and the approach velocity head, $h_a = v_a^2/2g = 5.9^2/64.4 = 0.5$ feet.

Assuming the friction coefficient in Manning's formula $n = 0.0225$, and assuming the hydraulic radius $r$ = the depth of approach, then the friction slope is equal to:

$$s = \left(\frac{v_a n}{1.486 r^{2/3}}\right)^2 = \left(\frac{5.9 \times 0.0225}{1.486 \times 7^{2/3}}\right)^2 = 0.0006$$

Therefore, the total approach channel friction loss, $h_f = 100\ (0.0006) = 0.06$ feet. Assuming an entrance loss into the approach channel equal to $0.1h_a$, the total loss of head in the approach is approximately $0.06 + (0.1 \times 0.5) = 0.11$ feet.

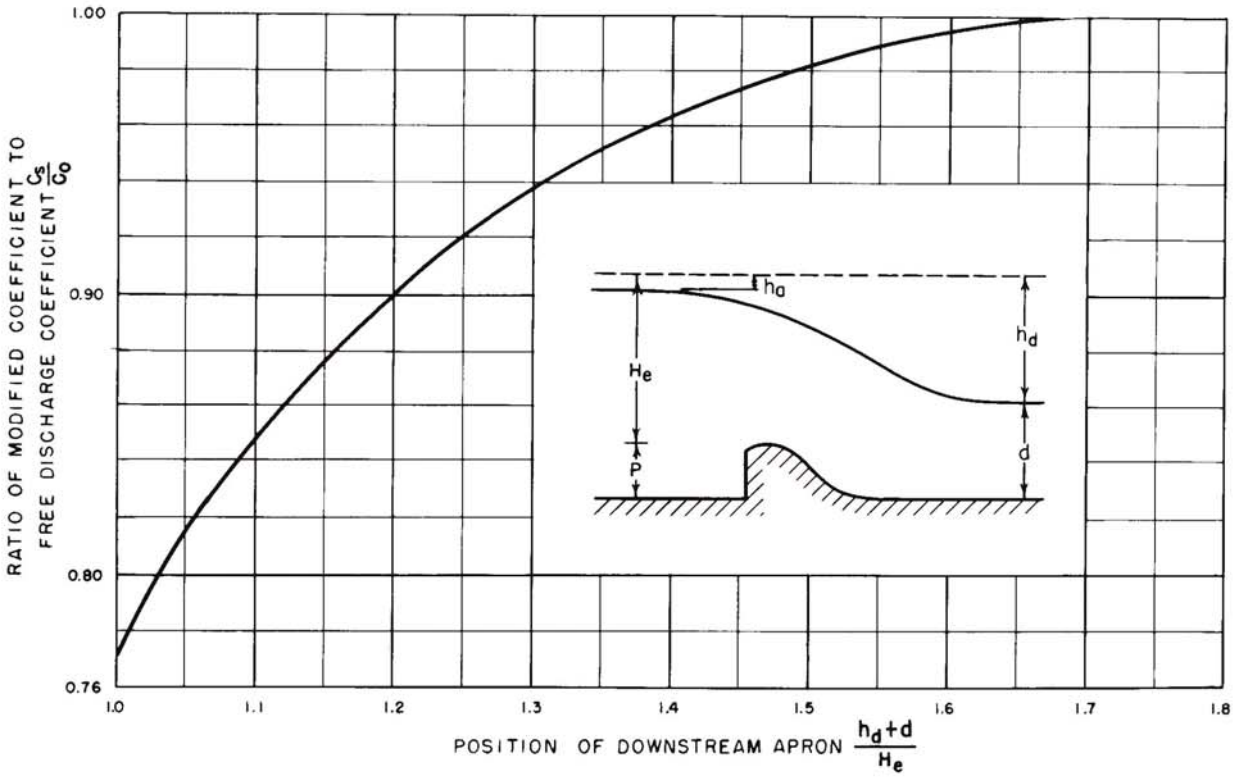


Figure 9-27.—Ratio of discharge coefficients resulting from apron effects. 288–D–2413.

The effective head, $H_o = 5.0 - 0.11 = 4.89$ feet, and $P/H_o = 2/4.89 = 0.41$. From figure 9-23, if $P/H_o = 0.41$, then $C_o = 3.77$.

Figure 9-25 is used to correct the discharge coefficient for the inclined upstream slope. For a 1:1 slope and $P/H_o = 0.41$, $C_i/C_v = 1.018$. Then, $C_4 = 1.018(3.77) = 3.84$.

Next, the relationships $(h_d + d)/H_e$ and $h_d/H_e$ are evaluated to determine the downstream effects. The value of $(h_d + d)/H_e$ is approximately 6.89/4.89 = 1.41. From figure 9-26, for $(h_d + d)/H_e = 1.41$, $h_d/H_e$ at supercritical flow = 0.91. If supercritical flow prevails, $h_d$ should be equal to $0.91H_e = 0.91(4.89) = 4.44$, and $d$ should be $6.89 - 4.44 = 2.45$ feet. With the indicated unit discharge of approximately 41 $ft^3/s$, the downstream velocity will be approximately 41/2.45 = 16.7 ft/s, and the velocity head, $h_v = 16.7^2/64.4 = 4.3$ feet. The closeness of $h_d$ and $h_v$ verifies that the flow is supercritical. From figure 9-26, it can be seen that the downstream effect is caused by apron influences only, and that the corrections shown on figure 9-27 will apply. The ratio of the modified $C_s$ to the coefficient $C_o$ for a downstream apron position determined by the $(h_d + d)/H_e$ ratio of 1.41 is 96.6 percent. The coefficient has now been corrected for all influencing effects.

The next step is to determine the required crest length. For the design head $H_o = 4.89$ feet, the required effective crest length is:

$$L = \frac{Q}{CH_o^{3/2}} = \frac{2{,}000}{3.71(4.89)^{3/2}} = 49.9 \text{ feet}$$

To correct for pier effects, the net length from equation (4) is:

$$L' = L + [2(NK_p + K_a)H_e]$$

If the bridge spans are not to exceed 20 feet, two piers will be required for the approximately 50-foot total span; therefore, $N = 2$. Therefore:

$$L' = 49.9 + [2(2[0.01] + 0)4.89 = 50.1 \text{ feet}$$

The foregoing procedure establishes a discharge coefficient for the design head. For computing a

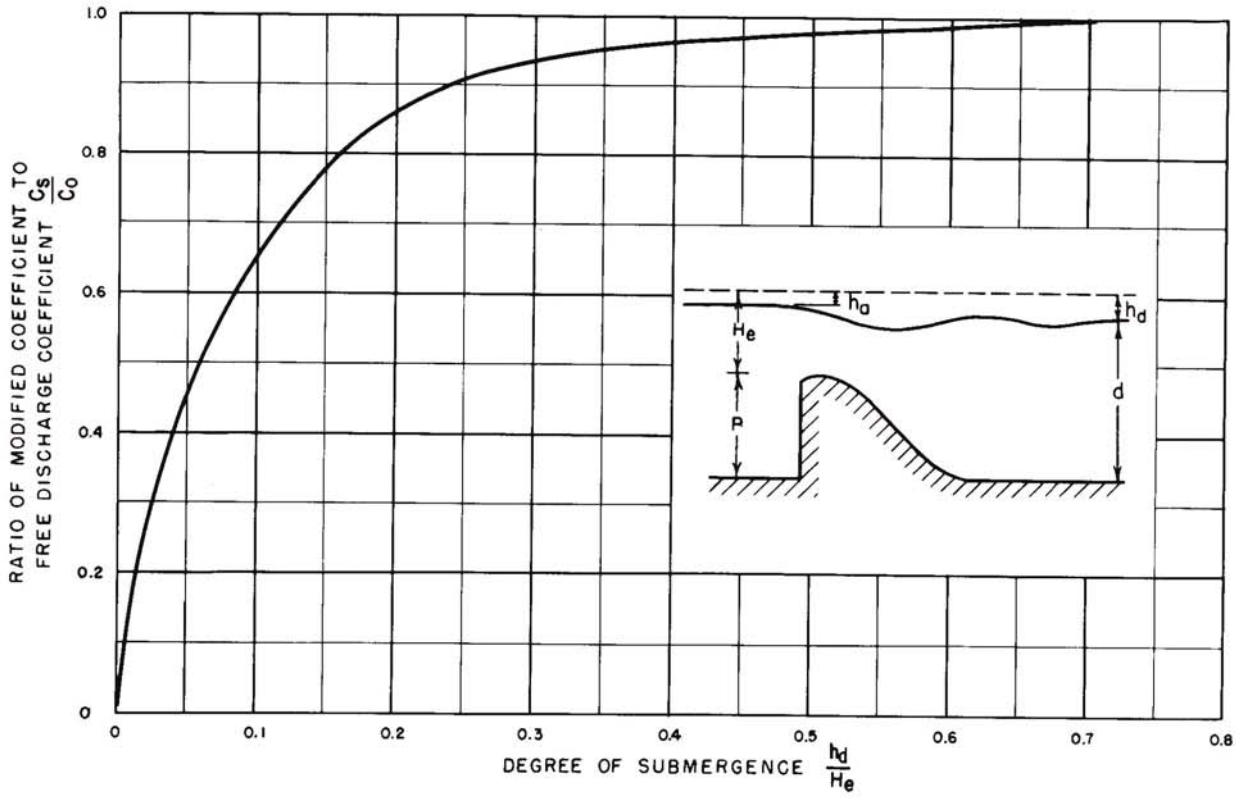


Figure 9-28.—Ratio of discharge coefficients caused by tailwater effects. 288–D–2414.

rating curve, coefficients for lesser heads must be obtained. Because the variations of the different corrections are not consistent, the procedure for correcting the coefficients must be repeated for each lesser head. The variables can be tabulated in a form similar to that used in table 9-2.

(2) *Procedure 2.*—First, assume an overall discharge coefficient, say 3.5. The discharge per unit length, $q$, is then equal to $3.5H_e^{3/2} = 39.2$ ft$^3$/s for $H_e = 5$ feet. Then the required effective length of the crest, $L$, is equal to $Q/q = 2{,}000/39.2 = 51$ feet.

Next, the approach depth is approximated from figure 9-23; for $C = 3.5$, $P/H_o$ is approximately 0.2. Thus, the approach depth cannot be less than 1 foot. To allow for other factors that may reduce the coefficient, an approach depth of about 2 feet might reasonably be assumed.

With a 2-foot approach depth, the computation for approach losses is the same as in the procedure 1 solution, and the effective head $H_o = 4.89$ feet. Similarly, $C_i = 3.84$.

Because the overall coefficient of 3.5 was assumed for the 5-foot gross head, the corresponding coefficient, $C_o$, for the 4.89-foot effective head can be calculated from the equation $C_o/C_g = H_g^{3/2}/H_e^{3/2}$; where the subscript $g$ refers to gross head. Therefore, $C_o = C_g\,(H_g/H_e)^{3/2} = 3.5(5.0/4.89)^{3/2} = 1.035(3.5) = 3.62$.

Therefore, submergence ratio $C_s/C_o = 3.62/3.84 = 0.94$, and from figure 9-27, $(h_d + d)/H_e = 1.3$. Thus, $h_d + d = 1.3(4.89) = 6.4$ feet. The downstream apron should therefore be placed 1.4 feet below the crest level.

Because it was demonstrated previously that pier and contraction effects are small, they can be neglected in this example, and the net crest length is, therefore, 51 feet. This crest length and downstream apron position can be varied by altering the assumptions of overall coefficient and approach depth.

The discharge rating curve may be developed by a process similar to that used in procedure 1.

(b) *Example 2.*—Design an uncontrolled overflow crest for a diversion dam to pass 2,000 ft$^3$/s

Table 9-2.—Design of an uncontrolled overflow ogee crest. Example 1, procedure 1; given $L$=50 feet[1], $H_o$=4.89 feet, and $P$=2 feet.

| $\frac{H_e}{H_o}$ | $H_e$, feet | $\frac{^2C}{C_o}$ | $C_i$ | $h_d+d$ | $\frac{h_d+d}{H_e}$ | $\frac{^4C_s}{C}$ | $C_s$ | $C_sH_e^{3/2}$ | $H_e+P$ | $v_a$ (approx.) | $h_a$ | $s$ | Entrance loss, 0.1 $h_a$ | Total approach losses, feet | Gross head, feet | Total discharge, ($Q = C_sLH_e^{3/2}$), ft$^3$/s |
|---|---|---|---|---|---|---|---|---|---|---|---|---|---|---|---|---|
| 0.1 | 0.49 | 0.82 | 3.15 | 2.49 | 5.08 | 1.00 | 3.15 | 1.1 | 2.49 | 0.44 | 0.003 | 0.00001 | 0.00 | 0.00 | 0.49 | 55 |
| .2 | .98 | .85 | 3.26 | 2.98 | 3.04 | 1.00 | 3.26 | 3.2 | 2.98 | 1.07 | .02 | .00006 | .00 | 0.1 | .99 | 160 |
| .4 | 1.96 | .90 | 3.46 | 3.96 | 2.02 | 1.00 | 3.46 | 9.5 | 3.96 | 2.40 | .09 | .0002 | .01 | .03 | 1.99 | 475 |
| .6 | 2.93 | .94 | 3.61 | 4.93 | 1.68 | 1.00 | 3.61 | 18.1 | 4.93 | 3.67 | .21 | .0004 | .02 | .06 | 2.99 | 905 |
| .8 | 3.91 | .97 | 3.73 | 5.91 | 1.51 | 0.982 | 3.66 | 28.3 | 5.91 | 4.79 | .36 | .0005 | .04 | .09 | 4.00 | 1,415 |
| 1.0 | 4.89 | 1.0 | [3]3.84 | 6.89 | 1.41 | .966 | 3.71 | 40.0 | 6.89 | 5.80 | .52 | .0006 | .05 | .11 | 5.00 | 2,000 |
| 1.2 | 5.87 | 1.03 | 3.96 | 7.87 | 1.34 | .95 | 3.76 | 53.5 | 7.87 | 6.80 | .72 | .0007 | .07 | .14 | 6.01 | 2,675 |

[1]The effective crest length and the net crest length for $H_o$ are 49.9 feet and 50.1 feet, respectively. Because of the small magnitude of the pier effects, an average length of 50 feet is taken for the effective crest length for all values of $H_e$. If the pier effects are significant, separate effective crest lengths should be computed for each $H_e$ value.
[2]From fig. 9-24.
[3]$C_i$ for $H_o$.
[4]From fig. 9-27.

with a depth of flow upstream from the dam not exceeding 5 feet above the crest. The overflow dam is 8 feet high. The abutment headwall is 90° to the direction of flow, and the edge adjacent to the crest is rounded to a 12-inch radius. For 2,000 ft$^3$/s flow, the tailwater will rise 3.5 feet above the crest.

For an approximate head, $H_e$, of 5 feet, a crest height of 8 feet, and a crest submergence of 3.5 feet, $(h_d + d)/H_e = 13/5 = 2.6$, and $h_d/H_e = 1.5/5 = 0.3$. Figure 9-26 shows that for these relations the downstream flow phenomena will be that of a drowned jump and that the coefficient will be reduced 6 percent.

Roughly, $P/H_o = 8/5 = 1.6$, and the unretarded coefficient from figure 9-23 is 3.93. Reducing this by 6 percent because of submergence results in an approximate coefficient of 3.7.

The approximate discharge per foot of crest $q = CH_o^{3/2} = 3.7(5)^{3/2} = 41.5$ ft$^3$/s. Therefore, the velocity of approach $v_a = 41.5/13 = 3.2$ ft/s, and the approach velocity head $h_a = 0.16$ feet. $H_o = 5.0 + 0.16 = 5.16$ feet.

The revised value of $P/H_o$ does not appreciably alter the coefficient obtained from figure 9-23. The revised value of $(h_d + d)/H_o = 13.16/5.16 = 2.55$, and the revised value of $h_d/H_o = 1.66/5.16 = 0.32$. The reduction in coefficient caused by submergence effects from figure 9-26 is 5 percent. The revised discharge coefficient, $C$, is 95 percent of 3.93 = 3.73.

The effective crest length $L$ equals $Q/CH_o^{3/2} = 2{,}000/3.73(5.16)^{3/2} = 45.7$ feet.

The net crest length is determined by using equation (4). Without piers the net crest length $L' = L + 2K_aH_e$. For 90° abutment walls rounded to a radius larger than $0.15H_o$, $K_a = 0.10$. Therefore, the net crest length, $L' = 45.7 + 2[0.10(5.16)] = 46.7$ feet.

**9.14. *Uncontrolled Ogee Crests Designed for Less than Maximum Head.*—**Economy in the design of an ogee crest may sometimes be effected by using a design head that is less than the maximum expected head. As discussed previously, use of a smaller design head results in increased discharges for the full range of heads. The increase in capacity makes it possible to achieve economy by reducing either the crest length or the maximum surcharge head.

Tests have shown that the subatmospheric pressures on a nappe-shaped crest do not exceed about one-half the design head when the design head is not less than about 75 percent of the maximum head. For most conditions in the design of spillways, these negative pressures will be small, and they can be tolerated because they will not approach absolute pressures that can induce cavitation. Care must be taken, however, in forming the surface of the crest where these negative pressures will occur, because unevenness caused by abrupt offsets, depressions, or projections will amplify the negative pressures

to a magnitude where cavitation conditions can develop.

The negative pressure on the crest may be resolved into a system of forces acting both upward and downstream. These forces should be considered in analyzing the structural stability of the crest structure.

An approximate force diagram of the subatmospheric pressures when the design head used to determine the crest shape is 75 percent of the maximum head is shown on figure 9-29. These data are based on average results of tests made on ideally shaped weirs with negligible approach velocities. Pressures for intermediate head ratios can be assumed to vary linearly, considering that no subatmospheric pressure prevails when $H_o/H_e = 1$.

**9.15. *Gate-Controlled Ogee Crests.*—**Releases for partial gate openings for gated crests occur as orifice flow. With full head on a gate that is opened a small amount, a free discharging trajectory will follow the path of a jet issuing from an orifice. For a vertical orifice the path of the jet can be expressed by the parabolic equation:

$$-y = \frac{x^2}{4H} \tag{5}$$

where $H$ is the head on the center of the opening. For an orifice inclined an angle $\theta$ from the vertical, the equation is:

$$-y = x \tan\theta + \frac{x^2}{4H \cos^2\theta} \tag{6}$$

If subatmospheric pressures are to be avoided along the crest contact, the shape of the ogee downstream from the gate sill must conform to the trajectory profile.

Gates operated with small openings under high heads produce negative pressures along the crest in the region immediately below the gate if the ogee profile drops below the trajectory profile. Tests showed the subatmospheric pressures would be equal to about one-tenth of the design head when the gate is operated at small openings and the ogee is shaped to the ideal nappe profile, equation (2), for maximum head $H_o$. The force diagram for this condition is shown on figure 9-30.

The adoption of a trajectory profile rather than a nappe profile downstream from the gate sill will result in a wider ogee, and reduced discharge efficiency for full gate opening. Where the discharge efficiency is unimportant and where a wider ogee shape is needed for structural stability, the trajectory profile may be adopted to avoid subatmospheric pressure zones along the crest. Where the ogee is shaped to the ideal nappe profile for maximum head, the subatmospheric pressure area can be minimized by placing the gate sill downstream from the crest of the ogee. This will provide an orifice that is inclined downstream for small gate openings and will result in a steeper trajectory closer to the nappe-shaped profile.

**9.16. *Discharge Over Gate-Controlled Ogee Crests.*—**The discharge for a gated ogee crest at partial gate openings will be similar to flow through an orifice and may be computed by the equation:

$$Q = CDL\sqrt{2gH} \tag{7}$$

where:

$H$ = head to the center of the gate opening (including the velocity head of approach),
$D$ = shortest distance from the gate lip to the crest curve, and
$L$ = crest width.

The coefficient, $C$, is primarily dependent upon the characteristics of the flow lines approaching and leaving the orifice. In turn, these flow lines are dependent on the shape of the crest and the type of gate. Figure 9-31, which shows coefficients of discharge for orifice flows for different $\theta$ angles, can be used for leaf gates or radial gates located at the crest or downstream of the crest. The $\theta$ angle for a particular opening is that angle formed by the tangent to the gate lip and the tangent to the crest curve at the nearest point of the crest curve for radial gates. This angle is affected by the gate radius and the location of the trunnion pin. For additional information and geometric computations see [20].

**9.17. *Side Channel Spillways.*—**(a) *General.*—The theory of flow in a side channel spillway [21] is based principally on the law of conservation of linear momentum, assuming that the only forces producing motion in the channel result from the fall in the water surface in the direction of the axis. This premise assumes that the entire energy of the flow over the crest is dissipated through its intermingling with the channel flow and is therefore of

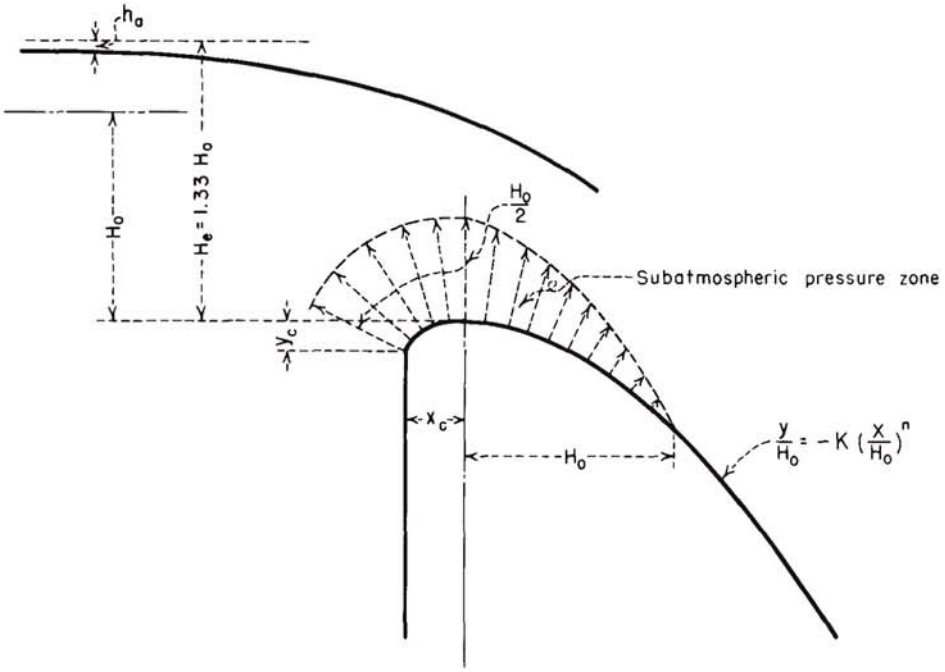


**Figure 9-29.—Subatmospheric crest pressures for $H_a/H_e$ = 0.75. 288–D–2415.**

no assistance in moving the water along the channel. Axial velocity is produced only after the incoming water particles join the channel stream.

For any short reach of the side channel, the momentum at the beginning of the reach plus any increase in momentum from external forces must equal the momentum at the end of the reach. If a short reach, $\Delta x$ in length, is considered and the velocity and discharge at the upstream section are $v$ and $Q$, respectively, then the velocity and discharge at the downstream section will be $v + \Delta v$ and $Q + q(\Delta x)$, where $q$ is the inflow per foot of length of weir crest. Therefore, the momentum[2] at the upstream section will be:

$$M_u = \frac{Qv}{g} \tag{8}$$

And the momentum at the downstream section will be:

$$M_d = \frac{[Q + q(\Delta x)]}{g}(v + \Delta v) \tag{9}$$

[2]The weight of 1 ft³ of water is taken as a unit force to eliminate the necessity of multiplying all forces and momenta by 62.4 to convert them into pounds.

Subtracting equation (8) from equation (9):

$$\Delta M = \frac{Q(\Delta v)}{g} + \frac{q(\Delta x)}{g}(v + \Delta v) \tag{10}$$

Dividing by $\Delta x$:

$$\frac{\Delta M}{\Delta x} = \frac{Q(\Delta v)}{g(\Delta x)} + \frac{q}{g}(v + \Delta v) \tag{11}$$

Since the rate of change of momentum with respect to time is $v$ times the rate of change with respect to $x$, and considering the average velocity = $v+(\Delta v/2)$, equation (11) can be written:

$$\frac{\Delta M}{\Delta t} = \frac{Q(\Delta v)}{g(\Delta x)}\left[v + \frac{1}{2}(\Delta v)\right] + \frac{q}{g}(v + \Delta v)\left[v + \frac{1}{2}(\Delta v)\right] \tag{12}$$

Since $\Delta M/\Delta t$ is the accelerating force, which is equal to the slope of the water surface, $\Delta y/\Delta x$, times the average discharge, equation (12) becomes:

$$\frac{\Delta y}{\Delta x}\left[Q+\frac{1}{2}(\Delta Q)\right]=\frac{Q(\Delta v)}{g(\Delta x)}\left[v+\frac{1}{2}(\Delta v)\right]+\frac{q}{g}(v+\Delta v)\left[v+\frac{1}{2}(\Delta v)\right] \quad (13)$$

from which the change in water surface elevation is:

$$\Delta y=\frac{Q\left[v+\frac{1}{2}(\Delta v)\right]}{g\left[Q+\frac{1}{2}(\Delta Q)\right]}\left[\Delta v+\frac{q(\Delta x)}{Q}(v+\Delta v)\right] \quad (14)$$

If $Q_1$ and $v_1$ are values at the beginning of the reach, and $Q_2$ and $v_2$ are the values at the end of the reach, the equation can be written:

$$\Delta y=\frac{Q_1}{g}\frac{(v_1+v_2)}{(Q_1+Q_2)}\left[(v_2-v_1)+\frac{v_2(Q_2-Q_1)}{Q_1}\right] \quad (15)$$

Similarly, the derivation can be developed so that:

$$\Delta y=\frac{Q_2}{g}\frac{(v_1+v_2)}{(Q_1+Q_2)}\left[(v_2-v_1)+\frac{v_1(Q_2-Q_1)}{Q_2}\right] \quad (16)$$

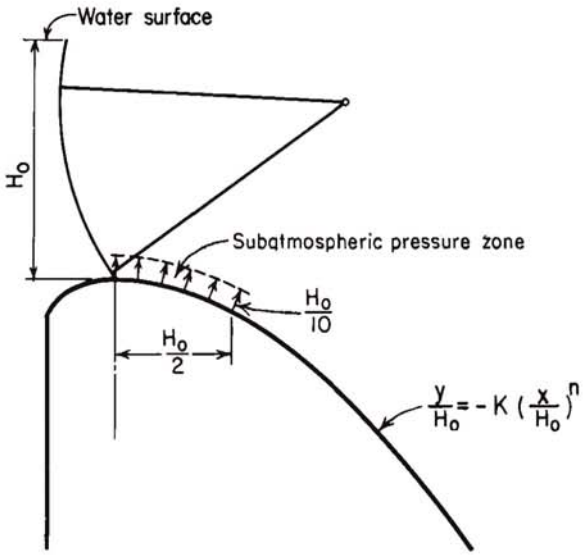


Figure 9-30.—Subatmospheric crest pressures for undershot gate flow. 288-D-2416.

By use of equation (15) or (16), the water surface profile can be determined for any particular side channel by assuming successive short reaches of channel once a starting point is found. The solution of equation (15) or (16) is obtained by a trial-and-error procedure. For a reach of length $\Delta x$ in a specific location, $Q_1$ and $Q_2$ will be known. If the depth at one end of the reach has been established, a trial depth at the other end of the reach can be found that will satisfy the indicated and computed values of $\Delta y$.

As in other water surface profile determinations, the depth of flow and the hydraulic characteristics of the flow will be affected by backwater influences from some control point or by critical conditions along the reach of the channel under consideration. The selection of a control for starting the water surface profile computations is treated in the subsequent discussion.

When the bottom of the side channel trough is selected so that its depth below the hydraulic gradient is greater than the minimum specific energy depth, flow will be either at the subcritical or supercritical stage, depending either on the relation of the bottom profile to critical slope or on the influences of a downstream control section. If the slope of the bottom is greater than critical and a control section is not established below the side channel trough, supercritical flow will prevail throughout the length of the channel. For this stage, velocities will be high and water depths will be shallow, resulting in a relatively high fall from the reservoir water level to the water surface in the trough. This flow condition is illustrated by profile B′ on figure 9-32. Conversely, if a control section is established downstream from the side channel trough to increase the upstream depths, the channel can be made to flow at the subcritical stage. Velocities at this stage will be less than critical, and the greater depths will result in a smaller drop from the reservoir water surface to the side channel water surface profile. The condition of flow for subcritical depths is illustrated on figure 9-32 by water surface profile A′.

The effect of the fall distance from the reservoir to the channel water surface for each type of flow is depicted on figure 9-32(B). It can be seen that for the subcritical stage, the incoming flow will not develop high transverse velocities because of the low drop before it meets the channel flow, thus effecting a good diffusion with the water bulk in the trough.

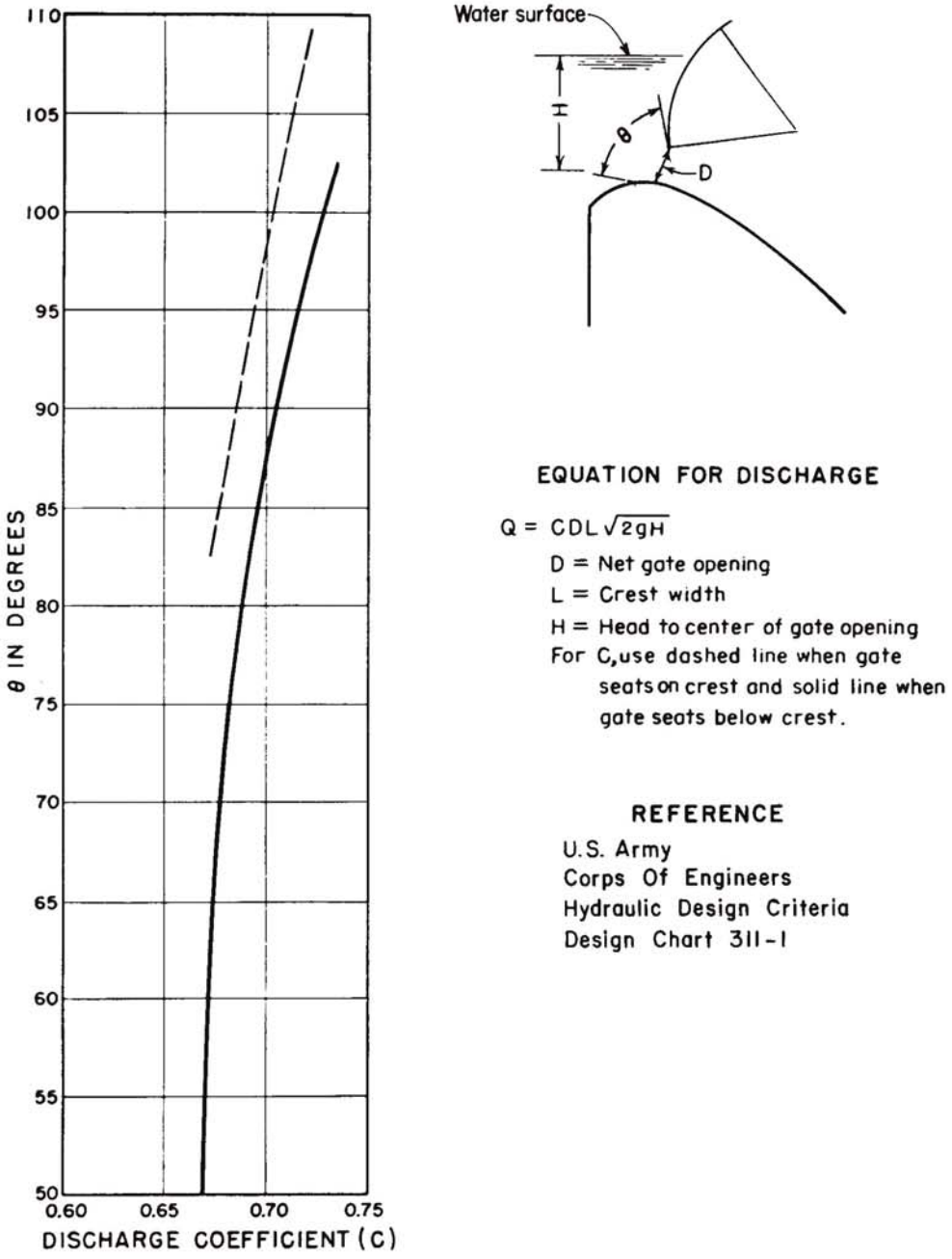


**Figure 9-31.—Discharge coefficient for flow under gates. 103-D-1875.**

Because both the incoming velocities and the channel velocities will be relatively slow, a fairly complete intermingling of the flows will occur, thereby producing a comparatively smooth flow in the side channel. Where the channel flow is at the supercritical stage, the channel velocities will be high, and the intermixing of the high-energy transverse flow with the channel stream will be rough and turbulent. The transverse flows will tend to sweep the channel flow to the far side of the channel, producing violent wave action with attendant vibrations. Therefore, it is evident that flows should be

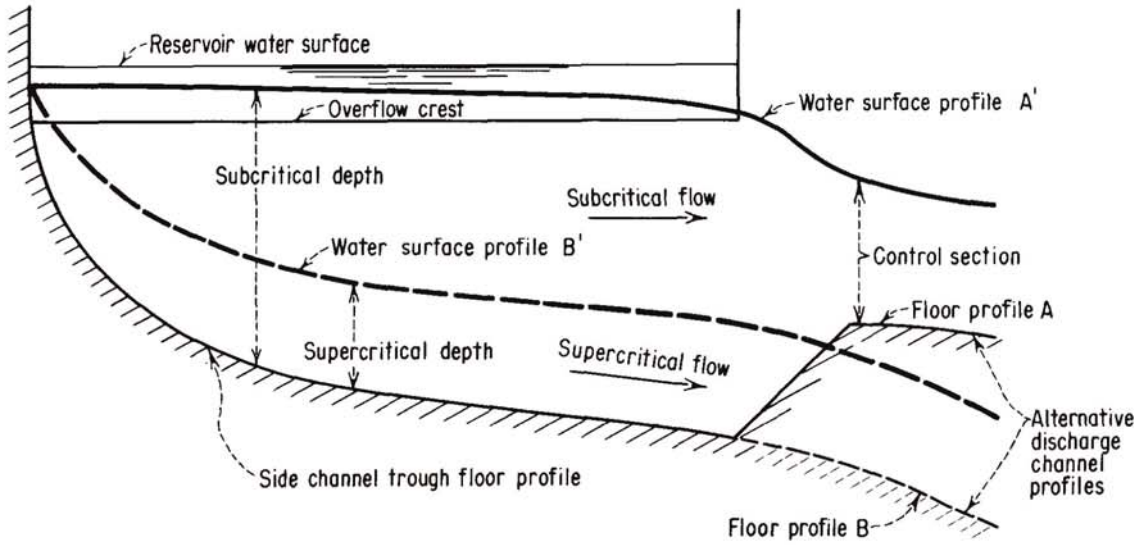


(A) SIDE CHANNEL PROFILE

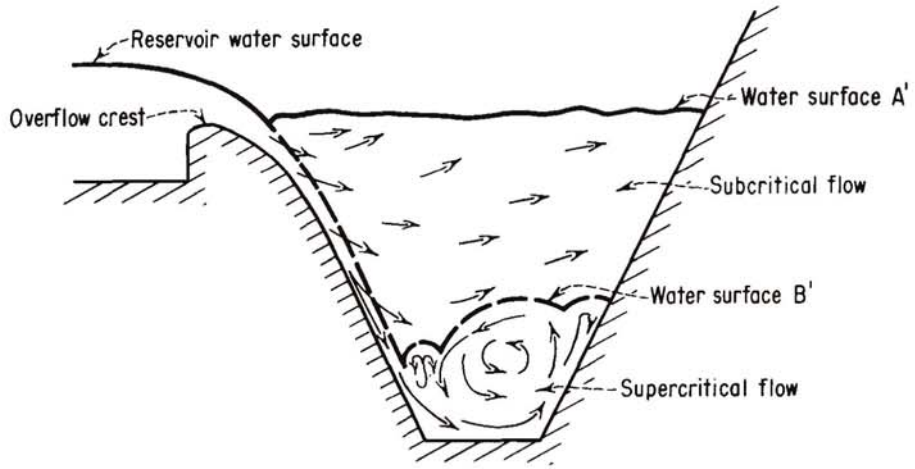


(B) SIDE CHANNEL CROSS SECTION

**Figure 9-32.—Side channel flow characteristics. 288-D-2418.**

maintained at subcritical stage for good hydraulic performance. This can be achieved by establishing a control section downstream from the side channel trough.

The cross-sectional shape of the side channel trough will be influenced by the overflow crest on the one side and by the bank conditions on the opposite side. Because of turbulence and vibrations inherent in side channel flow, a side channel design is ordinarily not considered except where a competent foundation such as rock exists. The channel sides will, therefore, usually be a concrete lining placed on a slope and anchored directly to the rock. A trapezoidal cross section is the one most often used for a side channel trough. The width of such a channel in relation to the depth should be considered. If the width to depth ratio is large, the depth of flow in the channel will be shallow, similar

to that depicted by the cross section *abfg* on figure 9-33. It is evident that for this condition a poor diffusion of the incoming flow with the channel flow will result. A cross section with a minimum width to depth ratio will provide the best hydraulic performance; this indicates that a cross section approaching *adj* (on fig. 9-33) would be the ideal choice both from the standpoint of hydraulics and economy. However, some bottom width is needed to avoid construction difficulties caused by confined working space. Furthermore, the stability of both the structure and the hillside, which might be jeopardized by an extremely deep cut in the abutment, must also be considered. Therefore, the minimum bottom width selected must be commensurate with both the practical and structural aspects of the problem.

A control section downstream from the side channel trough is achieved by constricting the channel sides or elevating the channel bottom to produce a point of critical flow. Flows upstream from the control will be at the subcritical stage and will provide a maximum of depth in the side channel trough. The side channel bottom and control dimensions are then selected so that flow in the trough opposite the crest will be at the greatest depth possible without submerging the flow over the crest. Flow in the discharge channel downstream from the control will be the same as that in an ordinary channel or chute spillway.

(b) *Design Example.*—A design example illustrates the procedures for determining the hydraulic design of a side channel spillway control structure. The problem is to design a side channel spillway 100 feet long (station 0+00 to station 1+00) to discharge a maximum of 2,000 ft³/s. The spillway crest is at elevation 1000.0 feet, and the discharge per foot of length $q$ = 2,000/100 = 20 ft³/s. Assume the crest coefficient $C$ = 3.6, $H_o = (q/C)^{2/3}$ = 3.1 feet.

For the side channel trough, assume a trapezoidal section with ½:1 side slopes and a bottom width of 10 feet, whose rise in bottom profile is 1.0 foot in the 100 feet of channel length. (The slope of the channel profile is arbitrary; however, a relatively flat slope will provide greater depths and lower velocities and, consequently, will ensure better intermingling of flows at the upstream end of the channel and avoid the possibility of accelerating or supercritical flows occurring in the channel for smaller discharges.) Furthermore, assume that a control section is placed downstream from the side channel trough with its bottom at the same elevation as the bottom of the side channel floor at the downstream end. Assume that a transition is made from the ½:1 slopes of the trough section to a rectangular section at the control. Arbitrarily assume a datum for the control section bottom at elevation 100.0.

Therefore, the critical depth for flow at the control is $d_c = (q_1^2/g)^{1/3}$.

For this example:

$$q_1 = \frac{2{,}000}{10} = 200 \text{ ft}^3\text{/s per foot of width}$$

$$d_c = \left(\frac{200^2}{32.2}\right)^{1/3} = 10.75 \text{ feet}$$

$$v_c = \frac{q_1}{d_c} = \frac{200}{10.75} = 18.6 \text{ ft/s}$$

$$h_{v_c} = \frac{v_c^2}{2g} = \frac{18.6^2}{64.4} = 5.37 \text{ feet}$$

Assume a transition loss from the end of the side channel trough to the control section (to provide for losses caused by contraction, by diffusion of the flows not affected in the side channel proper, and by friction losses) equal to 0.2 of the difference in velocity heads between the ends of the transition. The flow characteristics at the downstream end of the side channel can be obtained from Bernoulli's equation (app. B). For figure 9-34, Bernoulli's equation may be written as follows:

$$d_{(1+00)} + h_{v_{(1+00)}} = d_c + h_{v_c} + 0.2(h_{v_c} - h_{r_{(1+00)}})$$

This expression must be solved by trial and error. First, assume a value of $d_{(1+00)}$, and solve for $h_{v\,(1+00)}$. If the use of these values does not result in a balanced equation, a new value must be assumed for $d_{(1+00)}$ and the process repeated. A value of 16.34 feet for $d_{(1+00)}$ was found to satisfy the equation as follows:

For $d_{(1+00)}$ = 16.34, the area of flow at station 1+00 in the trapezoidal cross section with 10-foot bottom width and ½:1 side slopes = 297 ft².

$$v_{(1+00)} = \frac{2{,}000}{297} = 6.73 \text{ ft/s}$$

$$h_{v_{(1+00)}} = \frac{6.73^2}{64.4} = 0.70 \text{ foot}$$

$$0.2(h_{v_c} - h_{v(1+00)}) = 0.2\ (5.37 - 0.70) = 0.93 \text{ foot}$$

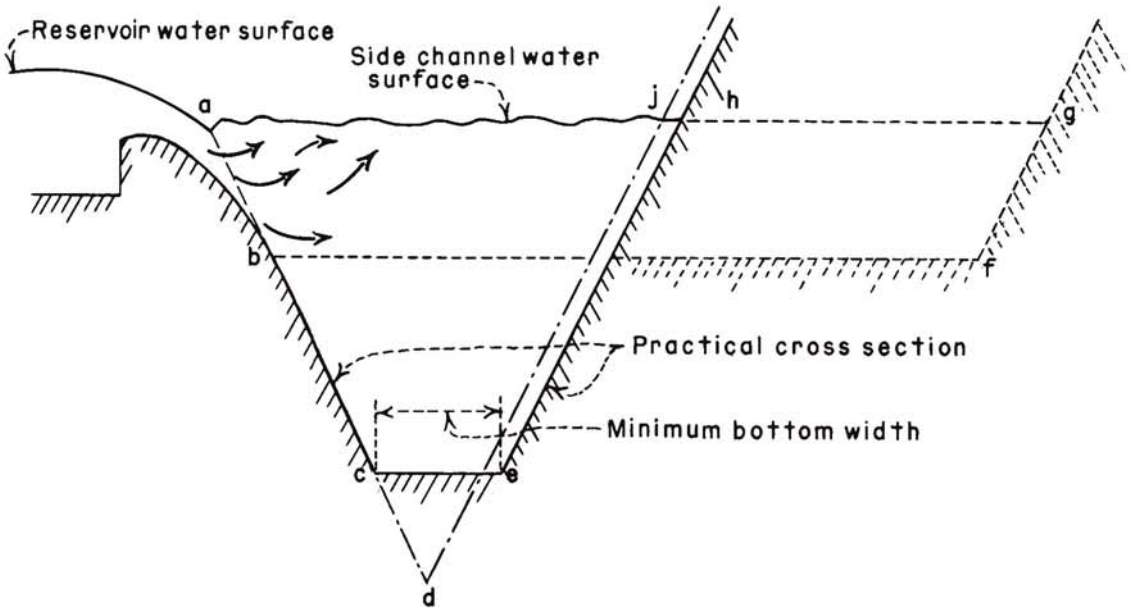


Figure 9-33.—Comparison of side channel cross sections. 288–D–2419.

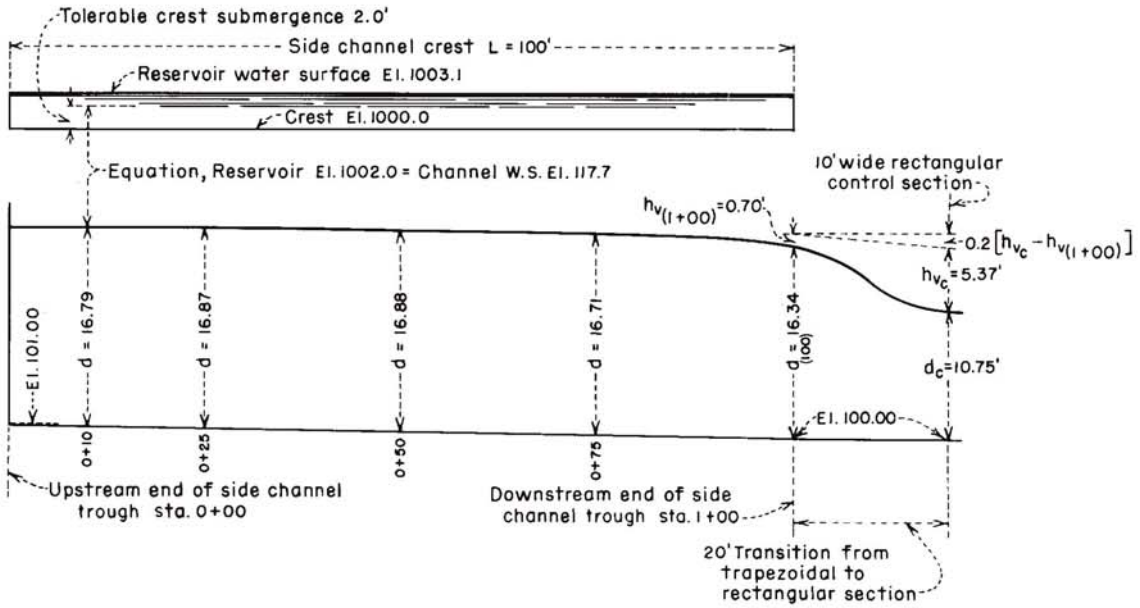


Figure 9-34.—Example of hydraulic design for side channel spillway. 288–D–2420.

Substituting the values in Bernoulli's equation:

$$16.34 + 0.70 = 10.75 + 5.37 + 0.93$$
$$17.04 = 17.05 \text{ (A satisfactory check)}$$

With the hydraulic properties of the side channel at station 1+00 determined, the water surface profile along the side channel trough can be determined from equation (15). The trial-and-error computations are shown in table 9-3. The resulting water surface profile is shown on figure 9-34.

Next, the channel profile is fitted to the crest datum by relating the water surface profile to the

Table 9-3.—Side channel spillway computations. Using eq(15) for design example in section 9.17(b): given $Q$ = 2,000 ft³/s, bottom width = 10 feet, side slopes = ½:1, and bottom slope = 1 foot in 100 feet.

| (1) | (2) | (3) | (4) | (5) | (6) | (7) | (8) | (9) | (10) | (11) | (12) | (13) | (14) | (15) | (16) | (17) | (18) | (19) |
|---|---|---|---|---|---|---|---|---|---|---|---|---|---|---|---|---|---|---|
| Station | $\Delta x$ | Elevation bottom | Trial $\Delta y$ | Water surface elevation | $d$ | $A$ | $Q$ | $v$ | $Q_1+Q_2$ | $\frac{Q_1}{g(Q_1+Q_2)}$ | $v_1+v_2$ | $v_2-v_1$ | $Q_2-Q_1$ | $\frac{Q_2-Q_1}{Q_1}$ | $\frac{v_2(Q_2-Q_1)}{Q_1}$ | (13)+(16) | $\Delta y$ = (11) ×(12)×(17) | Remarks |
| 1+00 | – | 100.0 | – | 116.34 | 16.34 | 297 | 2,000 | 6.73 | – | – | – | – | – | – | – | – | – | – |
| 0+75 | 25 | 100.25 | 1.00 | 117.34 | 17.09 | 317 | 1,500 | 4.73 | 3,500 | 0.01332 | 11.46 | 2.00 | 500 | 0.333 | 2.24 | 4.24 | 0.64 | Too low |
| | | | .62 | 116.96 | 16.71 | 307 | – | 4.89 | – | – | 11.62 | 1.84 | – | – | – | 4.08 | .63 | OK |
| 0+50 | 25 | 100.50 | .50 | 117.46 | 16.96 | 313 | 1,000 | 3.19 | 2,500 | .01244 | 8.08 | 1.70 | 500 | .50 | 2.44 | 4.14 | .42 | Too low |
| | | | .42 | 117.38 | 16.88 | 311 | – | 3.22 | – | – | 8.11 | 1.67 | – | – | – | 4.11 | .41 | OK |
| 0+25 | 25 | 100.75 | .30 | 117.68 | 16.93 | 313 | 500 | 1.60 | 1,500 | .01036 | 4.82 | 1.62 | 500 | 1.00 | 3.22 | 4.84 | .24 | Too low |
| | | | .24 | 117.62 | 16.87 | 311 | – | 1.61 | – | – | 4.83 | 1.61 | – | – | – | 4.83 | .24 | OK |
| 0+00 | 15 | 100.90 | .10 | 117.72 | 16.82 | 310 | 200 | .64 | 700 | .00888 | 2.25 | .97 | 300 | 1.50 | 2.41 | 3.38 | .07 | Too low |
| | | | .07 | 117.69 | 16.79 | 309 | – | .65 | – | – | 2.26 | .96 | – | – | – | 3.37 | .07 | OK |

reservoir water level. To obtain the assumed crest coefficient value of 3.6, excessive submergence of the overflow must be avoided. If it is assumed that a maximum of two-thirds submergence at the upstream end of the channel can be tolerated, the maximum water surface level in the channel will be $\frac{2}{3}H_o$ above the crest, or elevation 1002.0. Then at station 0+10, the channel datum water surface level elevation 117.7 will become elevation 1002.0, placing the channel floor level for station 0+00 at approximately elevation 985.3, and for station 1+00 at approximately elevation 984.3.

The design of the side channel control structure would be completed by designing the uncontrolled ogee crest by the methods shown in section 9.13, to obtain the crest coefficient value of 3.6 that was assumed.

Variations in the design can be made by assuming different bottom widths, different channel slopes, and varying control sections. A proper and economical design can usually be achieved after comparing several alternatives.

## D. HYDRAULICS OF FREE-FLOW DISCHARGE CHANNELS

**9.18.** ***General.***—Discharge generally passes through the critical stage in the spillway control structure and enters the discharge channel as supercritical or shooting flow. To avoid a hydraulic jump below the control, the flow must remain at the supercritical stage throughout the length of the channel. The flow in the channel may be uniform or it may be accelerated or decelerated, depending on the slopes and dimensions of the channel and on the total drop. Where it is desired to minimize the grade to reduce excavation at the upstream end of a channel, the flow might be uniform or decelerating, followed by accelerating flow in the steep drop leading to the downstream river level. Flow at any point along the channel will depend upon the specific energy, $d+h_v$, available at that point. This energy will equal the total drop from the reservoir water level to the floor of the channel at the point under consideration, less the head losses accumulated to that point. The velocities and depths of flow along the channel can be fixed by selecting the grade and the cross-sectional dimensions of the channel.

The velocities and depths of free surface flow in a channel, whether it be an open channel, a conduit, or a tunnel, conform to the principle of the conservation of energy as expressed by Bernoulli's theorem, which states "the absolute energy of flow at any cross section is equal to the absolute energy at a downstream section plus intervening losses of energy." As applied to figure 9-35 this relationship can be expressed as follows:

$$\Delta Z + d_1 + h_{v_2} = d_2 + h_{v_2} + \Delta h_L \qquad (17)$$

When the channel grades are not too steep, for practical purposes the normal depth, $d_n$, can be considered equal to the vertical depth $d$. The term $\Delta h_L$ includes all losses that occur in the reach of channel, such as friction, turbulence, impact, and transition losses. Because changes in most channels are made gradually, all losses except those from friction

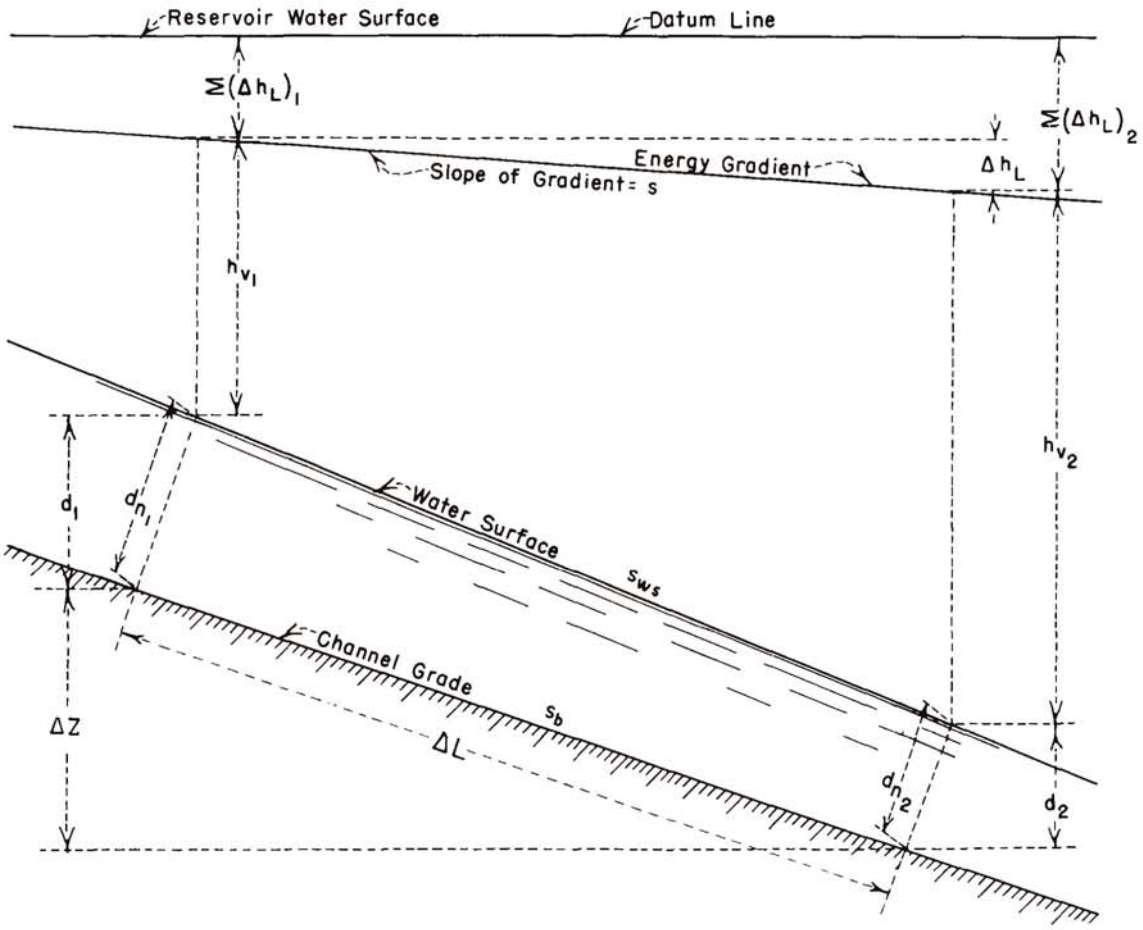


Figure 9-35.—Flow in open channels. 288–D–2421.

can ordinarily be neglected. The friction loss can then be expressed as:

$$\Delta h_L = s\Delta L \qquad (18)$$

where $s$ is the average friction slope expressed by either the Chezy or the Manning formula. For the reach $\Delta L$, the head loss can be expressed as:

$$\Delta h_L = \left(\frac{s_1 + s_2}{2}\right) \Delta L$$

From the Manning formula (eq. (30), app. B), $s = (vn/1.486r^{2/3})^2$.

The roughness coefficient, $n$, will depend on the nature of the channel surface. For conservative design the frictional loss should be maximized when evaluating depths of flow and minimized when evaluating the energy content of the flow. For determining depths of flow in a concrete-lined channel, an $n$ of about 0.014 should be assumed. For determining specific energies of flow needed to design the dissipating device, an $n$ of about 0.008 should be assumed.

Where only rough approximations of depths and velocities of flow in a discharge channel are desired, the total head loss $\Sigma\Delta h_L$ to any point along the channel might be expressed in terms of the velocity head. Thus, at any section the relationship can be stated: reservoir water surface elevation minus floor grade elevation = $d + h_v + Kh_v$. For spillways with small drops, $K$ can be assumed as approximately 0.2 for determining depths of flow and 0.1 or less for evaluating the energy of flow. Rough approximations of losses can also be obtained from figure B-5.

**9.19. *Open Channels.***—(a) *Profile.*—The profile of an open channel is usually selected to conform to topographic and geologic site conditions. It is generally defined as straight reaches connected

by vertical curves. Sharp convex and concave vertical curves would develop unsatisfactory flows in the channel and should be avoided. Convex curves should be flat enough to maintain positive pressures and thus preclude the tendency for the flow to separate from the floor. Concave curves should have a sufficiently long radius of curvature to minimize the dynamic forces on the floor brought about by the centrifugal force from a change in the direction of flow.

To avoid the tendency for the water to spring away from the floor and, thereby, reduce the surface contact pressure, the floor shape for convex curvature should be made slightly flatter than the trajectory of a free-discharging jet issuing under a head equal to the specific energy of flow as it enters the curve. The curvature should approximate a shape defined by the equation:

$$-y = x \tan\theta + \frac{x^2}{K[4(d + h_v)\cos^2\theta]} \qquad (19)$$

where $\theta$ is the slope angle of the floor upstream from the curve. Except for the factor $K$, the equation is that of a free-discharging trajectory issuing from an inclined orifice. To ensure positive pressure along the entire contact surface of the curve, $K$ should be equal to or greater than 1.5.

For the concave curvature, the pressure exerted upon the floor surface by the centrifugal force of the flow varies directly with the energy of the flow and inversely with the radius of curvature. An approximate relationship of these criteria can be expressed in the equations:

$$R = \frac{2qv}{p} \text{ and } R = \frac{2dv^2}{p} \qquad (20)$$

where:

$R$ = the minimum radius of curvature, in feet,
$q$ = the discharge, in cubic feet per second per foot of width,
$v$ = the velocity, in feet per second,
$d$ = the depth of flow, in feet, and
$p$ = the normal dynamic pressure exerted on the floor, in pounds per square foot.

An assumed value of $p$ = 1,000 will normally produce an acceptable radius; however, in no case should the radius be less than $10d$. For the reverse curve at the lower end of the ogee crest, radii of not less than $5d$ have been found acceptable.

(b) *Convergence and Divergence.*—The best hydraulic performance in a discharge channel is obtained when the confining sidewalls are parallel and the distribution of flow across the channel is maintained uniform. However, economy may dictate a channel section narrower or wider than either the crest or the terminal structure, thereby requiring converging or diverging transitions to fit the various components together. Sidewall convergence must be made gradual to avoid cross waves, wave runup on the walls, and uneven distribution of flow across the channel. Similarly, the rate of divergence of the sidewalls must be limited or else the flow will not spread to occupy the entire width of the channel uniformly. This will result in undesirable flow conditions at the terminal structure.

The inertial and gravitational forces of streamlined kinetic flow in a channel can be expressed by the Froude number parameter, $v/(gd)^{1/2}$. Variations from streamlined flow caused by outside interferences that cause an expansion or a contraction of the flow can also be related to this parameter. Experiments have shown that an angular variation of the flow boundaries not exceeding that produced by the equation,

$$\tan\alpha = \frac{1}{3F} \qquad (21)$$

will provide an acceptable transition for either a contracting or an expanding channel. In this equation, $F = v/(gd)^{1/2}$, and $\alpha$ is the angular variation of the sidewall with respect to the channel centerline; $v$ and $d$ are the velocity and depth at the start of the transition. Figure 9-36 is a nomograph from which the tangent of the flare angle or the flare angle in degrees may be obtained for known values of depth and velocity of flow.

(c) *Channel Freeboard.*—In a channel conducting flow at the supercritical stage, the surface roughness, wave action, air bulking, splash, and spray are related to the velocity and energy content of the flow. Expressed in terms of $v$ and $d$, the energy per foot of width $qh_v = v^3d/2g$. Therefore the relationship of velocity and depth to the flow energy also can be expressed in terms of $v$ and $d^{1/3}$. An empirical expression based on this relationship that gives a reasonable indication of desirable freeboard values is:

$$\text{Freeboard (in feet)} = 2.0 + 0.025v\sqrt[3]{d} \qquad (22)$$

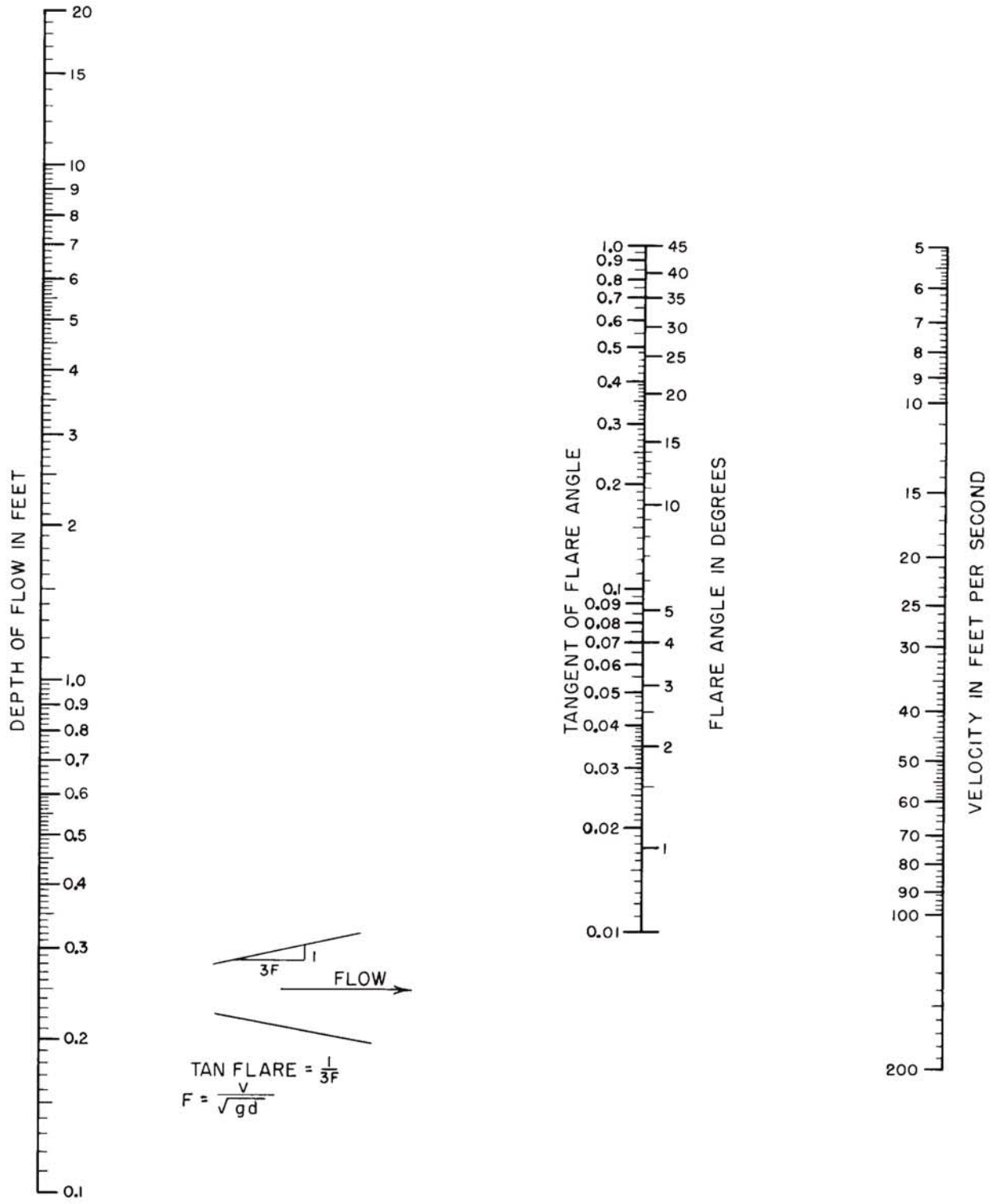


Figure 9-36.—Flare angle for divergent or convergent channels. 288-D-2422.

## E. HYDRAULICS OF TERMINAL STRUCTURES

**9.20. *Deflector Buckets.*—**Where the spillway discharge may be safely delivered directly to the river without providing a dissipating or stilling device, the jet is often projected beyond the structure by a deflector bucket or lip. Flow from these deflectors leaves the structure as a free-discharging upturned jet and falls into the stream channel some distance from the end of the spillway. The path the jet assumes depends on the energy of flow available at the lip and the angle at which the jet leaves the bucket.

With the origin of the coordinates taken at the end of the lip, the path of the trajectory is given by the equation:

$$y = x \tan \theta - \frac{x^2}{K[4(d + h_v) \cos^2 \theta]} \qquad (23)$$

where:

$\theta$ = angle of the edge of the lip with the horizontal, and
$K$ = a factor, equal to 1, for the theoretical jet.

To compensate for loss of energy and the velocity reduction caused by air resistance, internal turbulences, and disintegration of the jet, $K = 0.9$ should be assumed.

The horizontal range of the jet at the level of the lip is obtained by making $y = 0$ in equation (23). Then, $x = 4K(d+h_v)\tan\theta \cos^2\theta = 2K(d+h_v)\sin 2\theta$. The maximum value of $x$ will be $2K(d + h_v)$ when $\theta = 45°$. However, the angle of the lip is influenced by the bucket radius and the height of the lip above the bucket invert; ordinarily the exit angle should not be more than 30°.

The bucket radius should be made long enough to maintain concentric flow as the water moves around the curve. The rate of curvature must be limited, similar to that of a vertical curve in a discharge channel (sec. 9.19), so that the floor pressures will not alter the streamline distribution of the flow. The minimum radius of curvature, $R$, can be determined from equation (20), except that values of $p \leq 1{,}000$ lb/ft² will produce values of the radius that have proved satisfactory in practice. However, the radius should not be less than $5d$, five times the depth of water. Structurally, the cantilever bucket must be strong enough to withstand this normal dynamic force in addition to the other applied forces.

**9.21. *Hydraulic-Jump Basins.*—**(a) *General.*—Where the energy of flow in a spillway must be dissipated before the discharge is returned to the downstream river channel, the hydraulic-jump stilling basin is an effective device for reducing the exit velocity to a tranquil state. The jump that will occur in such a stilling basin has distinctive characteristics and assumes a definite form, depending on the relation between the energy of flow that must be dissipated and the depth of the flow.

A comprehensive series of tests have been performed by the Bureau of Reclamation [15] to determine the properties of the hydraulic jump. The jump form and the flow characteristics can be related to the kinetic flow factor, $v^2/gd$, of the discharge entering the basin; to the critical depth of flow, $d_c$ ; or to the Froude number parameter, $v/(gd)^{1/2}$. Forms of the hydraulic-jump phenomena for various ranges of the Froude number are illustrated on figure 9-37.

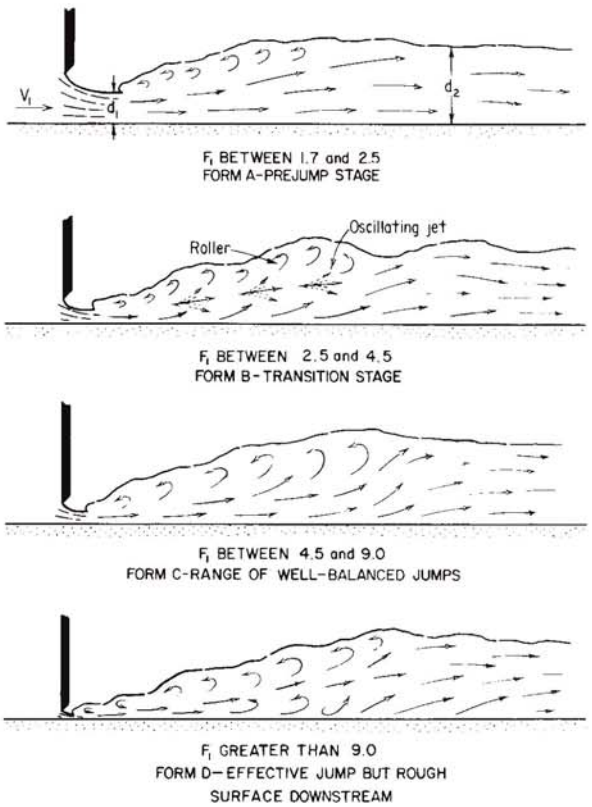


**Figure 9-37.—Characteristic forms of hydraulic jump related to the Froude number. 288-D-2423.**

When the Froude number of the incoming flow is 1.0, the flow is at critical depth and a hydraulic jump cannot form. For Froude numbers from 1.0 to about 1.7, the incoming flow is only slightly below critical depth, and the change from this low stage to the high stage flow is gradual and manifests itself only by a slightly ruffled water surface. As the Froude number approaches 1.7, a series of small rollers begins to develop on the surface. These become more intense with increasingly higher values of the number. Other than the surface roller phenomena, relatively smooth flows prevail throughout the Froude number range up to about 2.5. Stilling action for the range of Froude numbers from 1.7 to 2.5 is shown as form A on figure 9-37. Forms B, C, and D on figure 9-37 show characteristic forms at hydraulic jumps related to higher Froude numbers.

For Froude numbers between 2.5 and 4.5, an oscillating form of jump occurs. The entering jet intermittently flows near the bottom and then along the surface of the downstream channel. This oscillating flow causes objectionable surface waves that carry far beyond the end of the basin. The action represented through this range of flows is designated as form B on figure 9-37.

For Froude numbers between 4.5 and 9, a stable and well-balanced jump occurs. Turbulence is confined to the main body of the jump, and the water surface downstream is comparatively smooth. As the Froude number increases above 9, the turbulence within the jump and the surface roller becomes increasingly active, resulting in a rough water surface with strong surface waves downstream from the jump. Stilling action for Froude numbers between 4.5 and 9 is designed as form C on figure 9-37, and that above 9 is designated as form D.

Figure 9-38 plots relationships of conjugate depths and velocities for the hydraulic jump in a rectangular channel. The ranges for the various forms of jump described above are also indicated on the figure.

(b) *Basin Design in Relation to Froude Numbers.*—Stilling basin designs suitable to provide stilling action for the various forms of jump are described in the following paragraphs.

(1) *Basins for Froude Numbers Less Than 1.7.*—For a Froude number of 1.7, the conjugate depth, $d_2$, is about twice the incoming depth, or about 40 percent greater than the critical depth. The exit velocity, $v_2$, is about one-half the incoming velocity, or 30 percent less than the critical velocity. No special stilling basin is needed to still flows where the Froude number of the incoming flow is less than 1.7, except that the channel lengths beyond the point where the depth starts to change should be not less than about $4d_2$. No baffles or other dissipating devices are needed. These basins, designated type I, are not shown here (see [15]).

(2) *Basins for Froude Numbers Between 1.7 and 2.5.*—Flow phenomena for these basins will be in the form designated as the prejump stage, as shown on figure 9-37. Because such flows are not attended by active turbulence, baffles or sills are not required. The basin should be long enough to contain the flow prism while it is undergoing retardation. Conjugate depths and basin lengths shown on figure B-15 will provide acceptable basins. These basins, designated type I, are not shown here (see [15]).

(3) *Basins for Froude Numbers Between 2.5 and 4.5.*—Flows for these basins are considered to be in the transition flow stage because a true hydraulic jump does not fully develop. Stilling basins that accommodate these flows are the least effective in providing satisfactory dissipation because the attendant wave action ordinarily cannot be controlled by the usual basin devices. Waves generated by the flow phenomena will persist beyond the end of the basin and must often be dampened by means apart from the basin.

Where a stilling device must be provided to dissipate flows for this range of Froude number, the basin shown on figure 9-39(A), which is designated a type IV basin, has proved relatively effective for dissipating the bulk of the energy of flow. However, the wave action propagated by the oscillating flow cannot be entirely dampened. Auxiliary wave dampeners or wave suppressors must sometimes be used to provide smooth surface flow downstream.

Because of the tendency of the jump to sweep out and as an aid in suppressing wave action, the water depths in the basin should be about 10 percent greater than the computed conjugate depth.

Often, the need to design this type of basin can be avoided by selecting stilling basin dimensions that will provide flow conditions that fall outside the range of transition flow. For example, with an 800-$ft^3/s$ capacity spillway where the specific energy at the upstream end of the basin is about 15 feet and the velocity into the basin is about 30 ft/s, the Froude number will be 3.2 for a basin width of 10 feet. The Froude number can be raised to 4.6 by widening the basin to 20 feet. The selection of basin

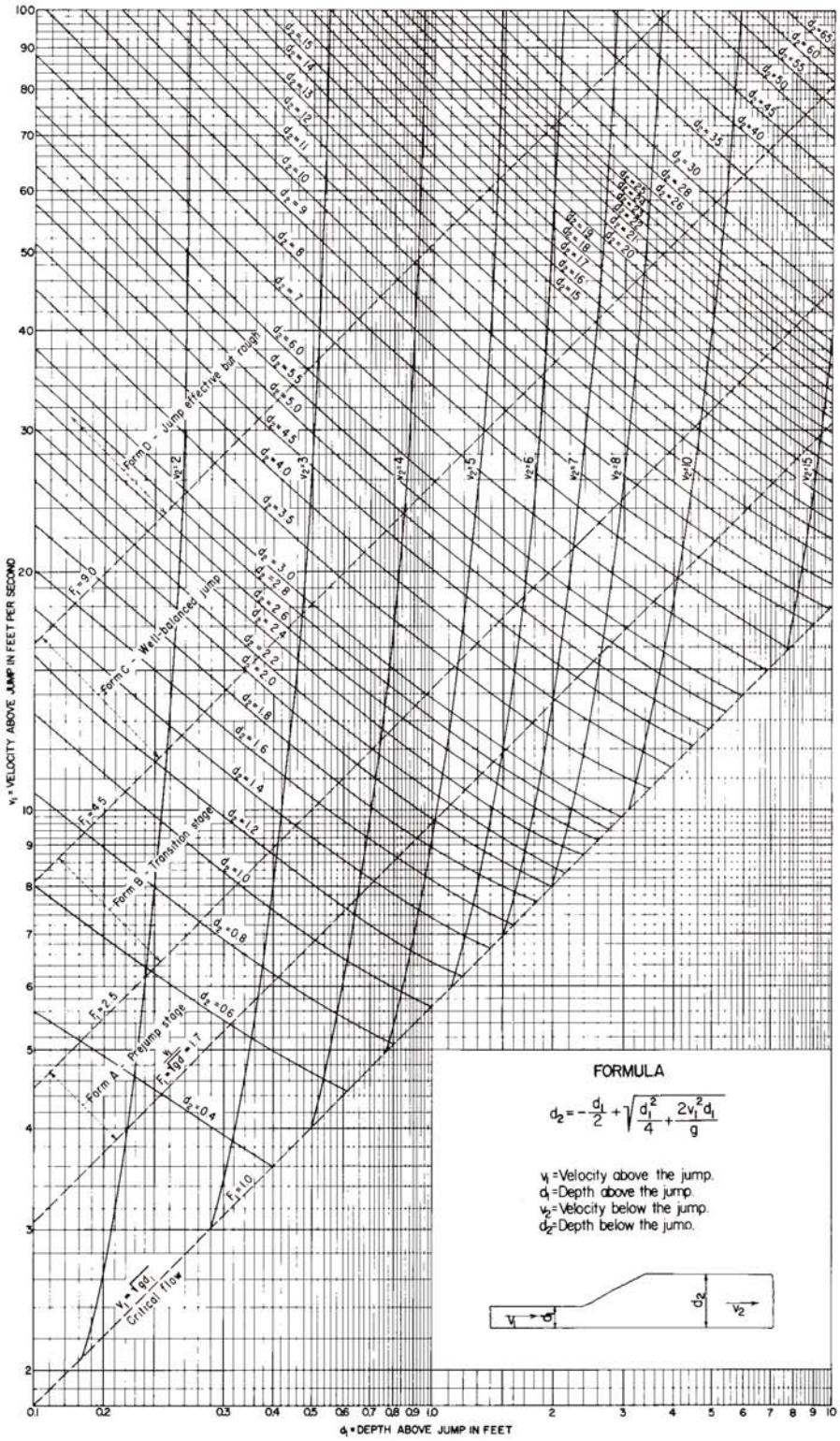


**Figure 9-38.—Relations between variables in hydraulic jump for rectangular channel. 288-D-2424.**

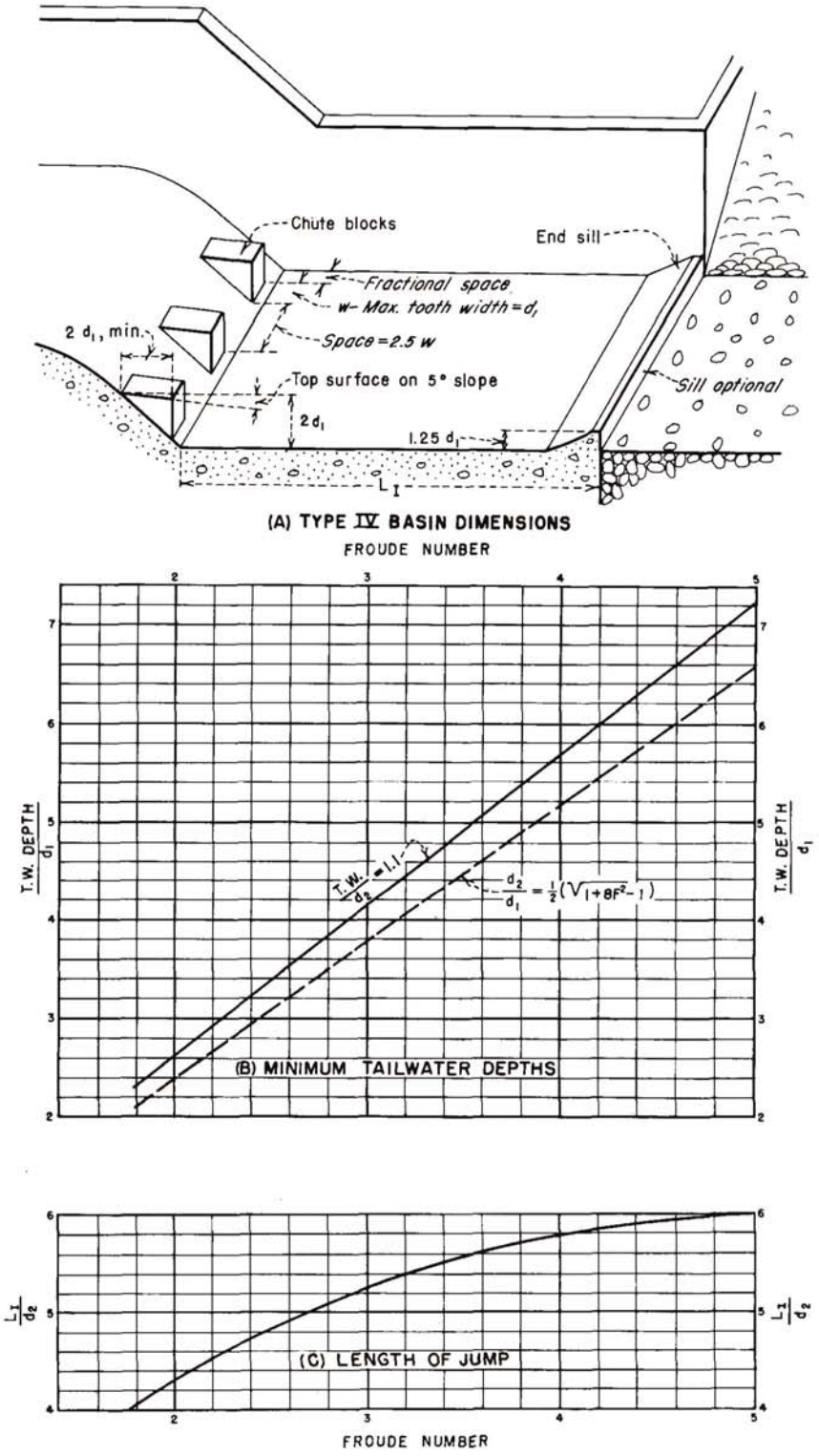


**Figure 9-39.—Stilling basin characteristics for Froude numbers between 2.5 and 4.5. 288–D–2425.**

width then becomes a matter of economics as well as hydraulic performance.

(4) *Alternative Low Froude Number Stilling Basins.*—Type IV basins are fairly effective at low Froude number flows for small canals and for structures with small unit discharges. However, recent model tests have developed designs quite different from the type IV basin design, even though the type IV basin design was included in the initial tests.

Palmetto Bend Dam stilling basin [22] is an example of a low Froude number structure, modeled in the Bureau of Reclamation Hydraulics Laboratory, whose recommended design is quite different from type IV design. The type IV design has large deflector blocks, similar to but larger than chute blocks, and an optional solid end sill; the Palmetto Bend design has no chute blocks, but has large baffle piers and a dentated end sill.

The foregoing generalized designs have not been suitable for some Bureau applications, and the increased use of low Froude number stilling basins has created a need for additional data on this type of design. A study was initiated to develop generalized criteria for the design of low Froude number hydraulic-jump stilling basins. The criteria and guidelines from previous studies were combined with the results of this study to formulate the design guidelines recommended for low Froude number stilling basins [23]. However, it should be noted that a hydraulic-jump stilling basin is not an efficient energy dissipator at low Froude numbers; that is, the efficiency of a hydraulic-jump basin is less than 50 percent in this Froude number range. Alternative energy dissipators, such as the baffled apron chute or spillway, should be considered for these conditions.

The recommended design has chute blocks, baffle piers, and a dentated end sill. All design data are presented on figure 9-40. The length is rather short, approximately three times $d_2$ (the conjugate depth after the jump). The size and spacing of the chute blocks and baffle piers are a function of $d_1$ (incoming depth) and the Froude number. The dentated end sill is proportioned according to $d_2$ and the Froude number. The end sill is placed at or near the downstream end of the stilling basin. Erosion tests were not included in the development of this basin. Observations of flow patterns near the invert downstream from the basin indicated that no erosion problem should exist. However, if hydraulic model tests are performed to confirm a design based on these criteria, erosion tests should be included. Tests should be made over a full range of discharges to determine whether abrasive materials will move upstream into the basin and to determine the erosion potential downstream from the basin. If the inflow velocity is greater than 50 ft/s, hydraulic model studies should be performed.

(5) *Basins for Froude Numbers Higher Than 4.5.*—For these basins, a true hydraulic jump will form. The elements of the jump will vary according to the Foude number, as shown on figure B-15. The installation of accessory devices such as blocks, baffles, and sills along the floor of the basin produce a stabilizing effect on the jump, which permits shortening the basin and provides a safety factor against sweepout caused by inadequate tailwater depth.

The basin shown on figure 9-41, which is designated a type III basin, can be adopted where incoming velocities do not exceed 60 ft/s. The type III basin uses chute blocks, impact baffle blocks, and an end sill to shorten the jump length and to dissipate the high-velocity flow within the shortened basin length. This basin relies on dissipation of energy by the impact blocks and on the turbulence of the jump phenomena for its effectiveness. Because of the large impact forces to which the baffles are subjected by the impingement of high incoming velocities and because of the possibility of cavitation along the surfaces of the blocks and floor, the use of this basin must be limited to heads where the velocity does not exceed 60 ft/s.

Cognizance must be taken of the added loads placed on the structure floor by the dynamic force brought against the upstream face of the baffle blocks. This dynamic force will approximate that of a jet impinging upon a plane normal to the direction of flow. The force, in pounds, may be expressed by the formula:

$$\text{Force} = 2wA(d_1+h_{v_1}) \qquad (24)$$

where:

$w$ = unit weight of water, in pounds per cubic foot,
$A$ = area of the upstream face of the block, in square feet, and
$(d_1+h_{v_1})$ = the specific energy of the flow entering the basin, in feet.

Negative pressure on the back face of the blocks

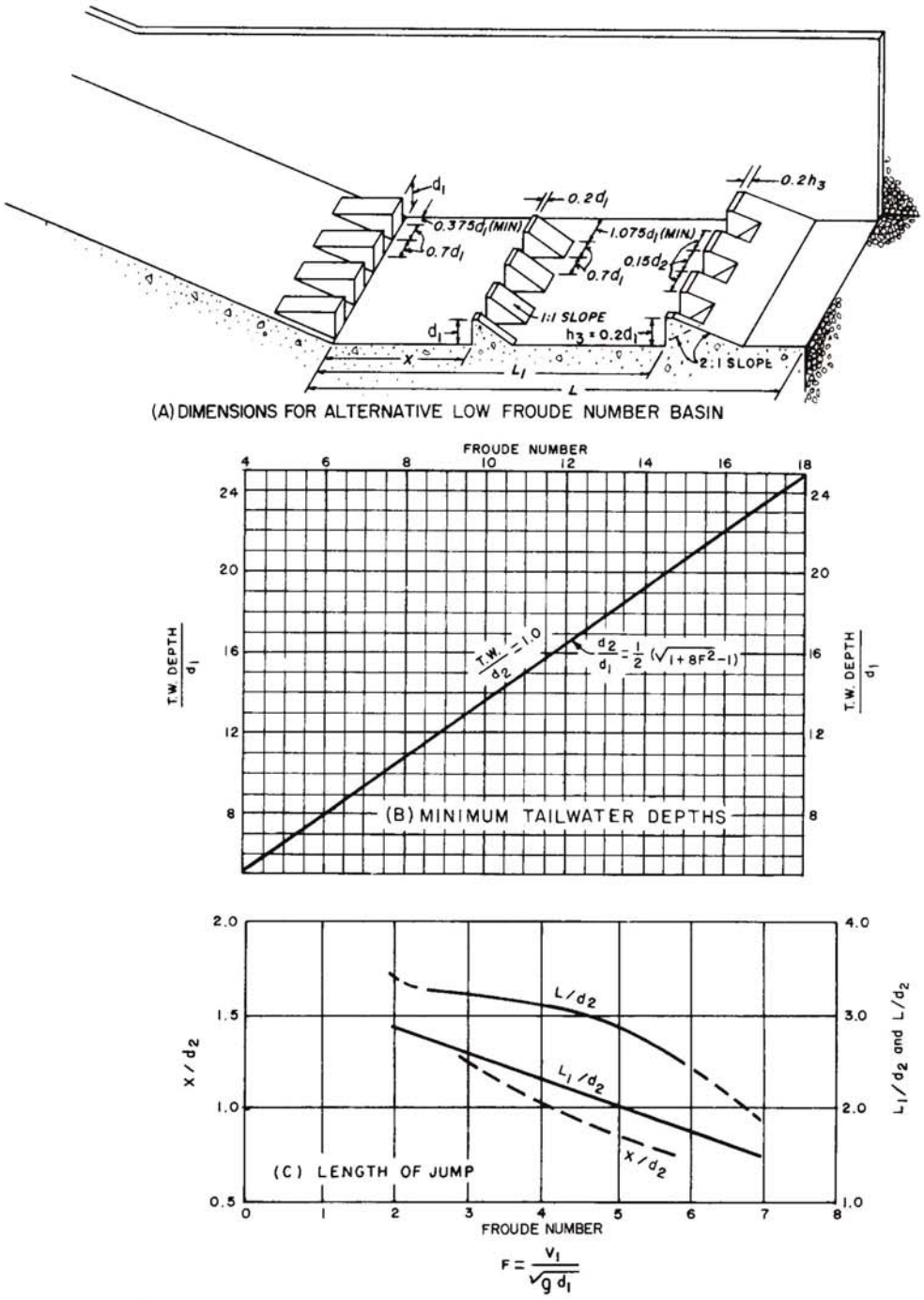


Figure 9-40.—Characteristics for alternative low Froude number stilling basins. 103–D–1876.

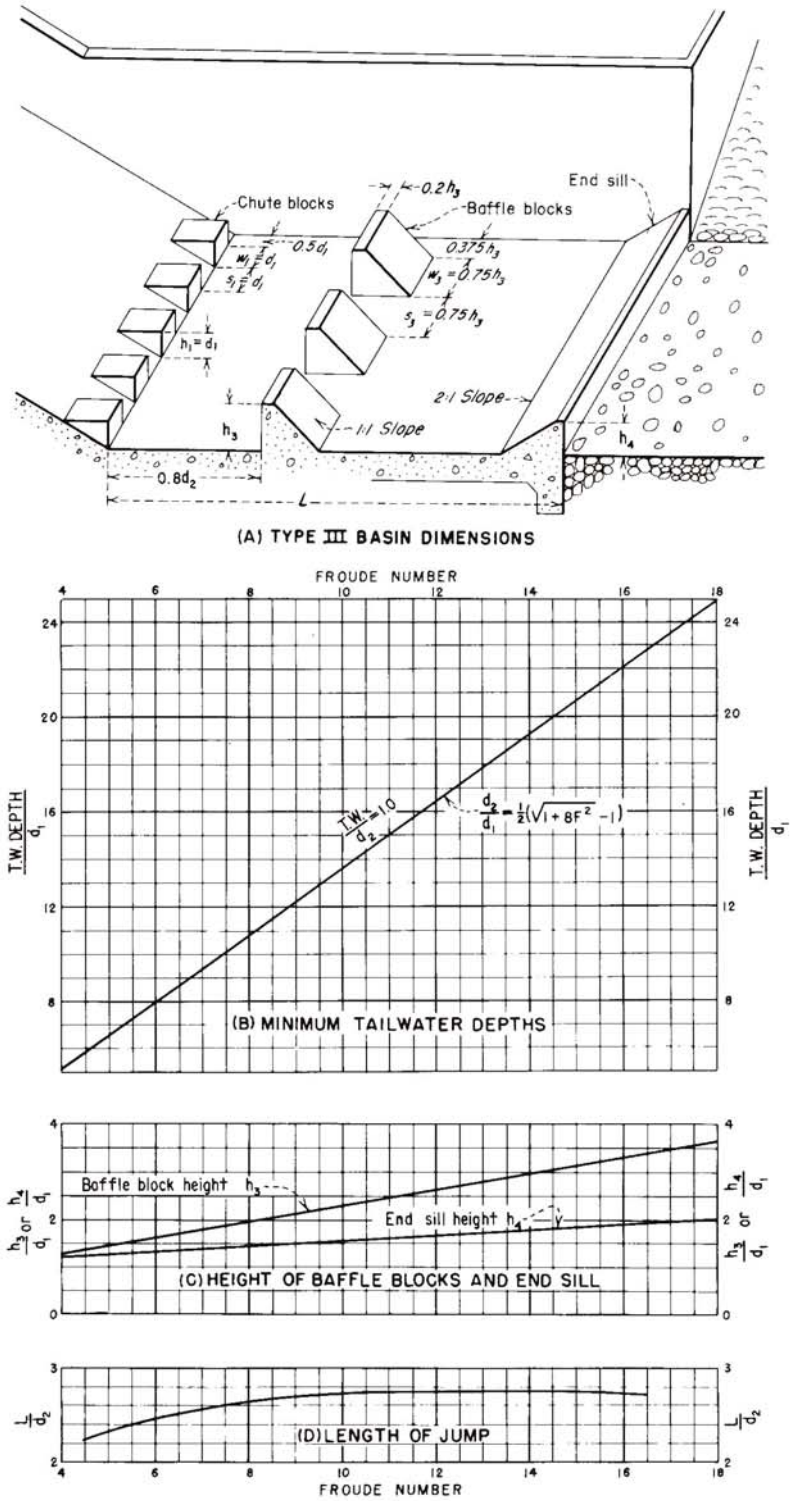


**Figure 9-41.—Stilling basin characteristics for Froude numbers above 4.5 where incoming velocity, $V_1 \leq 60$ ft/s. 288-D-2426.**

will further increase the total load. However, because the baffle blocks are placed a distance equal to $0.8d_2$ beyond the start of the jump, there will be some cushioning effect by the time the incoming jet reaches the blocks, and the force will be less than that indicated by the above equation. If the full force computed by equation (24) is used, the negative pressure force may be neglected.

Where incoming velocities exceed 60 ft/s, or where impact baffle blocks are not used, the type II basin (fig. 9-42) may be adopted. Because the dissipation is accomplished primarily by hydraulic-jump action, the basin length will be greater than that indicated for the type III basin. However, the chute blocks and dentated end sill will still effectively reduce the length. Because of the reduced margin of safety against sweepout, the water depth in the basin should be about 5 percent greater than the computed conjugate depth.

(c) *Rectangular Versus Trapezoidal Stilling Basin.*—The use of a trapezoidal stilling basin instead of a rectangular basin may often be proposed where economy favors sloped side lining over vertical wall construction. Model tests have shown, however, that the hydraulic-jump action in a trapezoidal basin is much less complete and less stable than it is in the rectangular basin. In a trapezoidal basin, the water in the triangular areas along the sides of the basin adjacent to the jump does not oppose the incoming high-velocity jet. The jump, which tends to occur vertically, cannot spread sufficiently to occupy the side areas. Consequently, the jump will form only in the central portion of the basin, while areas along the outside will be occupied by upstream-moving flows that ravel off the jump or come from the lower end of the basin. The eddy or horizontal roller action resulting from this phenomenon tends to interfere and interrupt the jump action to the extent that there is incomplete dissipation of the energy and severe scouring can occur beyond the basin. For good hydraulic performance, the sidewalls of a stilling basin should be vertical or as close to vertical as practicable.

(d) *Basin Depths Versus Hydraulic Heads.*—The nomograph on figure 9-43 can help determine approximate basin depths for various basin widths and for various differences between reservoir and tailwater levels. Plots are shown for the condition of no loss of head to the upstream end of the stilling basin, and for 10, 20, and 30 percent loss as scales A, B, C, and D, respectively. The required conjugate depths, $d_2$, will depend on the specific energy available at the entrance of the basin, as determined by the procedure discussed in section 9.18. Where the specific energy is known, the head loss in the channel upstream can be related to the velocity head, the percentage loss can be determined, and the approximate conjugate depth can be read for the nomograph. Where head losses have not been computed, a quick approximation of the head losses can be obtained from figure B-5. Where only a rough determination of basin depths is needed, the choice of the loss to be applied for various spillway designs may be generalized as follows:

(1) For a design of an overflow spillway where the basin is directly downstream from the crest, or where the chute is not longer than the hydraulic head, consider no loss of head.
(2) For a design of a channel spillway where the channel length is between one and five times the hydraulic head, consider 10 percent loss of head.
(3) For a design of a spillway where the channel length exceeds five times the hydraulic head, consider 20 percent loss of head.

The nomograph on figure 9-43 gives values of the conjugate depth of the hydraulic jump. Tailwater depths for the various types of basin described should be increased as noted earlier in this section.

(e) *Tailwater Considerations.*—Determination of the tailwater rating curve, which gives the stage-discharge relationship of the natural stream below the dam, is discussed in appendix B, part B. Tailwater rating curves for the regime of river below a dam are fixed by the natural conditions along the stream and ordinarily cannot be altered by the spillway design or by the release characteristics. As discussed in section 9.7(d), the retrogression or aggradation of the river below the dam, which will affect the ultimate stage-discharge conditions, must be recognized in selecting the tailwater rating curve to be used for stilling basin design. Usually, river flows that approach the maximum design discharges do not occur, and an estimate of the tailwater rating curve must either be extrapolated from known conditions or computed on a basis of assumed or empirical criteria. Thus, the tailwater rating curve is, at best, only approximate, and safety factors must be included in the design to compensate for variations in tailwater.

For a jump-type stilling basin, downstream water

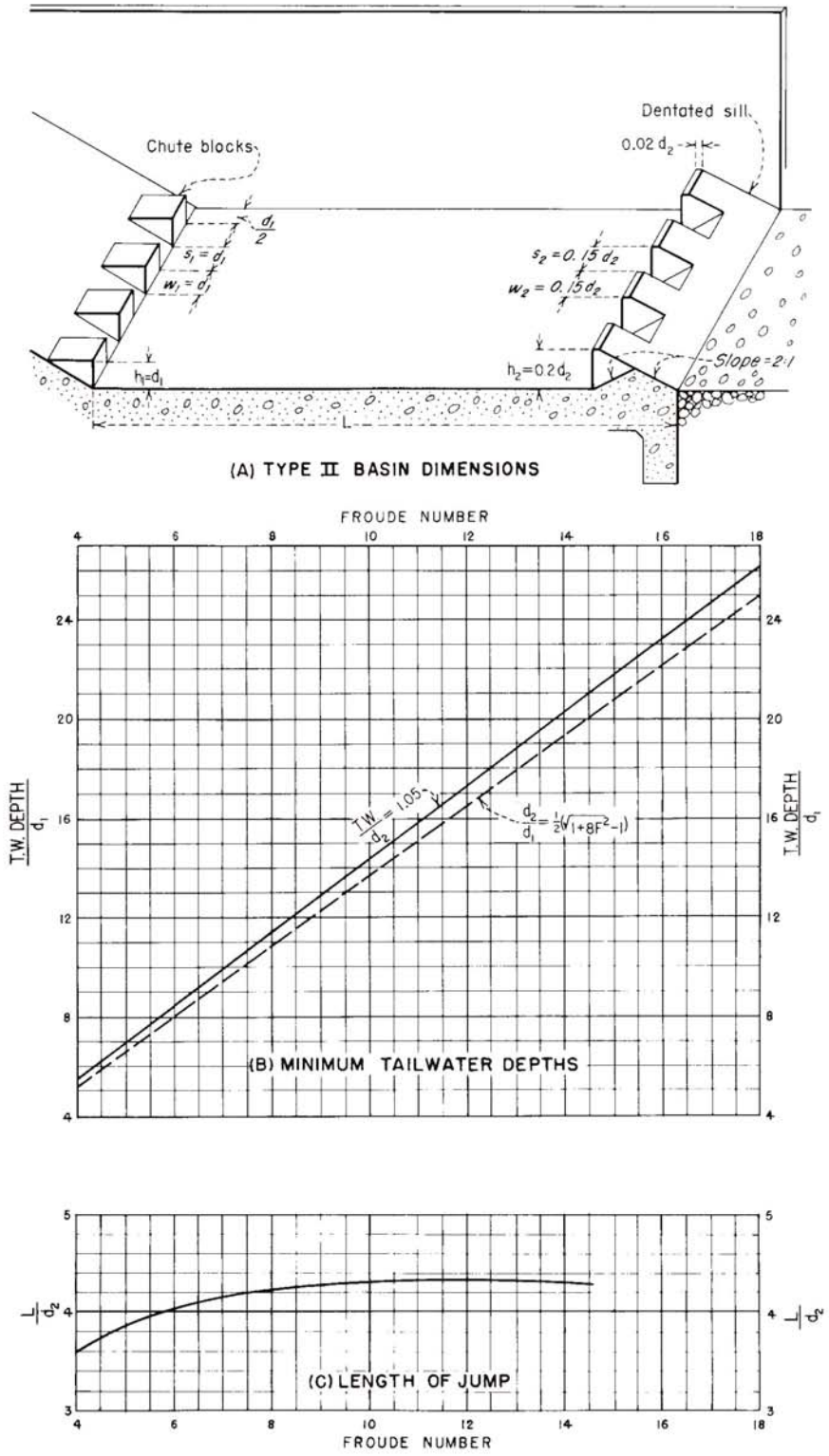


Figure 9-42.—Stilling basin characteristics for Froude numbers above 4.5. 288-D-2427.

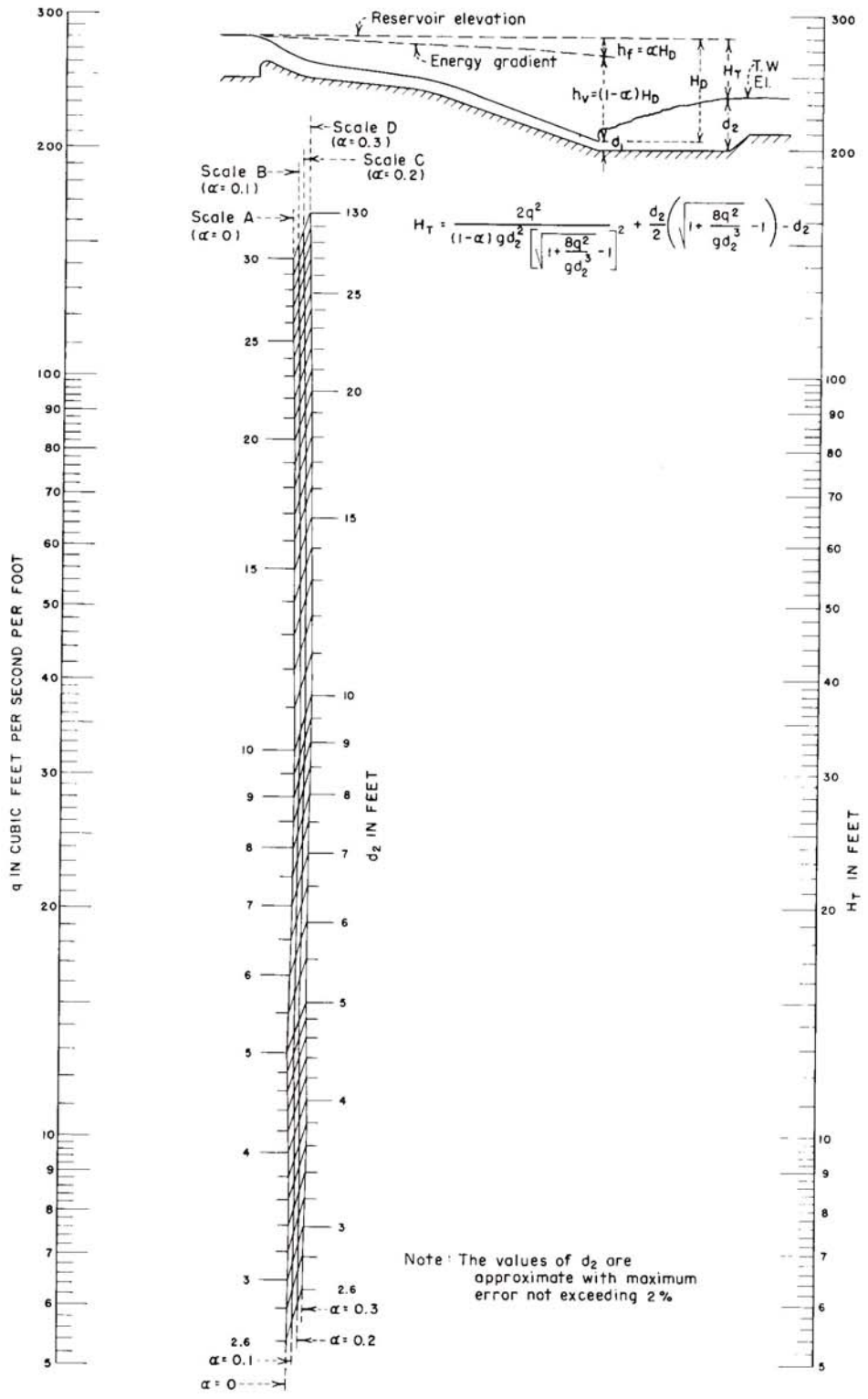


**Figure 9-43.—Stilling basin depths versus hydraulic heads for various channel losses. 288–D–2428.**

levels for various discharges must conform to the tailwater rating curve. The basin floor level must therefore be selected to provide jump depths that most nearly agree with the tailwater depths. For a given basin design, the tailwater depth for each discharge seldom corresponds to the conjugate depth needed to form a perfect jump. Thus, the relative shapes and relationships of the tailwater curve to the depth curve will determine the required minimum depth to the basin floor. This is shown on figure 9-44(A) where the tailwater rating curve is shown as curve 1, and a conjugate depth versus discharge curve for a basin of certain width is represented by curve 3. Because the basin must be deep enough to provide for full conjugate depth (or some greater depth to provide a safety factor) at the maximum spillway design discharge, the curves will intersect at point D. For lesser discharges the tailwater depth will be greater than the required conjugate depth, thus providing an excess of tailwater, which is conducive to the formation of a "drowned jump." (With the drowned jump condition, instead of achieving good jump-type dissipation by the intermingling of the upstream and downstream flows, the incoming jet plunges to the bottom and carries along the entire length of the basin floor at high velocity.) If the basin floor is higher than indicated by the position of curve 3 on figure 9-44, the depth curve and tailwater rating curve will intersect to the left of point D. This indicates an excess of tailwater for smaller discharges and a deficiency of tailwater for higher discharges.

As an alternative to the selected basin represented by curve 3, a wider basin might be considered for which conjugate depth curve 2 will apply. This design will provide a shallower basin, in which the ideal jump depths will more nearly match the tailwater depths for all discharges. The choice of basin widths, of course, involves consideration of economics, as well as of hydraulic performance.

Where a tailwater rating curve shaped similar to that represented by curve 4 on figure 9-44(B) is encountered, the level of the stilling basin floor must be determined for some discharge other than the maximum design capacity. If the tailwater curve intersects the required water surface elevation at the maximum design capacity, as in figure 9-44(A), there would be insufficient tailwater depth for most smaller discharges. In this case the basin floor elevation is selected so that there will be sufficient tailwater depth for all discharges. For a basin of

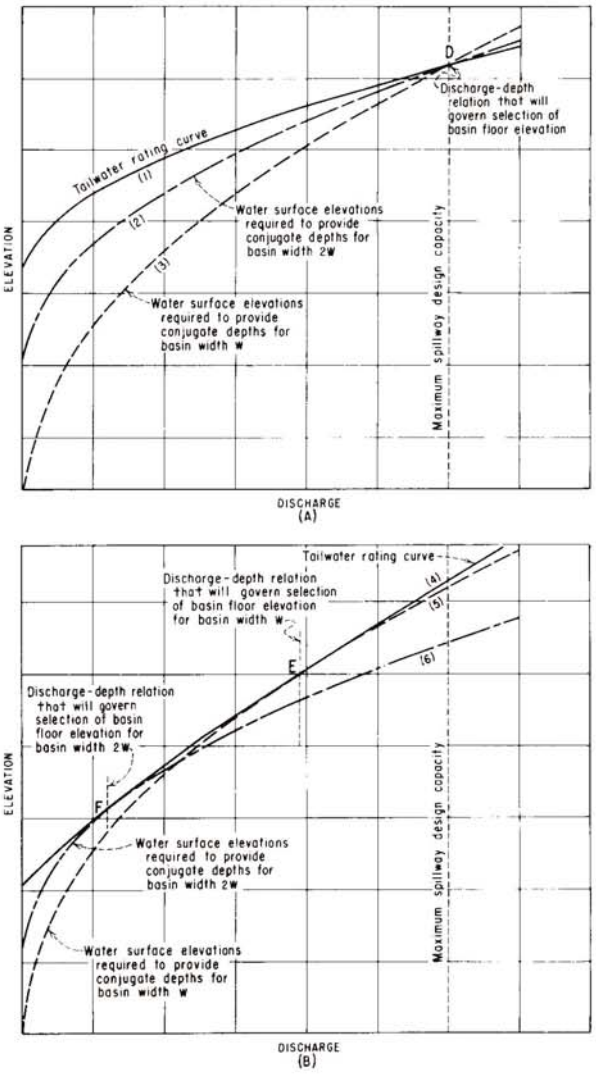


**Figure 9-44.—Relationships of conjugate depth curves to tailwater rating curves. 288–D–2429.**

width $W$, the floor level should be selected so that the two curves would coincide at the discharge represented by point E on the figure 9-44(B). For all other discharges the tailwater depth will be greater than that needed to form a satisfactory jump. Similarly, if a basin width of $2W$ were considered, the basin floor level would be selected so that curve 6 would intersect the tailwater curve at point F. Here also, the selection of basin widths should be based on economics as well as on hydraulic performance.

Where exact conjugate depth conditions for forming the jump cannot be attained, the relative desirability of having insufficient tailwater as com-

pared with having excessive tailwater should be considered. With insufficient tailwater the back pressure will be deficient and sweepout of the basin will occur. With an excess of tailwater the jump will be formed, and energy dissipation within the basin will be complete until the drowned-jump phenomenon becomes critical. Chute blocks, baffles, and end sills will also assist in energy dissipation, even with a drowned jump.

(f) *Stilling Basin Freeboard.*—Freeboard is ordinarily provided so that the stilling basin walls will not be overtopped by surges, splash and spray, and wave action set up by the turbulence of the jump. The surface roughness of the flow is related to the energy dissipated in the jump and to the depth of flow in the basin. The following empirical expression provides values that have proved satisfactory for most basins:

$$\text{Freeboard in feet} = 0.1(v_1 + d_2) \qquad (25)$$

**9.22. *Submerged Bucket Dissipators.***—When the tailwater depth is too great for the formation of a hydraulic jump, the high energy can be dissipated by the use of a submerged bucket deflector. The hydraulic behavior in this type of dissipator is manifested primarily by the formation of two rollers: one occurs on the surface, moves counterclockwise, and is contained within the region above the curved bucket; the other is a ground roller, moves clockwise, and is situated downstream from the bucket. The movements of these rollers, along with the intermingling of the incoming flows, effectively dissipate the high energy of the water and prevent excessive scouring downstream from the bucket.

Two types of roller buckets have been developed and model tested [15]. Their shape and dimensions are shown on figure 9-45. The general nature of the dissipating action for each type is represented on figure 9-46. The hydraulic actions of the two buckets have the same characteristics, but distinctive features of their flows differ to the extent that each has certain limitations. The high-velocity flow leaving the deflector lip of the solid bucket is directed upward (fig. 9-46(A)). This creates a high boil on the water surface and a violent ground roller moving clockwise downstream from the bucket. This ground roller continuously pulls loose material back towards the lip of the bucket and keeps some of the intermingling material in a constant state of agitation. The typical scour pattern that results from this action is shown on figure 9-47. The high-velocity jet leaves the lip of a slotted bucket at a flatter angle, and only a part of the high-velocity flow finds its way to the surface (fig. 9-46(B)). Thus, a less violent surface boil occurs, and there is a better dissipation of flow in the region above the ground roller. This results in less concentration of high-energy flow throughout the bucket and a smoother downstream flow.

Use of a solid bucket dissipator may be objectionable because of the abrasion on the concrete surfaces caused by material that is swept back along the lip of the deflector by the ground roller. In addition, the more turbulent surface roughness induced by the severe surface boil carries farther down the river, causing objectionable eddy currents that contribute to riverbank sloughing. Although the slotted bucket provides better energy dissipation with less severe surface and streambed disturbances, it is more sensitive to sweepout at lower tailwaters and is conducive to a diving and scouring action at excessive tailwaters. This is not the case with the solid bucket. Thus, the tailwater range that provides good performance with the slotted bucket is much narrower than that of the solid bucket. A

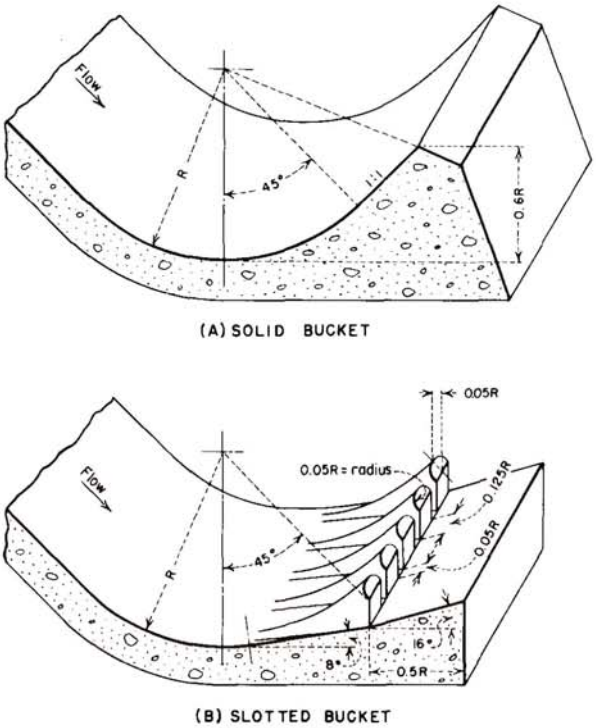


**Figure 9-45.—Submerged buckets. 288-D-2430.**

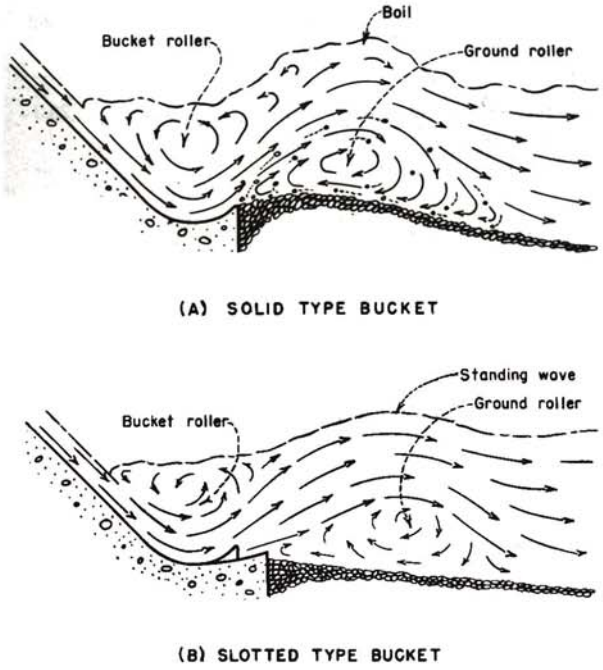


Figure 9-46.—Hydraulic action of solid and slotted buckets. 288–D–2431.

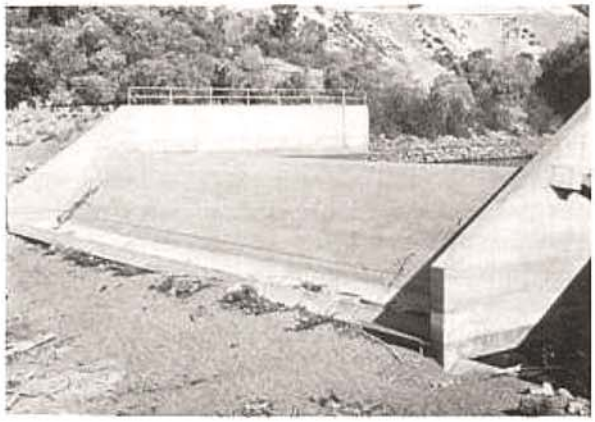

Figure 9-47.—Scour patterns downstream from a solid bucket dissipator for an ogee overflow crest. 288–D–2904.

solid bucket dissipator should not be used where the tailwater limitations of the slotted bucket can be met. Therefore, only the design of the slotted bucket will be discussed.

Flow characteristics of the slotted bucket are shown on figure 9-48. For deficient tailwater depths the incoming jet will sweep the surface roller out

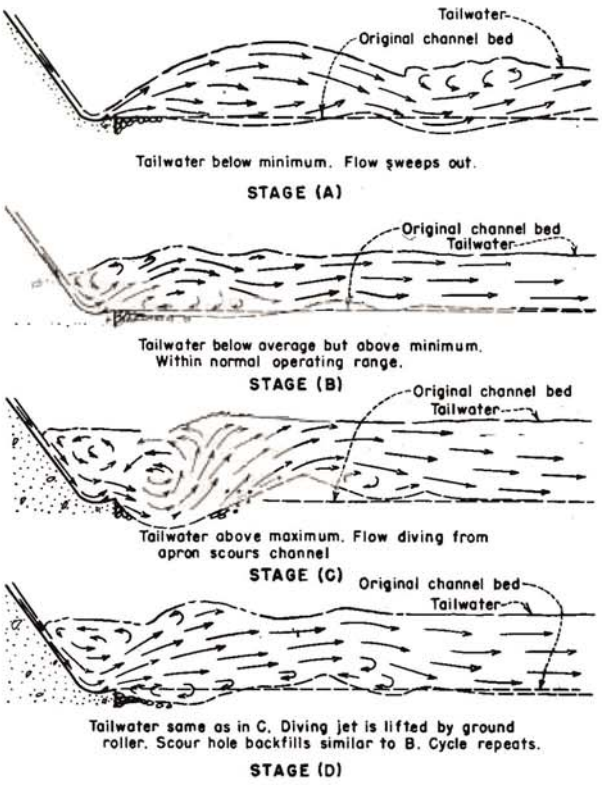


Figure 9-48.—Flow characteristics of a slotted bucket. 288–D–2432.

of the bucket and will produce a high-velocity flow downstream, both along the water surface and along the riverbed. This action is depicted as stage (A) on figure 9-48. As the tailwater depth is increased, there will be a depth at which instability of flow will occur, where sweepout and submergence will alternately prevail. To obtain continuous operation at the submerged stage, the minimum tailwater depth must be above this unstable state. Flow action within the acceptable operating stage is depicted as stage (B) on figure 9-48.

When the tailwater becomes excessively deep, the phenomenon called "diving flow" will occur. At this stage the jet issuing from the lip of the bucket will no longer rise and continue along the surface, but will intermittently become depressed and dive to the riverbed.

The position of the downstream roller will change with the change in position of the jet. It will occur at the surface when the jet dives and will form along the river bottom as a ground roller when the

jet rides the surface. Scour will occur in the streambed at the point of impingement when the jet dives, but will be filled in by the ground roller when the jet rides. The characteristic flow pattern for the diving stage is depicted in (C) and (D) of figure 9-48. Maximum tailwater depths must be limited to forestall the diving flow phenomenon.

The design of the slotted bucket involves determination of the radius of curvature of the bucket and the allowable range of tailwater depths. These criteria, as determined from experimental results, are plotted on figure 9-49 in relation to the Froude number. The Froude numbers are for flow at the point where the incoming jet enters the bucket. Symbols and criteria are defined on figure 9-50.

**9.23. *Examples of Designs of a Stilling Basin and an Alternative Submerged Bucket Dissipator.*—**The designs of a stilling basin and of a submerged bucket dissipator are best explained by examples. Consider that it is required to make comparative designs of a stilling basin and of a submerged bucket dissipator for an overflow dam whose maximum discharge is 2,000 ft³/s and whose controlling dimensions and tailwater conditions are shown on figure 9-51.

For a first trial design, assume a crest length of 20 feet. The criteria for different discharges are then as follows:

| | | | |
|---|---|---|---|
| Total discharge, Q, in cubic feet per second | 2,000 | 1,000 | 500 |
| Unit discharge, $q$, in cubic feet per second per foot | 100 | 50 | 25 |
| Assumed coefficient of discharge, $C$ | 3.9 | 3.7 | 3.5 |
| Head, in feet on crest, $H_e = (q/C)^{2/3}$ | 8.7 | 5.7 | 3.7 |
| Reservoir water level, elevation | 1008.7 | 1005.7 | 1003.7 |
| Tailwater level, elevation | 985.0 | 981.0 | 978.0 |
| Reservoir water level minus tailwater level, in feet | 23.7 | 24.7 | 25.7 |
| Velocity head at tailwater level, $h_{v_t}$, in feet (assuming no loss of specific energy) | 23.7 | 24.7 | 25.7 |
| Velocity of flow, in feet per second at tailwater level, $v_t = \sqrt{2gh_{v_t}}$ | 39.1 | 39.9 | 40.7 |
| Depth of flow, in feet, at tailwater level, $d_t = q/v_t$ | 2.56 | 1.25 | 0.61 |
| Froude number at tailwater level, $F_t = v_t/\sqrt{gd_t}$ | 4.3 | 6.3 | 9.2 |
| Specific energy at tailwater level, $d_t + h_{v_t}$ | 26.3 | 25.9 | 26.3 |

Table 9-4 shows computations for a hydraulic-jump basin design. Conjugate depths and the required apron elevation for the various discharges are calculated to determine the critical condition. The lowest apron elevation is for the 2,000-ft³/s discharge. The Froude number of 6.2 and the incoming velocity not exceeding 60 ft/s determine that the type III stilling basin shown on figure 9-41 should be used for this design. The basin length will be 42 feet and the apron elevation will be 968.3.

For the submerged slotted bucket design, the minimum bucket radius for the maximum discharge is determined by use of figure 9-49. For a Froude number at tailwater level $F_t = 4.3$, the minimum radius is $0.42(d_t + h_{v_t}) = (0.42)(26.3) = 11.0$ feet. In this instance the riverbed slopes up, and the use of figure 9-49 results in the following values for the maximum and minimum tailwater for $F_t = 4.3$ and $R/(d_t + h_{v_t}) = 0.42$:

$$T_{max} = 7.5d_t = (7.5)(2.56) = 19.2 \text{ feet}$$
$$T_{min} = 6.5d_t = (6.5)(2.56) = 16.6 \text{ feet}$$

An average tailwater depth of 18 feet will place the bucket invert at elevation 985.0 − 18.0 = 967.0. It is now necessary to check the radius and tailwater conditions for less than maximum flows to determine whether the design is satisfactory throughout the range of discharge.

For a unit discharge of 50 ft³/s and for $F_t = 6.3$, the minimum radius is $0.26(d_t + h_{v_t}) = 0.26(25.9) = 6.8$ feet. Therefore, the minimum radius of 11.0 feet determined for the maximum discharge will govern. The maximum and minimum tailwater values for $F_t = 6.3$ and $R/(d_t + h_{v_t}) = 11/25.9 = 0.42$ are:

$$T_{max} = 20.0d_t = 20.0(1.25) = 25.0 \text{ feet}$$
$$T_{min} = 10.1d_t = 10.1(1.25) = 12.6 \text{ feet}$$

The bucket invert level at elevation 967.0 as determined for the maximum discharge will provide a tailwater depth of 981.0 − 967.0 = 14 feet, which is within the safe limit for producing satisfactory roller action.

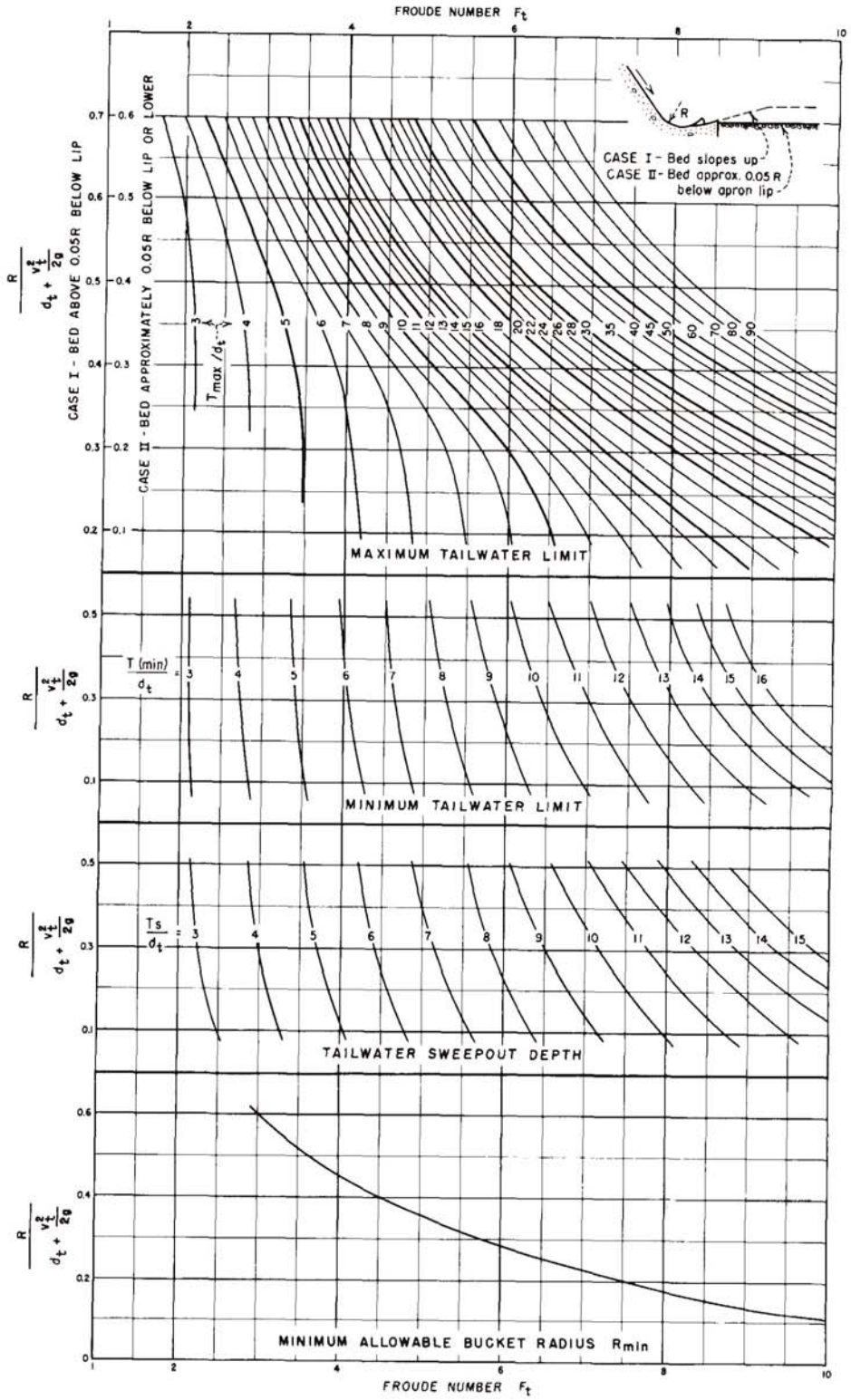


**Figure 9-49.—Limiting criteria for slotted bucket design. 288–D–2433.**

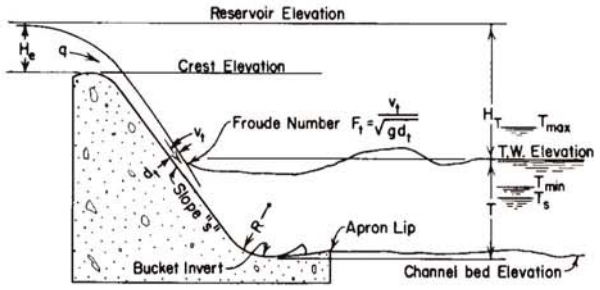


Figure 9-50.—Definition of symbols for submerged buckets. 288–D–2434.

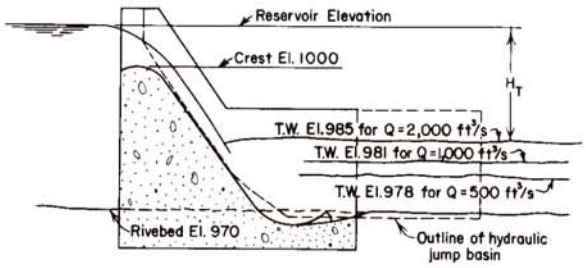


Figure 9-51.—Example of design of stilling device for overflow spillway. 288–D–2435.

Table 9-4.—Computations for hydraulic-jump basin design. For design example in section 9.23.

| Discharge, $Q$, ft³/s | Discharge per foot, $q$, ft³/s | Reservoir level minus tailwater, feet | Conjugate depth, $d_2$, feet[1] | Tailwater elevation, feet | Required apron elevation, feet | Specific energy, $H_E$, at upstream end of basin,[2] feet | Upstream depth of flow at basin floor level,[3] $d_1$, feet | Upstream velocity at basin floor level,[3] $v_1$ ft/s | Froude number,[4] $F_1$ |
|---|---|---|---|---|---|---|---|---|---|
| 2,000 | 100 | 23.7 | 16.7 | 985.0 | 968.3 | 40.4 | 2.01 | 49.8 | 6.2 |
| 1,000 | 50 | 24.7 | 11.8 | 981.0 | 969.2 | 36.5 | 1.05 | 47.6 | 8.1 |
| 500 | 25 | 25.7 | 8.6 | 978.0 | 969.4 | 34.3 | 0.54 | 46.3 | 11.1 |

[1]From figure 9-43, assuming no loss in specific energy.
[2]$H_E$ = Reservoir water surface minus apron elevation, assuming no loss in specific energy.
[3]$H_E = d_1 + (v_1^2/2g)$.
[4]$F_1 = v_1/\sqrt{gd}$.

The same procedure should be followed to verify that satisfactory roller action will result for a unit discharge of 25 ft³/s. In this case the minimum radius of 11.0 feet determined for the maximum discharge was found to govern. $T_{max}$ and $T_{min}$ were found to be 50 feet and 10.4 feet, respectively, compared with the 11 feet of tailwater depth provided by the invert elevation placed at 967.0 feet. It may now be considered that the design based on maximum discharges will be satisfactory for all lower discharges.

If a wider range of safe tailwater depths is desired, the radius of curvature of the bucket can be increased. Thus, for a bucket radius of 12 feet, for the maximum discharge, $T_{min} = 6.5d_t = 16.6$, and $T_{max} = 8.5\ d_t = 22.5$ feet. An average tailwater depth of 20 feet, placing the bucket invert at elevation 965.0, will provide more leeway for tailwater variations.

**9.24. *Plunge Basins.*—**When a free jet falls vertically into a pool in a riverbed, a plunge pool will be scoured to a depth that is related to the discharge, the height of the fall, the depth of tailwater, and the bed material [2]. The riverbed will be scoured as a result of the abrading action of the churning water and sediment in the pool. Ultimately, the scour will reach a limiting depth as the energy of the jet is no longer able to remove bed material from the scour hole. A simple empirical approximation of the ultimate scour depth is:

$$D = 1.32H^{0.225}q^{0.54} \qquad (26)$$

where:

$D$ = the ultimate scour depth below tailwater level, in feet,
$H$ = the elevation drop from reservoir to tailwater, in feet, and
$q$ = the unit discharge, in cubic feet per second per foot.

When a jet is issued from a structure in a more horizontal direction, a trapezoidal plunge pool may be used. Such a basin should be used only where the jet discharges into the air and then plunges

downward into the basin. Tests have shown that if the angle of impingement is less than about 25° above the horizontal, the jet will ride and skip across the surface at high velocity. This will cause waves and eddies in the basin sufficient to erode the side slopes, and there will be high exit velocities.

No fixed criteria have yet been established for plunge basins that will provide satisfactory dissipation for all heads, discharges, and incoming jet conditions. However, criteria established for several small outlet works plunge basins that have operated reasonably satisfactorily are presented only as a preliminary guide for approximate basin geometry (the general arrangement of this basin is shown on fig. 9-52): The basin depths were about one-fifth of the difference in elevation between maximum reservoir water surfaces and maximum tailwater levels. The minimum bottom widths were the width of the incoming jet or the width required to limit the average velocity at the end of the basin to about 3 ft/s, whichever was greater.

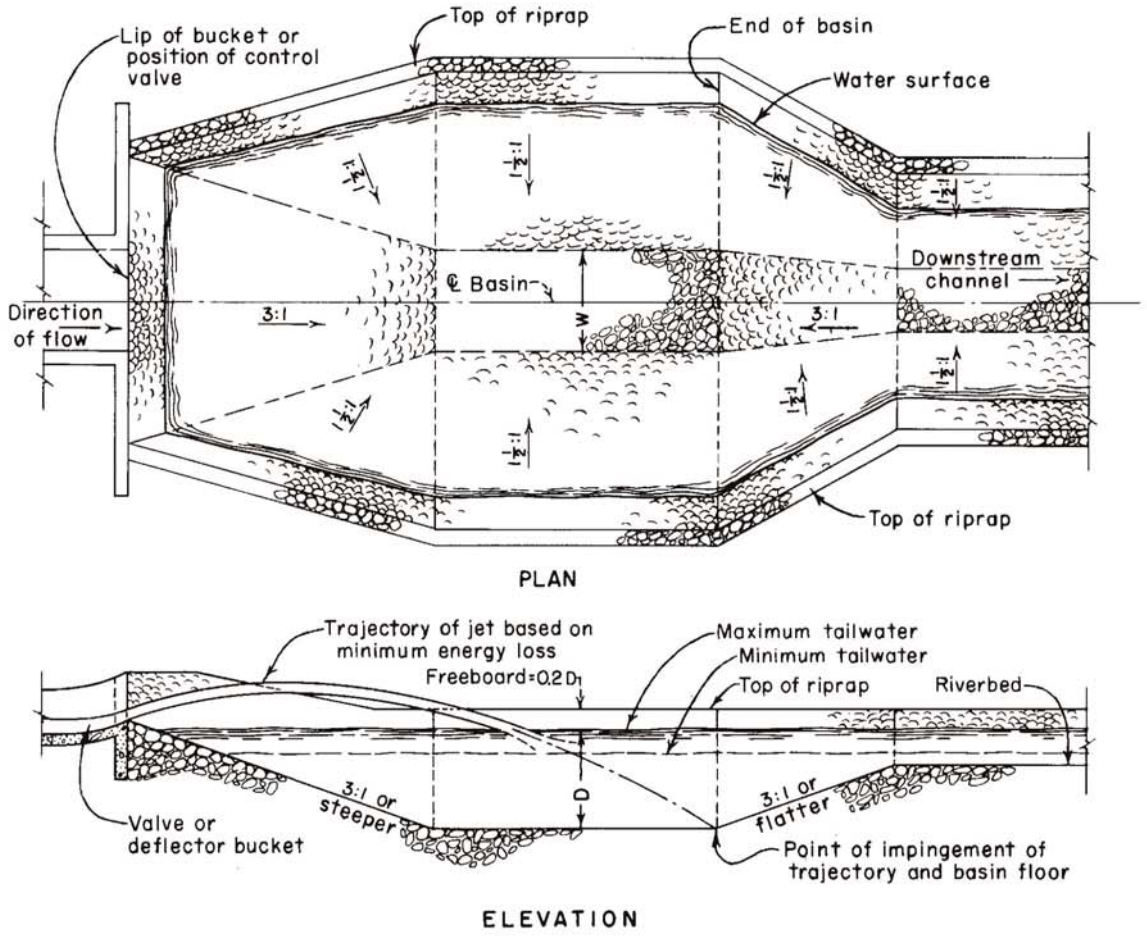


Figure 9-52.—Plunge basin energy dissipator. 288–D–2534.

## F. HYDRAULICS OF SPILLWAYS

**9.25. *Free Overfall (Straight Drop) Spillways.*—**(a) *General.*—The hydraulic problems of the free overfall spillway are concerned with the characteristics of the control and with the dissipation of flow in the downstream basin. Flow over the control ordinarily is free discharging; air is admitted to the underside of the nappe to avoid depression of the jet by reduced underneath pres-

sure. The flow in the downstream basin may be dissipated by the hydraulic jump, by impact and turbulence induced in a basin with impact blocks, or by a slotted grating dissipator installed immediately downstream from the control.

The control may be either sharp-crested to provide a fully contracted vertical jet, broad-crested to effect a fully suppressed jet, or shaped to increase the crest efficiency. Discharge coefficients will approximate those indicated in section 9.12. The sides of the control usually are arranged to allow full-side contraction to provide side space for the access of air to the underside of the nappe. This contraction is effected by providing square abutment headwalls or by installing square-cornered vertical offsets along the piers or walls opposite the crest. The effective length of the crest is then determined according to equation (4) where both $K_p$ and $K_a$ are approximately 0.20.

The dimensions of the stilling basin for the free overfall spillway can be related to two independent variables: the drop distance, $Y$, and the unit discharge, $q$. These variables, which are dimensional terms, can be expressed in a dimensionless ratio by expressing $q$ in lineal form by means of the equation for critical depth, $d_c = \sqrt[3]{q^2/g}$; dividing by $Y$: $d_c/Y = \sqrt[3]{q^2/gY^3}$. From this expression it can be seen that $q^2/gY^3$ is a dimensionless ratio that can be used as an independent variable to which the individual dimensions may be related. This ratio is called the "drop number" and is designated $\overline{D}$. It can be shown that $\overline{D}$ is the product of $F_1^2$ and $(D_1/Y)^3$, where the Froude number $F_1 = v_1/\sqrt{d_1 g}$ at the point where the nappe meets the basin floor.

(b) *Hydraulic-Jump Basins.*—The jump characteristics of the straight drop basin are basically the same as those for other jump basins, except that the position of the start of the jump cannot be determined as readily. On figure 9-53, the point of the start of the jump (point $X$) will vary with the vertical drop distance and is influenced by the upper nappe pool depth, $d_f$. The basin design downstream from point $X$ will be patterned after the designs discussed in section 9.21, once distance $L_d$ is determined. Values of the depth $d_1$, and of the Froude number, $F_1$, at the start of the jump in relation to the drop number, $\overline{D}$, are shown on figure 9-53. These relations may be used for determining the basin dimensions.

Where tailwater depths are greater than the conjugate depth $d_2$, the jump will move back on the free-falling nappe, raising the depth $d_f$ of the undernappe pool. With greater depths of the undernappe pool, the nappe will not plunge immediately to the floor of the basin, but will be deflected upward along the top of the underpool so that it will meet the floor to the right of point $X$. The distance to the start of the jump, $L_d$, will become progressively longer as the tailwater depth is increased. Average values of $L_d$ in relation to $h_d/H_e$, as determined from tests, are plotted on figure 9-53. For a basin with excessive depth, the type III basin discussed in section 9.21 is most adaptable. The impact block type basin, discussed below, also can be adopted for low drop spillways with excessive tailwater depths.

(c) *Impact Block Type Basins.*—An impact block basin that has been developed [4] for low heads dissipates energy reasonably well for a wide range of tailwater depths. The high energy is principally dissipated by turbulence induced by the impingement of the incoming flow on the impact blocks. The required tailwater depths, therefore, become more or less independent of the drop height. The linear proportions are as follows:

Minimum basin length $L_B = L_p + 2.55d_c$
Minimum length to upstream face of baffle block $= L_p + 0.8d_c$
Minimum tailwater depth $d_{tw} = 2.15d_c$
Optimum baffle block height $= 0.8d_c$
Width and spacing of baffle blocks $= \pm 0.4d_c$
Optimum height of end sill $= 0.4d_c$

(d) *Slotted-Grating Dissipators.*—An effective dissipator for small drops is shown on figure 9-54. This device has been tested for values of the Froude number, $F_1$, as determined at basin apron level, in the range of 2.5 to 4.5. For this arrangement the overfalling sheet is separated into a number of long, thin segments that fall nearly vertically into the basin below, where the energy is dissipated by turbulence. To be effective, the length of the grating, $L_G$, must be such that the entire incoming flow falls through the slots before reaching the downstream end. The length is therefore a function of the total discharge, the velocity of the incoming flow, and the area of the grating slots. Experimental tests indicate that the following relation gives an effective design:

$$L_G = \frac{Q}{0.245wN\sqrt{2gH_e}} \qquad (27)$$

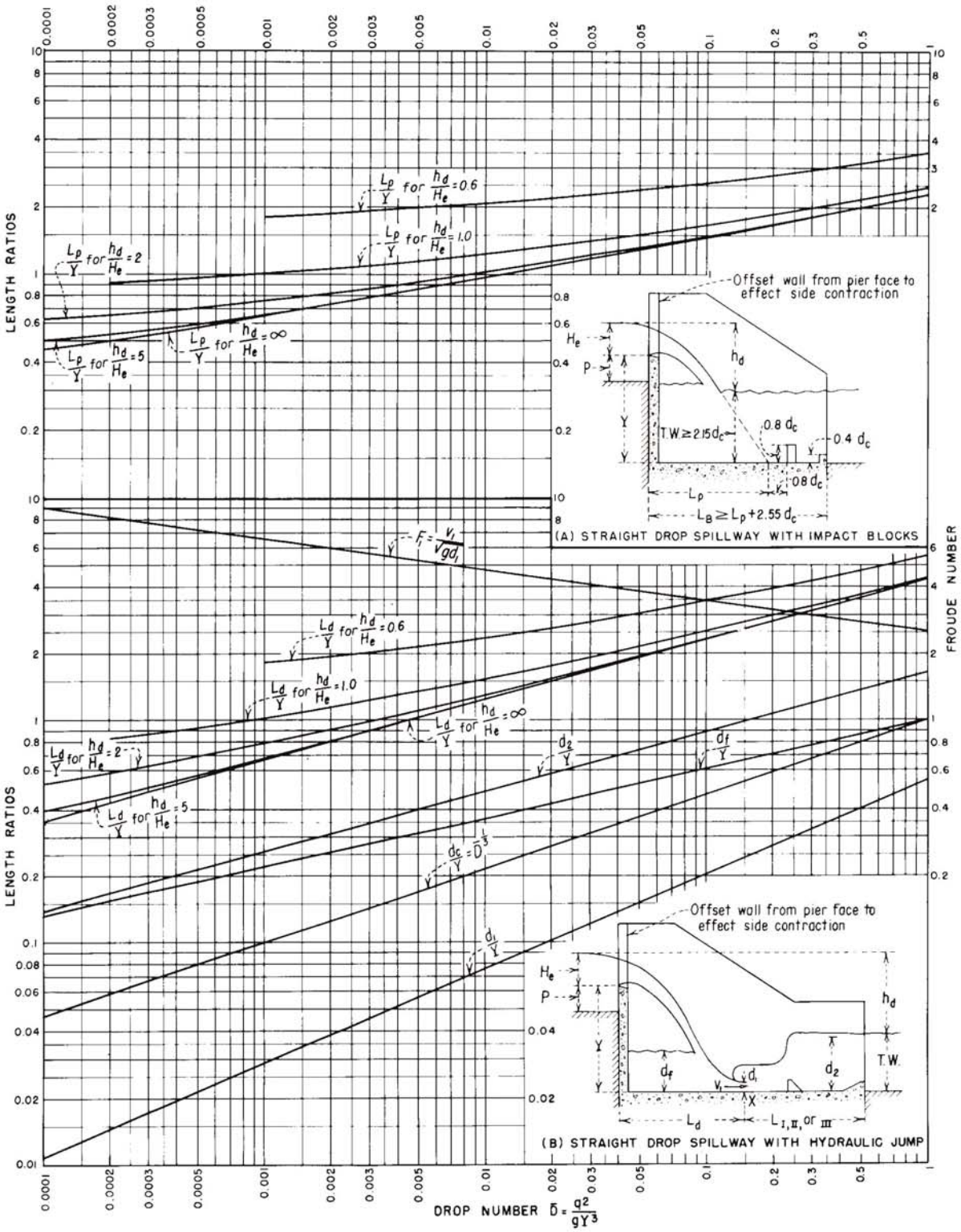


**Figure 9-53.—Hydraulic characteristics of straight drop spillways with hydraulic jump or with impact blocks. 288-D-2437.**

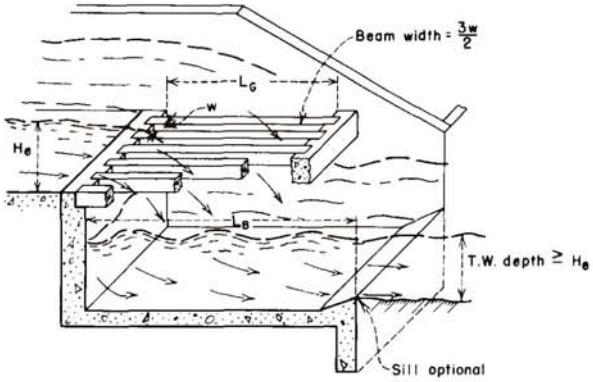


Figure 9-54.—Slotted-grating dissipator. 288–D–2438.

where:

$L_G$ = the length of the grating, in feet,
$w$ = the width of the slot, in feet,
$N$ = the number of slots, and
$H_e$ = the depth of flow upstream from the drop.

The length of the basin, $L_B$, should be approximately $1.2L_G$. An end sill similar to that for basin type I, discussed in section 9.21, may be provided to improve the hydraulic action.

(e) *Example of Design of a Free Overfall Spillway.*—The procedure for designing a free overfall spillway is best shown by means of an example. Consider that such a spillway must be designed to discharge 500 ft³/s. The drop from the spillway crest to the tailwater level for a flow of 500 ft³/s is 12 feet. The tailwater elevation is 108.0. The approach channel is 20 feet long, and the approach floor is level with the spillway crest, which is at elevation 120.0. Each type of energy dissipator is to be investigated.

The procedure for designing a hydraulic-jump basin is as follows: First, assume the effective length of the spillway crest is 15 feet and that $C$ is approximately 3.0. The unit discharge $q = 500/15 = 33.3$ ft³/s and $H_e = (q/C)^{2/3} = (33.3/3.0)^{2/3} = 5.0$ feet. The reservoir water surface elevation, therefore, is 120.0 + 5.0 = 125.0. Therefore, the drop from reservoir level to tailwater level will be approximately 17 feet.

Assume that an offset of 0.5 foot is provided along each side of the weir to effect side contractions for aerating the underside of the sheet, and that the offset is square-cornered. Then the net crest length, which will also be the stilling basin width, is $L' = L+2K_aH_e+2(0.5) = 15+2(0.2)(5)+1.0 = 18.0$ feet.

The nomograph on figure 9-43 is used to determine the approximate apron level of the jump basin, assuming the effective width of the basin is 15 feet and (for the first trial) that there will be no loss of energy between the reservoir and the point where the jet strikes the basin floor. From scale A, the conjugate depth $d_2 = 8.8$ feet for $q = 33.3$ ft³/s and $H_T = 17$ feet. This places the apron floor at elevation 99.2. The drop distance $Y = 120-99.2 = 70.8$ feet, and drop number $\overline{D} = q^2/gY^3 = 33.3^2/32.2(20.8)^3 = 0.0038$. From the figure 9-53, for $\overline{D} = 0.0038$, $d_2/Y = 0.375$, and $d_2 = 7.8$ feet. The apron level then must be adjusted to an elevation that is $d_2$ below the tailwater elevation 108.0, or elevation 100.2.

For the second trial, the adjusted value of $Y$ is 19.8, and $\overline{D} = 33.3^2/32.2\ (19.8)^3 = 0.0044$. From figure 9-53, for $\overline{D} = 0.0044$ and $h_d/H_e = 17/5 = 3.4$, $L_d/Y = 1.02$, and $L_d = 20.2$ feet, $d_1 = 1.1$ feet, and $F_1 = 5.3$.

With $F_1 = 5.3$, $d_1 = 1.1$, and $d_2 = 7.8$, the type III basin arrangement, shown on figure 9-41, can be used. From figure 9-41, $L/d^2 = 2.37$, and $L = 18.5$ feet. The length of the basin measured from the vertical crest is equal to $L_d+L = 20.2+18.5 = 38.7$ feet. The distance of the baffle blocks from the vertical crest for this basin will be 20.2 feet + $0.8d_2$ = 20.2 + 0.8(7.8) = 26.4 feet, approximately.

The baffle blocks will be approximately $1.5d_1$, or 1.6 feet, high and will be about 14 inches wide and spaced at about 28-inch centers.

For the impact block basin, the procedure is as follows: The critical depth $d_c = \sqrt[3]{33.3^3/32.2} = 3.3$ feet. Then from figure 9-53, for $\overline{D} = 0.0044$ and $h_d/H_e = 3.4$, $L_p/Y = 0.85$, and $L_p = 17.0$ feet. The minimum length of the basin $L_B = L_P + 2.55d_c = 17.0 + 2.55(3.3) = 25.4$ feet, say 26 feet. The minimum tailwater depth of $2.15d_c = 7.1$ feet, which places the basin floor at elevation 100.9. The distance from the vertical crest to the baffle blocks will be $L + 0.8d_c = 17.0 + 0.8(3.3) = 19.6$ feet, say 20 feet. The baffle blocks will be about $0.8d_c = 3.0$ feet high and about 18 inches wide, spaced at about 3-foot centers. The end sill will be $0.4d_c = 1.5$ feet high.

It can be seen from the above result that an impact block basin can be almost 13 feet shorter than a hydraulic-jump basin, and that the impact block basin will be 0.7 foot shallower. The baffle blocks

for the hydraulic-jump basin will be smaller and spaced closer together than those for the impact block basin.

This example shows that the impact block basin is considerably smaller than the hydraulic-jump basin. However, the impact block basin should be limited to uses where the drop distance does not exceed 20 feet. Furthermore, as previously explained, the foundation for an impact block basin must be of better quality because of the concentrated forces involved. The hydraulic-jump basin, therefore, has a much wider application.

The slotted-grating dissipator is not suitable in this case because the Froude number of 5.3 is greater than 4.5, which is the tested limit for a practical slotted-grating design.

**9.26. *Drop Inlet (Shaft or Morning Glory) Spillways.*** —(a) *General Characteristics.*—Typical floor conditions and discharge characteristics of a drop inlet spillway are shown on figure 9-55. The discharge curve shows that crest control (condition 1) will prevail for heads between the ordinates of *a* and *g*; orifice or tube control (condition 2) will govern for heads between the ordinates of *g* and *h*; and the spillway conduit will flow full for heads above the ordinate of *h* (condition 3).

The flow characteristics of a drop inlet spillway vary according to the proportional sizes of the different elements. Changing the diameter of the crest will change the curve *ab* on figure 9-55 so that the ordinate of *g* on curve *cd* will be either higher or lower. For a larger diameter crest, greater outflows can be discharged over the weir at low heads, the transition will fill up, and tube control will occur with a lesser head on the crest. Similarly, by altering the size of the throat of the tube, the position of curve *cd* will change, indicating the heads above which tube control will prevail. If the transition is made of such size that curve *cd* is moved to coincide with or lie to the right of point *j*, the control will shift directly from the crest to the downstream end of the conduit. The details of the hydraulic flow characteristics are discussed in the following subsections.

(b) *Crest Discharge.*—For small heads, flow over the drop inlet spillway is governed by the characteristics of crest discharge. The vertical transition beyond the crest will flow partly full and the flow will cling to the sides of the shaft. As the discharge over the crest increases, the overflowing annular nappe will become thicker and, eventually, the nappe flow will converge into a solid vertical jet. The point where the annular nappe joins the solid jet is called the crotch. After the solid jet forms, a "boil" will occupy the region above the crotch; both the crotch and the top of the boil become progressively higher with large discharges. For high heads the crotch and boil may almost flood out, showing only a slight depression and eddy at the surface.

Until the nappe converges to form a solid jet, free-discharging weir flow prevails. After the crotch and boil form, submergence begins to affect the weir flow and, ultimately, the crest will drown out. Flow is then governed either by the contracted jet formed by the overflow entrance, or by the shape and size of the vertical transition if it does not conform to the jet shape. Vortex action must be minimized to maintain converging flow into the drop inlet. Guide piers are often installed along the crest for this purpose [13, 14].

If the crest profile and transition conform to the shape of the lower nappe of a jet flowing over a sharp-crested circular weir, the discharge for flow over the crest and through the transition can be expressed as $Q = CLH^{3/2}$ (see eq. (3)); where $H$ is the head measured either to the apex of the undernappe of the overflow, to the spring point of the circular sharp-crested weir, or to some other established point on the overflow. Similarly, the choice of the length, $L$, is related to some specific point of measurement such as the length of the circle at the apex, along the periphery at the upstream face of the crest, or along some other chosen reference line. $C$ will change with different definitions of $L$ and $H$. If $L$ is taken at the outside periphery of the overflow crest (the origin of the coordinates on figure 9-56) and if the head is measured to the apex of the overflow shape, equation (3) can be written:

$$Q = C_o(2\pi R_s)H_o^{3/2} \qquad (28)$$

It is apparent that the discharge coefficient for a circular crest differs from that for a straight crest because of the effects of submergence and back pressure incident to the joining of the converging flows. Thus, $C_o$ must be related to both $H_o$ and $R_s$, and can be expressed in terms of $H_o/R_s$. The relationship of $C_o$, as determined from model tests [24], to $H_o/R_s$ for three conditions of approach depth is plotted on figure 9-57. These coefficients are valid only if the crest profile and transition shape conform to that of the jet flowing over a

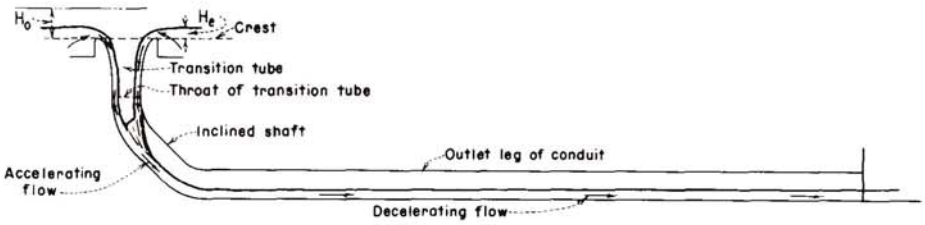


CONDITION 1. CREST CONTROL

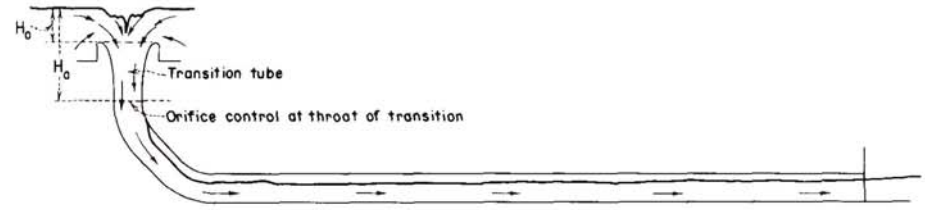


CONDITION 2. TUBE OR ORIFICE CONTROL

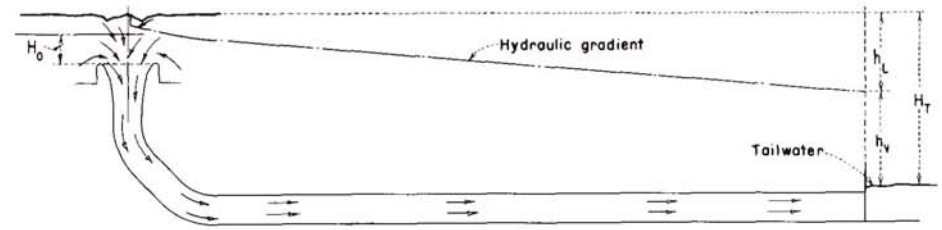


CONDITION 3. FULL PIPE FLOW

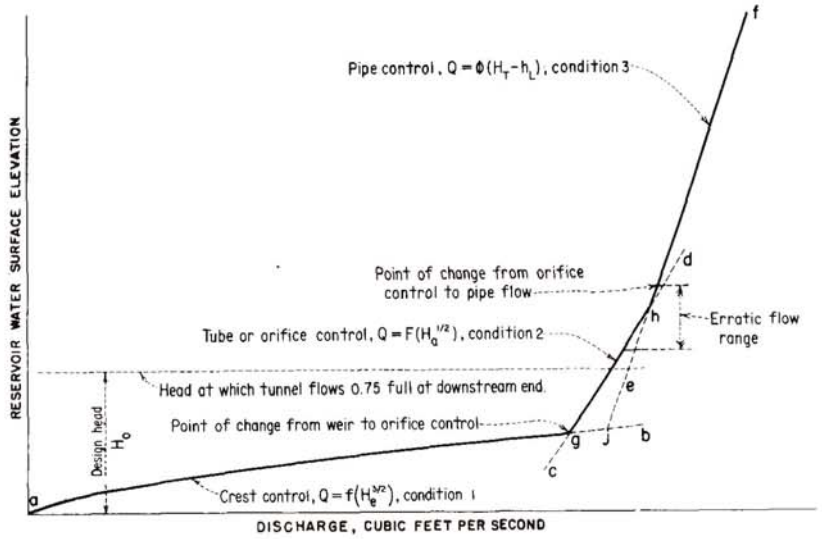


**Figure 9-55.—Nature of flow and discharge characteristics of a morning glory spillway. 288-D-2439.**

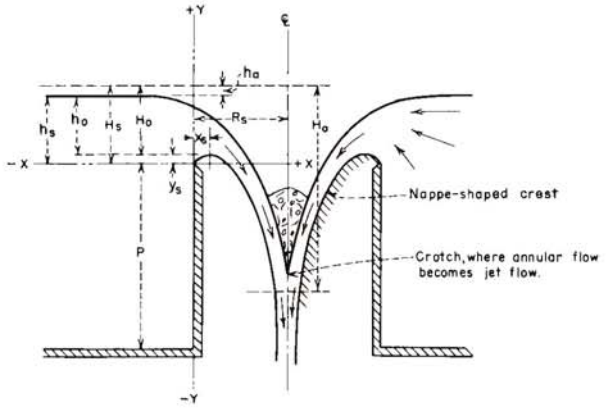


**Figure 9-56.—Elements of nappe-shaped profile for circular weir. 288-D-2440.**

sharp-crested circular weir at $H_o$ head and if aeration is provided so that subatmospheric pressures do not exist along the lower nappe surface contact.

When the crest outline and transition shape conform to the profile of the nappe shape for an $H_o$ head over the crest, free flow prevails for $H_o/R_s$ up to approximately 0.45, and weir control governs. As $H_o/R_s$ increases above 0.45, the weir partly submerges, and flow showing characteristics of a submerged weir is the controlling condition. When the $H_o/R_s$ ratio approaches 1.0, the water surface above the weir is completely submerged. For this and higher stages of $H_o/R_s$, the flow phenomenon is that of orifice flow. The weir formula, $Q = CLH^{3/2}$, is used as the measure of flow through the drop inlet entrance regardless of the submergence, by using a coefficient that reflects the flow conditions through the various $H_o/R_s$ ranges. Thus, from figure 9-57 it can be seen that the weir coefficient only changes slightly from that normally indicated for $H_o/R_s < 0.45$, but reduces rapidly for the higher $H_o/R_s$ values.

It should be noted that for most conditions of flow over a circular weir, the discharge coefficient increases with a reduction in the approach depth; whereas, the opposite is true for a straight weir. For both weirs, a shallower approach lessens the upward vertical velocity component and, consequently, suppresses the contraction of the nappe. However, for the circular weir, the submergence effect is reduced because of a depressed upper nappe surface, giving the jet a quicker downward impetus, which lowers the position of the crotch and increases the discharge.

Discharge coefficients for partial heads of $H_e$ on the crest can be determined from figure 9-58 to prepare a discharge-head relationship. The designer must be cautious in applying the above criteria because subatmospheric pressure or submergence effects may alter the flow conditions differently for various profile shapes. This criteria, therefore, should not be applied for flow conditions where $H_e/R_s > 0.4$.

(c) *Crest Profiles.*—Values of coordinates that define the shape of the lower surface of a nappe flowing over an aerated sharp-crested circular weir for various conditions of $P/R_s$ and $H_s/R_s$ are shown in tables 9-5, 9-6, and 9-7. These data are based on experimental tests [24] conducted by the Bureau of Reclamation. The relationships of $H_s$ to $H_o$ are shown on figure 9-59. Typical upper and lower nappe profiles for various values of $H_s/R_s$ are plotted on figure 9-60 in terms of $X/H_s$ and $Y/H_s$ for the condition of $P/R_s = 2.0$.

Figure 9-61 shows typical lower nappe profiles, plotted for various values of $H_s$ for a given value of $R_s$. In contrast to the straight weir where the nappe springs farther from the crest as the head increases, it can be seen from figure 9-61 that the lower nappe profile for the circular crest springs farther only in the region of the high point of the trace, and then only for $H_s/R_s$ values up to about 0.5.

The profiles become increasingly suppressed for larger $H_s/R_s$ values. Below the high point of the profile, the traces cross and the shapes for the higher heads fall inside those for the lower heads. Thus, if the crest profile is designed for heads where $H_s/R_s$ exceeds about 0.25 to 0.3, it appears that subatmospheric pressure will occur along some portion for the profile when heads are less than the designed maximum. If subatmospheric pressures are to be avoided along the crest profile, the crest shape selected should give support to the overflow nappe for the smaller $H_s/R_s$ ratios. Figure 9-62 shows the approximate increase in radius required to minimize subatmospheric pressures on the crest. The crest shape for the enlarged crest radius is then based on $H'_s/R'_s = 0.3$.

(d) *Transition Design.*—The diameter of a jet issuing from a horizontal orifice can be determined for any point below the water surface if it is assumed that the continuity equation, $Q = av$, is valid and if friction and other losses are neglected.

For a circular jet the area is equal to $\pi R^2$. The discharge is equal to $av = \pi R^2\sqrt{2gH_a}$. Solving for $R$,

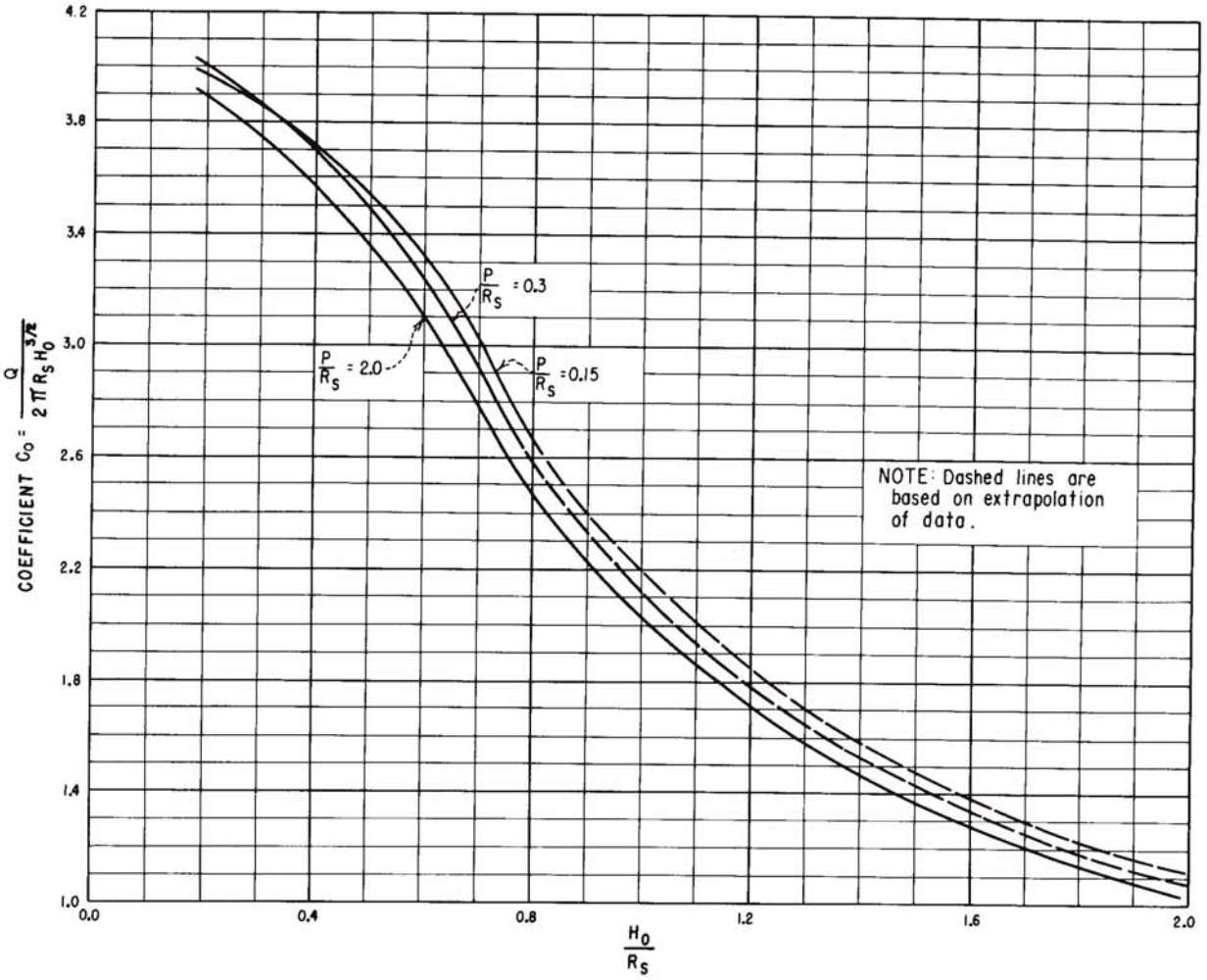


**Figure 9-57.—Relationship of circular crest coefficient $C_o$ to $H_o/R_s$ for different approach depths (aerated nappe). 288–D–2441.**

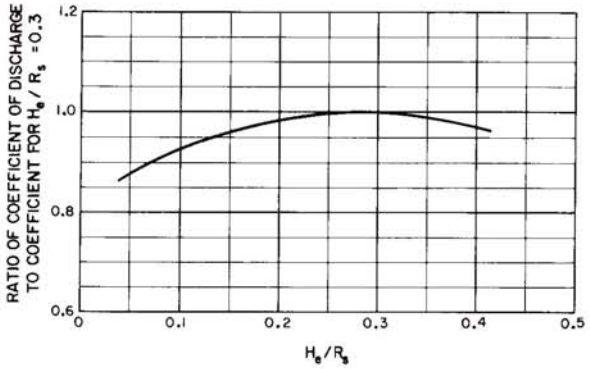


**Figure 9-58.—Circular crest discharge coefficient for other than design head. 288–D–2442.**

$R = Q_a^{1/2}/5H_a^{1/4}$; where $H_a$ is equal to the distance between the water surface and the elevation under consideration. The diameter of the jet thus decreases with the distance of the free vertical fall for normal design applications.

If an assumed total loss (including jet contraction losses, friction losses, velocity losses from direction changes, etc.) is taken as 0.1 $H_a$, the equation for determining the approximate required shaft radius may be written:

$$R = 0.204 \frac{Q_a^{1/2}}{H_a^{1/4}} \qquad (29)$$

Because this equation is for the shape of the jet,

Table 9-5.—Coordinates of lower nappe surface for different values of $H_s/R_s$ when $P/R_s$ = 2.0.

[Negligible approach velocity and aerated nappe]

| $H_s/R_s$ | 0.00 | 0.10* | 0.20 | 0.25 | 0.30 | 0.35 | 0.40 | 0.45 | 0.50 | 0.60 | 0.80 | 1.00 | 1.20 | 1.50 | 2.00 |
|---|---|---|---|---|---|---|---|---|---|---|---|---|---|---|---|
| $X/H_s$ | $Y/H_s$ for portion of profile above weir crest | | | | | | | | | | | | | | |
| 0.000 | 0.0000 | 0.0000 | 0.0000 | 0.0000 | 0.0000 | 0.0000 | 0.0000 | 0.0000 | 0.0000 | 0.0000 | 0.0000 | 0.0000 | 0.0000 | 0.0000 | 0.0000 |
| .010 | .0150 | .0145 | .0133 | .0130 | .0128 | .0125 | .0122 | .0119 | .0116 | .0112 | .0104 | .0095 | .0086 | .0077 | .0070 |
| .020 | .0280 | .0265 | .0250 | .0243 | .0236 | .0231 | .0225 | .0220 | .0213 | .0202 | .0180 | .0159 | .0140 | .0115 | .0090 |
| .030 | .0395 | .0365 | .0350 | .0337 | .0327 | .0317 | .0308 | .0299 | .0289 | .0270 | .0231 | .0198 | .0168 | .0126 | .0085 |
| .040 | .0490 | .0460 | .0435 | .0417 | .0403 | .0389 | .0377 | .0363 | .0351 | .0324 | .0268 | .0220 | .0176 | .0117 | .0050 |
| .050 | .0575 | .0535 | .0506 | .0487 | .0471 | .0454 | .0436 | .0420 | .0402 | .0368 | .0292 | .0226 | .0168 | .0092 | |
| .060 | .0650 | .0605 | .0570 | .0550 | .0531 | .0510 | .0489 | .0470 | .0448 | .0404 | .0305 | .0220 | .0147 | .0053 | |
| .070 | .0710 | .0665 | .0627 | .0605 | .0584 | .0560 | .0537 | .0514 | .0487 | .0432 | .0308 | .0201 | .0114 | .0001 | |
| .080 | .0765 | .0710 | .0677 | .0655 | .0630 | .0603 | .0578 | .0550 | .0521 | .0455 | .0301 | .0172 | .0070 | | |
| .090 | .0820 | .0765 | .0722 | .0696 | .0670 | .0640 | .0613 | .0581 | .0549 | .0471 | .0287 | .0135 | .0018 | | |
| .100 | .0860 | .0810 | .0762 | .0734 | .0705 | .0672 | .0642 | .0606 | .0570 | .0482 | .0264 | .0089 | | | |
| .120 | .0940 | .0880 | .0826 | .0790 | .0758 | .0720 | .0683 | .0640 | .0596 | .0483 | .0195 | | | | |
| .140 | .1000 | .0935 | .0872 | .0829 | .0792 | .0750 | .0 05 | .0654 | .0599 | .0460 | .0101 | | | | |
| .160 | .1045 | .0980 | .0905 | .0855 | .0812 | .0768 | .0710 | .0651 | .0585 | .0418 | | | | | |
| .180 | .1080 | .1010 | .0927 | .0872 | .0820 | .0766 | .0705 | .0637 | .0559 | .0361 | | | | | |
| .200 | .1105 | .1025 | .0938 | .0877 | .0819 | .0756 | .0688 | .0611 | .0521 | .0292 | | | | | |
| .250 | .1120 | .1035 | .0926 | .0850 | .0773 | .0683 | .0596 | .0495 | .0380 | .0068 | | | | | |
| .300 | .1105 | .1000 | .0850 | .0764 | .0668 | .0559 | .0446 | .0327 | .0174 | | | | | | |
| .350 | .1060 | .0930 | .0750 | .0650 | .0540 | .0410 | .0280 | .0125 | | | | | | | |
| .400 | .0970 | .0830 | .0620 | .0500 | .0365 | .0220 | .0060 | | | | | | | | |
| .450 | .0845 | .0700 | .0450 | .0310 | .0170 | .000 | | | | | | | | | |
| .500 | .0700 | .0520 | .0250 | .0100 | | | | | | | | | | | |
| .550 | .0520 | .0320 | .0020 | | | | | | | | | | | | |
| .600 | .0320 | .0080 | | | | | | | | | | | | | |
| .650 | .0090 | | | | | | | | | | | | | | |
| $Y/H_s$ | $X/H_s$ for portion of profile below weir crest | | | | | | | | | | | | | | |
| 0.000 | 0.668 | 0.615 | 0.554 | 0.520 | 0.487 | 0.450 | 0.413 | 0.376 | 0.334 | 0.262 | 0.158 | 0.116 | 0.093 | 0.070 | 0.048 |
| −.020 | .705 | .652 | .592 | .560 | .526 | .488 | .452 | .414 | .369 | .293 | .185 | .145 | .120 | .096 | .074 |
| −.040 | .742 | .688 | .627 | .596 | .563 | .524 | .487 | .448 | .400 | .320 | .212 | .165 | .140 | .115 | .088 |
| −.060 | .777 | .720 | .660 | .630 | .596 | .557 | .519 | .478 | .428 | .342 | .232 | .182 | .155 | .129 | .100 |
| −.080 | .808 | .752 | .692 | .662 | .628 | .589 | .549 | .506 | .454 | .363 | .250 | .197 | .169 | .140 | .110 |
| −.100 | .838 | .784 | .722 | .692 | .657 | .618 | .577 | .532 | .478 | .381 | .266 | .210 | .180 | .150 | .118 |
| −.150 | .913 | .857 | .793 | .762 | .725 | .686 | .641 | .589 | .531 | .423 | .299 | .238 | .204 | .170 | .132 |
| −.200 | .978 | .925 | .860 | .826 | .790 | .745 | .698 | .640 | .575 | .459 | .326 | .260 | .224 | .184 | .144 |
| −.250 | 1.040 | .985 | .919 | .883 | .847 | .801 | .750 | .683 | .613 | .490 | .348 | .280 | .239 | .196 | .153 |
| −.300 | 1.100 | 1.043 | .976 | .941 | .900 | .852 | .797 | .722 | .648 | .518 | .368 | .296 | .251 | .206 | .160 |
| −.400 | 1.207 | 1.150 | 1.079 | 1.041 | 1.000 | .944 | .880 | .791 | .706 | .562 | .400 | .322 | .271 | .220 | .168 |
| −.500 | 1.308 | 1.246 | 1.172 | 1.131 | 1.087 | 1.027 | .951 | .849 | .753 | .598 | .427 | .342 | .287 | .232 | .173 |
| −.600 | 1.397 | 1.335 | 1.260 | 1.215 | 1.167 | 1.102 | 1.012 | .898 | .793 | .627 | .449 | .359 | .300 | .240 | .179 |
| −.800 | 1.563 | 1.500 | 1.422 | 1.369 | 1.312 | 1.231 | 1.112 | .974 | .854 | .673 | .482 | .384 | .320 | .253 | .184 |
| −1.000 | 1.713 | 1.646 | 1.564 | 1.508 | 1.440 | 1.337 | 1.189 | 1.030 | .899 | .710 | .508 | .402 | .332 | .260 | .188 |
| −1.200 | 1.846 | 1.780 | 1.691 | 1.635 | 1.553 | 1.422 | 1.248 | 1.074 | .933 | .739 | .528 | .417 | .340 | .266 | |
| −1.400 | 1.970 | 1.903 | 1.808 | 1.748 | 1.653 | 1.492 | 1.293 | 1.108 | .963 | .760 | .542 | .423 | .344 | | |
| −1.600 | 2.085 | 2.020 | 1.918 | 1.855 | 1.742 | 1.548 | 1.330 | 1.133 | .988 | .780 | .553 | .430 | | | |
| −1.800 | 2.196 | 2.130 | 2.024 | 1.957 | 1.821 | 1.591 | 1.358 | 1.158 | 1.008 | .797 | .563 | .433 | | | |
| −2.000 | 2.302 | 2.234 | 2.126 | 2.053 | 1.891 | 1.630 | 1.381 | 1.180 | 1.025 | .810 | .572 | | | | |
| −2.500 | 2.557 | 2.475 | 2.354 | 2.266 | 2.027 | 1.701 | 1.430 | 1.221 | 1.059 | .838 | .588 | | | | |
| −3.000 | 2.778 | 2.700 | 2.559 | 2.428 | 2.119 | 1.748 | 1.468 | 1.252 | 1.086 | .853 | | | | | |
| −3.500 | ..... | 2.916 | 2.749 | 2.541 | 2.171 | 1.777 | 1.489 | 1.267 | 1.102 | | | | | | |
| −4.000 | ..... | 3.114 | 2.914 | 2.620 | 2.201 | 1.796 | 1.500 | 1.280 | | | | | | | |
| −4.500 | ..... | 3.306 | 3.053 | 2.682 | 2.220 | 1.806 | 1.509 | | | | | | | | |
| −5.000 | ..... | 3.488 | 3.178 | 2.734 | 2.227 | 1.811 | | | | | | | | | |
| −5.500 | ..... | 3.653 | 3.294 | 2.779 | 2.229 | | | | | | | | | | |
| −6.000 | ..... | 3.820 | 3.405 | 2.812 | 2.232 | | | | | | | | | | |
| $H_s/R_s$ | 0.00 | 0.10 | 0.20 | 0.25 | 0.30 | 0.35 | 0.40 | 0.45 | 0.50 | 0.60 | 0.80 | 1.00 | 1.20 | 1.50 | 2.00 |

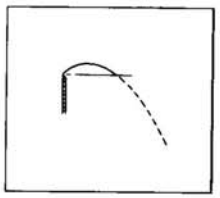

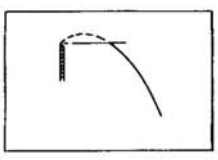

*The tabulation for $H_s/R_s$ = 0.10 was obtained by interpolation between $H_s/R_s$ = 0 and 0.20.

Table 9-6.—Coordinates of lower nappe surface for different values of $H_s/R_s$ when $P/R_s = 0.30$.

| $H_s/R_s$ | 0.20 | 0.25 | 0.30 | 0.35 | 0.40 | 0.45 | 0.50 | 0.60 | 0.80 |
|---|---|---|---|---|---|---|---|---|---|
| $X/H_s$ | $Y/H_s$ for portion of profile above weir crest | | | | | | | | |
| 0.000 | 0.0000 | 0.0000 | 0.0000 | 0.0000 | 0.0000 | 0.0000 | 0.0000 | 0.0000 | 0.0000 |
| .010 | .0130 | .0130 | .0130 | .0125 | .0120 | .0120 | .0115 | .0110 | .0100 |
| .020 | .0245 | .0242 | .0240 | .0235 | .0225 | .0210 | .0195 | .0180 | .0170 |
| .030 | .0340 | .0335 | .0330 | .0320 | .0300 | .0290 | .0270 | .0240 | .0210 |
| .040 | .0415 | .0411 | .0390 | .0380 | .0365 | .0350 | .0320 | .0285 | .0240 |
| .050 | .0495 | .0470 | .0455 | .0440 | .0420 | .0395 | .0370 | .0325 | .0245 |
| .060 | .0560 | .0530 | .0505 | .0490 | .0460 | .0440 | .0405 | .0350 | .0250 |
| .070 | .0610 | .0575 | .0550 | .0530 | .0500 | .0470 | .0440 | .0370 | .0245 |
| .080 | .0660 | .0620 | .0590 | .0565 | .0530 | .0500 | .0460 | .0385 | .0235 |
| .090 | .0705 | .0660 | .0625 | .0595 | .0550 | .0520 | .0480 | .0390 | .0215 |
| .100 | .0740 | .0690 | .0660 | .0620 | .0575 | .0540 | .0500 | .0395 | .0190 |
| .120 | .0800 | .0750 | .0705 | .0650 | .0600 | .0560 | .0510 | .0380 | .0120 |
| .140 | .0840 | .0790 | .0735 | .0670 | .0615 | .0560 | .0515 | .0355 | .0020 |
| .160 | .0870 | .0810 | .0750 | .0675 | .0610 | .0550 | .0500 | .0310 | |
| .180 | .0885 | .0820 | .0755 | .0675 | .0600 | .0535 | .0475 | .0250 | |
| .200 | .0885 | .0820 | .0745 | .0660 | .0575 | .0505 | .0435 | .0180 | |
| .250 | .0855 | .0765 | .0685 | .0590 | .0480 | .0390 | .0270 | | |
| .300 | .0780 | .0670 | .0580 | .0460 | .0340 | .0220 | .0050 | | |
| .350 | .0660 | .0540 | .0425 | .0295 | .0150 | | | | |
| .400 | .0495 | .0370 | .0240 | .0100 | | | | | |
| .450 | .0300 | .0170 | .0025 | | | | | | |
| .500 | .0090 | −.0060 | | | | | | | |
| .550 | | | | | | | | | |
| $Y/H_s$ | $X/H_s$ for portion of profile below weir crest | | | | | | | | |
| −0.000 | 0.519 | 0.488 | 0.455 | 0.422 | 0.384 | 0.349 | 0.310 | 0.238 | 0.144 |
| −.020 | .560 | .528 | .495 | .462 | .423 | .387 | .345 | .272 | .174 |
| −.040 | .598 | .566 | .532 | .498 | .458 | .420 | .376 | .300 | .198 |
| −.060 | .632 | .601 | .567 | .532 | .491 | .451 | .406 | .324 | .220 |
| −.080 | .664 | .634 | .600 | .564 | .522 | .480 | .432 | .348 | .238 |
| −.100 | .693 | .664 | .631 | .594 | .552 | .508 | .456 | .368 | .254 |
| −.150 | .760 | .734 | .701 | .661 | .618 | .569 | .510 | .412 | .290 |
| −.200 | .831 | .799 | .763 | .723 | .677 | .622 | .558 | .451 | .317 |
| −.250 | .893 | .860 | .826 | .781 | .729 | .667 | .599 | .483 | .341 |
| −.300 | .953 | .918 | .880 | .832 | .779 | .708 | .634 | .510 | .362 |
| −.400 | 1.060 | 1.024 | .981 | .932 | .867 | .780 | .692 | .556 | .396 |
| −.500 | 1.156 | 1.119 | 1.072 | 1.020 | .938 | .841 | .745 | .595 | .424 |
| −.600 | 1.242 | 1.203 | 1.153 | 1.098 | 1.000 | .891 | .780 | .627 | .446 |
| −.800 | 1.403 | 1.359 | 1.301 | 1.227 | 1.101 | .970 | .845 | .672 | .478 |
| −1.000 | 1.549 | 1.498 | 1.430 | 1.333 | 1.180 | 1.028 | .892 | .707 | .504 |
| −1.200 | 1.680 | 1.622 | 1.543 | 1.419 | 1.240 | 1.070 | .930 | .733 | .524 |
| −1.400 | 1.800 | 1.739 | 1.647 | 1.489 | 1.287 | 1.106 | .959 | .757 | .540 |
| −1.600 | 1.912 | 1.849 | 1.740 | 1.546 | 1.323 | 1.131 | .983 | .778 | .551 |
| −1.800 | 2.018 | 1.951 | 1.821 | 1.590 | 1.353 | 1.155 | 1.005 | .797 | .560 |
| −2.000 | 2.120 | 2.049 | 1.892 | 1.627 | 1.380 | 1.175 | 1.022 | .810 | .569 |
| −2.500 | 2.351 | 2.261 | 2.027 | 1.697 | 1.428 | 1.218 | 1.059 | .837 | |
| −3.000 | 2.557 | 2.423 | 2.113 | 1.747 | 1.464 | 1.247 | 1.081 | .852 | |
| −3.500 | 2.748 | 2.536 | 2.167 | 1.778 | 1.489 | 1.263 | 1.099 | | |
| −4.000 | 2.911 | 2.617 | 2.200 | 1.796 | 1.499 | 1.274 | | | |
| −4.500 | 3.052 | 2.677 | 2.217 | 1.805 | 1.507 | | | | |
| −5.000 | 3.173 | 2.731 | 2.223 | 1.810 | | | | | |
| −5.500 | 3.290 | 2.773 | 2.228 | | | | | | |
| −6.000 | 3.400 | 2.808 | | | | | | | |
| $H_s/R_s$ | 0.20 | 0.25 | 0.30 | 0.35 | 0.40 | 0.45 | 0.50 | 0.60 | 0.80 |

Table 9-7.—Coordinates of lower nappe surface for different values of $H_s/R_s$ when $P/R_s = 0.15$.

| $H_s/R_s$ | 0.20 | 0.25 | 0.30 | 0.35 | 0.40 | 0.45 | 0.50 | 0.60 | 0.80 |
|---|---|---|---|---|---|---|---|---|---|
| $X/H_s$ | $Y/H_s$ for portion of profile above weir crest | | | | | | | | |
| 0.000 | 0.0000 | 0.0000 | 0.0000 | 0.0000 | 0.0000 | 0.0000 | 0.0000 | 0.0000 | 0.0000 |
| .010 | .0120 | .0120 | .0115 | .0115 | .0110 | .0110 | .0105 | .0100 | .0090 |
| .020 | .0210 | .0200 | .0195 | .0190 | .0185 | .0180 | .0170 | .0160 | .0140 |
| .030 | .0285 | .0270 | .0265 | .0260 | .0250 | .0235 | .0225 | .0200 | .0165 |
| .040 | .0345 | .0335 | .0325 | .0310 | .0300 | .0285 | .0265 | .0230 | .0170 |
| .050 | .0405 | .0385 | .0375 | .0360 | .0345 | .0320 | .0300 | .0250 | .0170 |
| .060 | .0450 | .0430 | .0420 | .0400 | .0380 | .0355 | .0330 | .0265 | .0165 |
| .070 | .0495 | .0470 | .0455 | .0430 | .0410 | .0380 | .0350 | .0270 | .0150 |
| .080 | .0525 | .0500 | .0485 | .0460 | .0435 | .0400 | .0365 | .0270 | .0130 |
| .090 | .0560 | .0530 | .0510 | .0480 | .0455 | .0420 | .0370 | .0265 | .0100 |
| .100 | .0590 | .0560 | .0535 | .0500 | .0465 | .0425 | .0375 | .0255 | .0065 |
| .120 | .0630 | .0600 | .0570 | .0520 | .0480 | .0435 | .0365 | .0220 | |
| .140 | .0660 | .0620 | .0585 | .0525 | .0475 | .0425 | .0345 | .0175 | |
| .160 | .0670 | .0635 | .0590 | .0520 | .0460 | .0400 | .0305 | .0110 | |
| .180 | .0675 | .0635 | .0580 | .0500 | .0435 | .0365 | .0260 | .0040 | |
| .200 | .0670 | .0625 | .0560 | .0465 | .0395 | .0320 | .0200 | | |
| .250 | .0615 | .0560 | .0470 | .0360 | .0265 | .0160 | .0015 | | |
| .300 | .0520 | .0440 | .0330 | .0210 | .0100 | | | | |
| .350 | .0380 | .0285 | .0165 | .0030 | | | | | |
| .400 | .0210 | .0090 | | | | | | | |
| .450 | .0015 | | | | | | | | |
| .500 | | | | | | | | | |
| .550 | | | | | | | | | |
| $Y/H_s$ | $X/H_s$ for portion of profile below weir crest | | | | | | | | |
| −0.000 | 0.454 | 0.422 | 0.392 | 0.358 | 0.325 | 0.288 | 0.253 | 0.189 | 0.116 |
| −.020 | .499 | .467 | .437 | .404 | .369 | .330 | .292 | .228 | .149 |
| −.040 | .540 | .509 | .478 | .444 | .407 | .368 | .328 | .259 | .174 |
| −.060 | .579 | .547 | .516 | .482 | .443 | .402 | .358 | .286 | .195 |
| −.080 | .615 | .583 | .550 | .516 | .476 | .434 | .386 | .310 | .213 |
| −.100 | .650 | .616 | .584 | .547 | .506 | .462 | .412 | .331 | .228 |
| −.150 | .726 | .691 | .660 | .620 | .577 | .526 | .468 | .376 | .263 |
| −.200 | .795 | .760 | .729 | .685 | .639 | .580 | .516 | .413 | .293 |
| −.250 | .862 | .827 | .790 | .743 | .692 | .627 | .557 | .445 | .319 |
| −.300 | .922 | .883 | .843 | .797 | .741 | .671 | .594 | .474 | .342 |
| −.400 | 1.029 | .988 | .947 | .893 | .828 | .749 | .656 | .523 | .381 |
| −.500 | 1.128 | 1.086 | 1.040 | .980 | .902 | .816 | .710 | .567 | .413 |
| −.600 | 1.220 | 1.177 | 1.129 | 1.061 | .967 | .869 | .753 | .601 | .439 |
| −.800 | 1.380 | 1.337 | 1.285 | 1.202 | 1.080 | .953 | .827 | .655 | .473 |
| −1.000 | 1.525 | 1.481 | 1.420 | 1.317 | 1.164 | 1.014 | .878 | .696 | .498 |
| −1.200 | 1.659 | 1.610 | 1.537 | 1.411 | 1.228 | 1.059 | .917 | .725 | .517 |
| −1.400 | 1.780 | 1.731 | 1.639 | 1.480 | 1.276 | 1.096 | .949 | .750 | .531 |
| −1.600 | 1.897 | 1.843 | 1.729 | 1.533 | 1.316 | 1.123 | .973 | .770 | .544 |
| −1.800 | 2.003 | 1.947 | 1.809 | 1.580 | 1.347 | 1.147 | .997 | .787 | .553 |
| −2.000 | 2.104 | 2.042 | 1.879 | 1.619 | 1.372 | 1.167 | 1.013 | .801 | .560 |
| −2.500 | 2.340 | 2.251 | 2.017 | 1.690 | 1.423 | 1.210 | 1.049 | .827 | |
| −3.000 | 2.550 | 2.414 | 2.105 | 1.738 | 1.457 | 1.240 | 1.073 | .840 | |
| −3.500 | 2.740 | 2.530 | 2.153 | 1.768 | 1.475 | 1.252 | 1.088 | | |
| −4.000 | 2.904 | 2.609 | 2.180 | 1.780 | 1.487 | 1.263 | | | |
| −4.500 | 3.048 | 2.671 | 2.198 | 1.790 | 1.491 | | | | |
| −5.000 | 3.169 | 2.727 | 2.207 | 1.793 | | | | | |
| −5.500 | 3.286 | 2.769 | 2.210 | | | | | | |
| −6.000 | 3.396 | 2.800 | | | | | | | |
| $H_s/R_s$ | 0.20 | 0.25 | 0.30 | 0.35 | 0.40 | 0.45 | 0.50 | 0.60 | 0.80 |

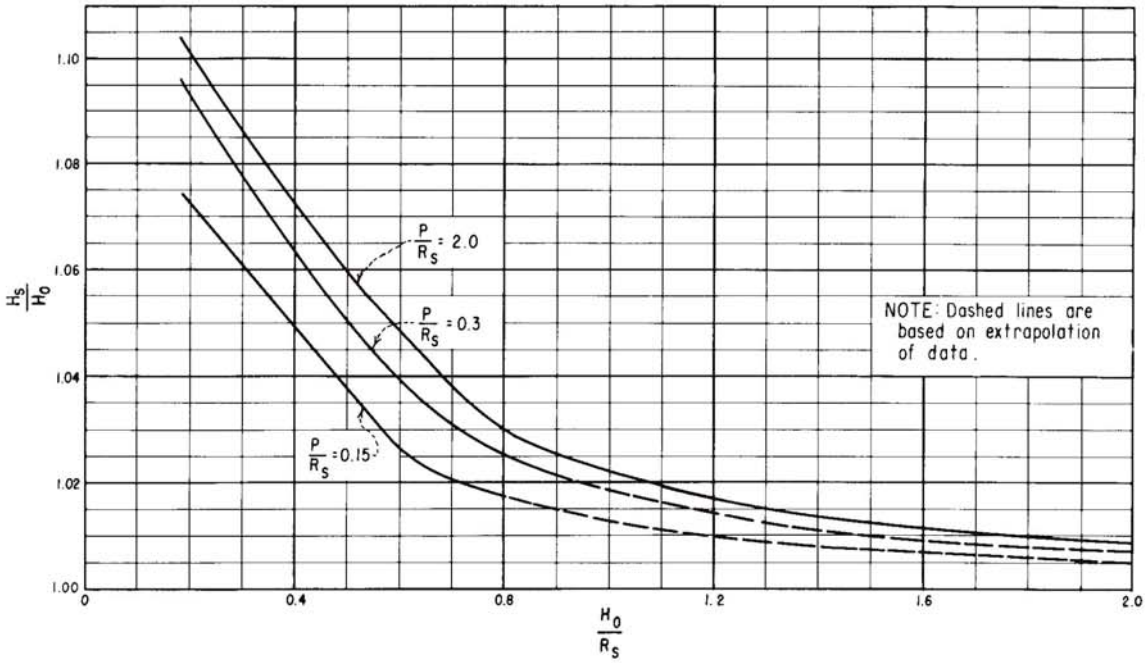


**Figure 9-59.—Relationship of $H_s/H_o$ to $H_o/R_s$ for circular sharp-crested weirs. 288–D–2443.**

its use for determining the shape of the shaft will result in the minimum size that will accommodate the flow without restrictions and without developing pressures along the side of the shaft.

A typical shaft profile obtained by equation (29) is shown by the lines designated *abc* on figure 9-63. If the shaft profile, *abc*, is enlarged above selected points *b*, as shown by the dashed lines *db*, the flow at section A-A will be under pressure; below section A-A the free jet profile should follow lines *bc*.

Aeration is required at the control either through the introduction of air into a sudden enlargement of the shaft or the installation of a deflector to ensure free flow below the control section A-A. Elbows and passageway sizes and slopes must be such that free flow is maintained below the point of control. Failure to provide adquate aeration at the point of control could introduce cavitation and make-and-break siphonic action that could cause severe vibration. For a profile (e.g., *abe*) established for a specific head, the control must remain at section A-A for any higher head so that above the section pressure flow will prevail. The flow below section A-A must be kept free flow. If the profile *dbe* is adopted, once a head is reached to make the shaft flow full at point *b*, section A-A will be the point of control, and pressure flow above the control will prevail for that and all greater heads.

For submerged crest flow, the corresponding nappe shape, as determined from section 9.26(c), for design head $H_o$ will be such that along its lower levels it will closely follow the profile determined from equation (29) if $H_e$ approximates $H_o$. It must be remembered that on the basis of the losses assumed in equation (29), profile *abc* will be the minimum shaft size that will accommodate the required flow and that no part of the crest shape should be permitted to project inside this profile. As noted in section 9.14, small subatmospheric crest pressures can be tolerated if proper precautions are taken to obtain a smooth surface and if the negative pressure forces are recognized in the structural design. The choice of the minimum crest and transition shapes rather than wider shapes, then becomes a matter of economics, structural arrangement, and layout adaptability.

Where the transition profile corresponds to the continuation of the crest shape as determined by tables 9-5, 9-6, and 9-7, the discharge can be computed from equation (28) using a coefficient from figure 9-57. Where the transition profile differs

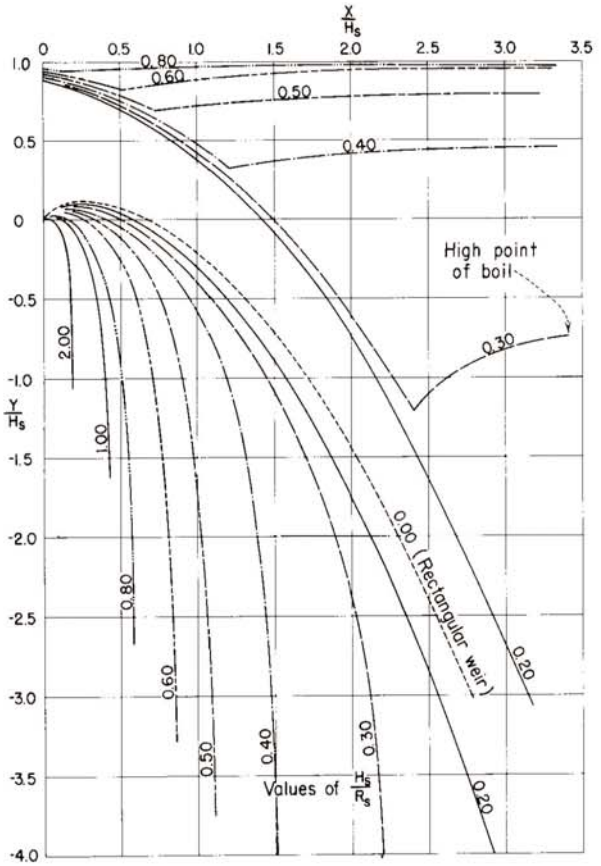


**Figure 9-60.—Upper and lower nappe profiles for circular weir (aerated nappe and negligible approach velocity). 288–D–2444.**

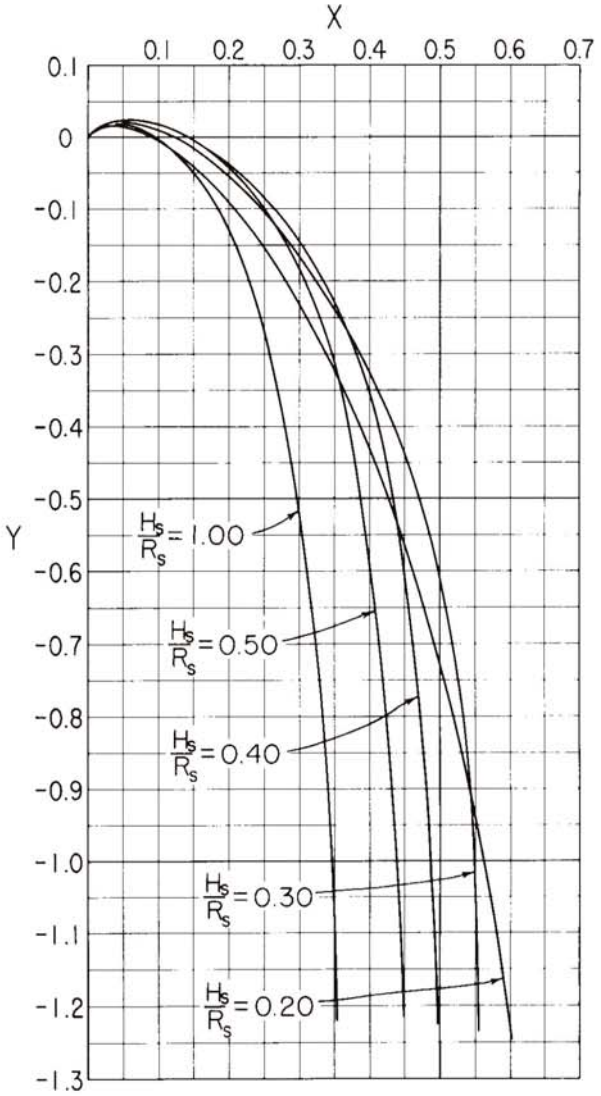


**Figure 9-61.—Comparison of lower nappe shapes for circular weir for different heads. 288–D–2445.**

from the crest shape profile so that a constricted control section is established, the discharge must be determined from equation (29). On figure 9-55, the discharge-head relationship curve *ag* can then be computed from the coefficients determined from figure 9-58, while the discharge-head relationship curve *gh* will be based on equation (29).

(e) *Conduit Design.*—If, for a designated discharge, the conduit of a drop inlet spillway were to flow full below the transition without being under pressure, the required size of the shaft and outlet leg would vary according to the available net head along its length. So long as the slope of the hydraulic gradient that is dictated by the hydraulic losses is flatter than the slope of the conduit, the flow will accelerate and the required size of conduit will decrease. When the conduit slope is flatter than the slope of the hydraulic gradient, the flow will decelerate and the required size of conduit will increase. All points along the conduit will act simultaneously to control the rate of flow. For heads greater than that used to size it, the conduit will flow under pressure with the control at the downstream end; for heads less than that used to size it, the conduit will flow partly full for its entire length, and the control will remain in the transition upstream. On figure 9-55, the head at which the conduit just flows full is represented by point *h*. At heads above point *h*, the conduit flows full under pressure; at heads less than *h* the conduit flows partly full with controlling conditions dictated by the transition design.

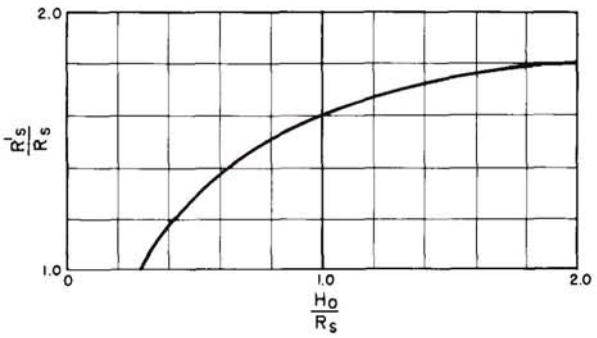


**Figure 9-62.—Increased circular crest radius needed to minimize subatmospheric pressure along crest. 288-D-2446.**

Because it is impractical to build a conduit with a varying diameter, it's size is ordinarily constant beyond the inlet transition. Thus, the conduit from the control point in the transition to the downstream end will have an excess of area. If atmospheric pressure can be maintained along the portion of the conduit flowing partly full, it will continue to flow at that stage even though the downstream end fills. Progressively greater discharges will not alter the partly full flow in the upper lengths of the conduit, but full-flow conditions under pressure will occupy increasing lengths of the downstream end of the conduit. At the discharge represented by point *h* on figure 9-55, the full flow condition has moved back to the transition control section and the conduit will flow full for its entire length.

If the conduit flows at such a stage that the downstream end flows full, both the inlet and outlet will be sealed. To forestall siphon action by the withdrawal of air from the conduit would require an adequate venting system. Unless venting is effected over the entire length of conduit, it may prove inadequate to prevent subatmospheric pressures along some portion of the length because of the possibility of sealing at any point by surging, wave action, or eddy turbulences. Thus, if no venting is provided or if the venting is inadequate, a make-and-break siphon action will attend the flow in the range of discharges approaching full-flow conditions. This action is accompanied by erratic discharges, by thumping and vibration, and by surges at the entrance and outlet of the spillway.

To avoid siphonic flow conditions, the size of the downstream conduit for ordinary designs (especially for those handling higher heads) should be chosen so that it will never flow full beyond the inlet transition. To allow for air bulking, surging, etc., the conduit size should ordinarily be selected so that it will not flow more than 75 percent full (in area) at the downstream end at maximum discharge. Under this limitation, air will be able to pass up the conduit from the downstream portal and thus prevent the formation of subatmospheric pressure along the conduit length. Care must be taken, however, in selecting the vertical and horizontal curvatures of the conduit profile and alignment to prevent sealing along some portion by surging or wave action.

(f) *Design Example.*—The following example problem illustrates the procedure for designing a morning glory drop inlet spillway: Design an ungated drop inlet spillway that will operate under a maximum surcharge head of 10 feet, but will limit the outflow to 2,000 ft³/s. Determine alternative overflow crest shapes and discharge head relationships, considering that (1) the overflow crest radius must be minimized because the intake is formed as a tower away from the abutment, and subatmospheric pressures along the crest can be tolerated; and (2) the crest radius may be any size because it is located on a knoll at the abutment, and subatmospheric pressures along the crest should be minimized. In both cases the conduit must not flow more than 75 percent full at the downstream end. The controlling dimensions are shown on figure 9-64.

(1) *Case 1.*—The radius of the overflow crest must be minimized, and subatmospheric pressures may be tolerated:

Assume $P/R_s \geq 2$ (see fig. 9-57). $R_s$ is determined by a trial-and-error procedure of assuming values of $R_s$ and computing the discharge.

Assume $R_s = 7.0$ feet; then $H_o/R_s = 10/7 = 1.43$. For $H_o/R_s = 1.43$ and $P/R_s \geq 2$, from figure 9-57, $C_o = 1.44$. Then; $Q = C_o(2\pi R_s)H_o^{3/2} = 1.44(2\pi)(7.0)10^{3/2} = 2{,}010$ ft³/s, which is approximately the required discharge. From figure 9-59, for $H_o/R_s = 1.43$ and $P/R_s \geq 2$, $H_s/H_o = 1.014$, $H_s = 1.014\ H_o$, and $H_s = 1.014(10) = 10.14$ feet. Then, $H_s/R_s = 10.14/7.0 = 1.45$.

Using table 9-5, points on the profile of the crest shape that conforms to the lower nappe surface for $H_s/R_s = 1.45$ are computed by interpolation. These points are then plotted as shown on figure 9-65.

The next step is to determine the transition shape required to pass 2,000 ft³/s with an $H_o$ of 10 feet above the crest (water surface elevation 110.0).

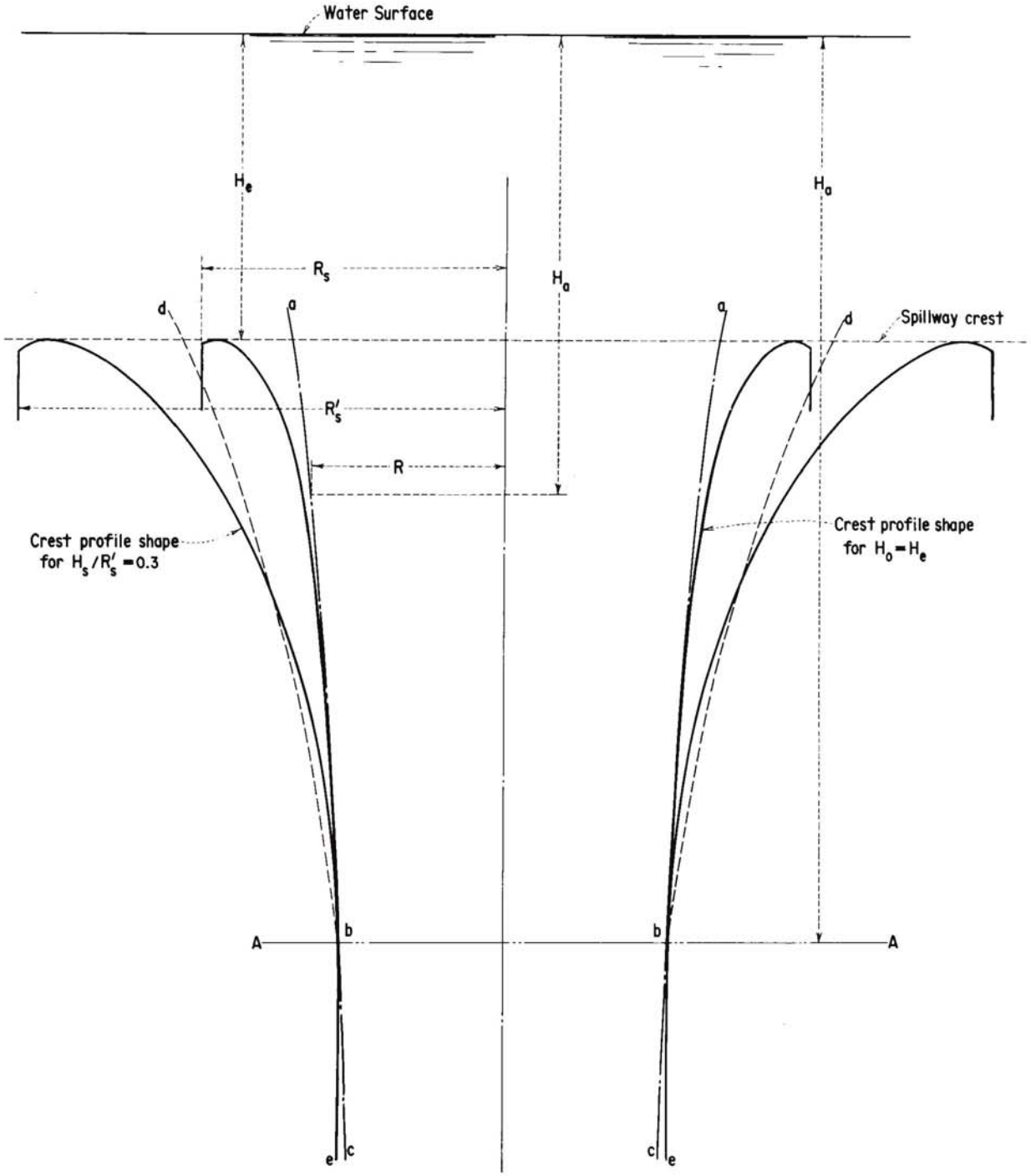


Figure 9-63.—Comparison of drop inlet profiles for various flow conditions. 288–D–2447.

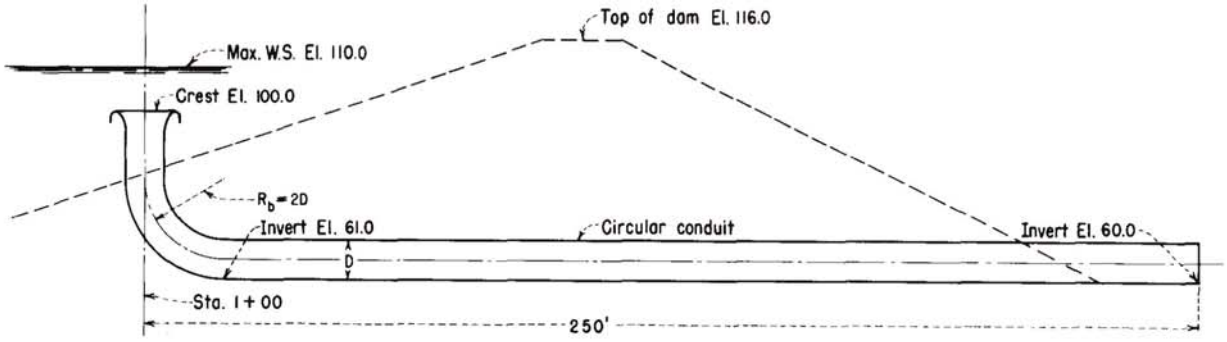


**Figure 9-64.—Drop inlet spillway profile. For design example in section 9.26(f). 228–D–2448.**

This shape is determined by the use of equation (29):

$$R = 0.204 \frac{Q_a^{1/2}}{H_a^{1/4}} = 0.204 \frac{(2{,}000)^{1/2}}{H_a^{1/4}} = \frac{9.12}{H_a}$$

Points on the transition are computed as shown in the following table and are plotted on the same graph on which points for the crest shape have already been plotted (fig. 9-65).

| *Elevation of section* | $H_a$ | $H_a^{1/4}$ | $R=\frac{9.12}{H_a^{1/4}}$ |
|---|---|---|---|
| 100 | 10 | 1.78 | 5.13 |
| 98 | 12 | 1.86 | 4.90 |
| 96 | 14 | 1.93 | 4.72 |
| 94 | 16 | 2.00 | 4.56 |
| 92 | 18 | 2.06 | 4.43 |
| 88 | 22 | 2.17 | 4.20 |

A smooth curve should be drawn through the controlling points on the crest and transition shapes to determine the final shape of the crest and transition.

The final step is to determine the minimum uniform conduit diameter that will pass the flow from the transition section to the conduit portal without the conduit flowing more than 75 percent full. The procedure is as follows: (1) Select a trial conduit and throat diameter and find the corresponding throat location, (2) compute the length from transition throat to outlet portal, (3) approximate the friction losses in the conduit by assuming the conduit flows three-fourths full for its entire length, and (4) check the elevation of the invert at the outlet portal required to pass the design discharge through the selected size conduit. After an approximate conduit size has been determined in this manner, it should be checked by computing the water surface profile through the conduit by open channel flow computations.

For this problem assume a conduit diameter of 9.0 feet. From figure 9-65, a radius of 4.5 feet is found to be at 6.9 feet below the crest; therefore, the elevation of the 9.0-foot-diameter throat is 93.1. The tunnel length may be scaled or calculated by approximate methods. In this example the approximate tunnel length is 270 feet.

Assuming that the conduit flows 75 percent full, area = $0.75\pi(4.5^2)$ = 47.7 ft², velocity = 2,000/47.7 = 41.9 ft/s, and $h_v = 41.9^2/64.4$ = 27.3 feet.

From table B-3, for 75 percent full flow, $d/D$ = 0.702, and the hydraulic radius $r$ = 0.2964(9.0) = 2.67.

Using a value of $n$ = 0.014 to maximize the losses, by Manning's equation (equation (30), app. B):

$$s = \left(\frac{vn}{1.486r^{2/3}}\right)^2 = \left[\frac{(41.9)\ (.014)}{(1.486)\ (2.67)^{2/3}}\right]^2 = 0.04$$

and $h_f$ = 0.04(270) = 10.8 feet.

The invert elevation at the downstream portal of the conduit will then be equal to (1) the elevation of the throat, plus (2) the velocity head at the throat, minus (3) the velocity head in the conduit flowing 75 percent full, minus (4) the friction losses in the conduit, minus (5) the depth of flow at the downstream portal. The required portal invert elevation for this trial conduit diameter is approximately 93.1 + (1/1.1)(110.0 − 93.1) − 27.3 − 10.8 − 0.702(9.0) = 64.1.

Although this elevation is somewhat higher than the established portal invert elevation, 60.0, actual losses through the conduit will be larger than those

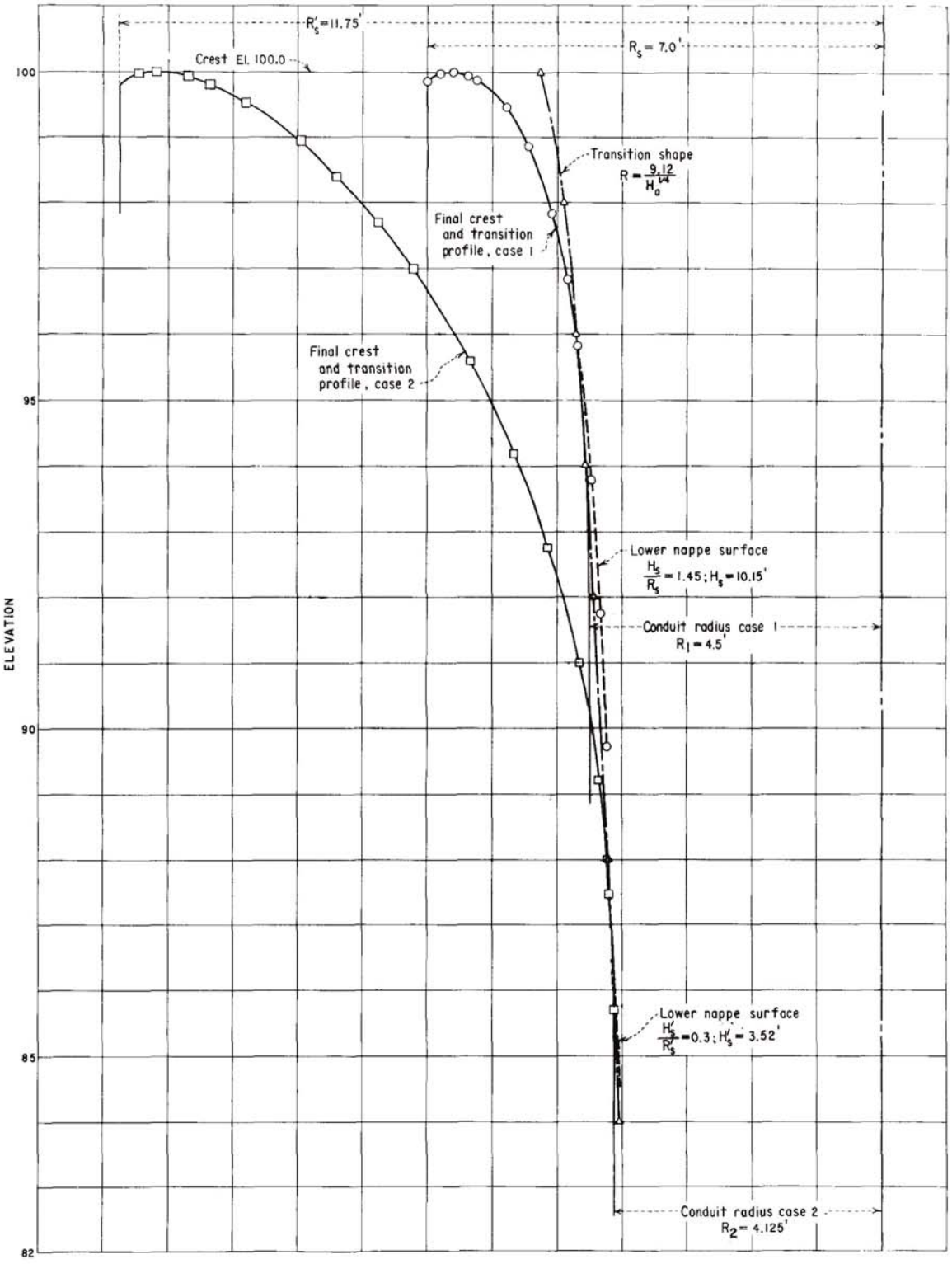


**Figure 9-65.—Drop inlet crest, transition, and conduit plottings. For design example in section 9.26(f). 288–D–2515.**

estimated because the conduit will flow 75 percent full throughout its length.

Therefore, the 9.0-foot-diameter conduit appears to be, for all practical purposes, the minimum uniform diameter conduit that will meet the requirements of the problem. Computations of the water surface profile through the 9.0-foot-diameter conduit, shown in table 9-8, are then performed to verify the approximate solution given above. These computations are based on Bernoulli's theorem (eq. (32), app. B).

Discharge-head computations for this design are shown in table 9-9. For the lower range of heads, the coefficient relationships of various $H_e/R_s$ values are obtained from figure 9-58, assuming a coefficient of 3.75 for $H_e/R_s = 0.3$. For the higher ranges of head, the discharges can be obtained from equation (29) using a throat radius of 4.50 at elevation 93.1. Smooth curves are then plotted for both head range computations. The intersection of the curves is replaced by an approximate transition curve to more nearly represent actual conditions. The discharge curve is plotted on figure 9-66. The computations show that the conduit will be only 76 percent full at the downstream end; therefore, the design is satisfactory.

(2) *Case 2.*—The radius of the overflow crest may be any size, and subatmospheric pressures along crest must be minimized:

First, determine the minimum crest radius for the given: $H_o = 10$ feet, and $Q = 2{,}000$ ft$^3$/s for case 1. Assume $P/R_s = 0.15$ and, as in case 1, determine $R_s$ by trial and error.

Assuming $R_s = 7.0$ feet, $H_o/R_s = 10/7 = 1.43$. For $H_o/R_s = 1.43$ and $P/R_s = 0.15$ from figure 9-57, $C_o = 1.55$. Then, $Q = C_o(2\pi R_s)H_o^{3/2} = 1.55(2\pi)7.0(10)^{3/2} = 2{,}155$ ft$^3$/s. Since a 2,000-ft$^3$/s discharge is required, the assumed value of $R_s$ is too large.

Assuming $R_s = 6.7$ feet, $H_o/R_s = 10/6.7 = 1.49$. From figure 9-57, $C_o = 1.49$ and $Q = 1{,}985$ ft$^3$/s, which is approximately the required discharge.

Using $H_o/R_s = 1.49$, enter figure 9-62 and find the approximate increased crest radius required to minimize subatmospheric pressures. For $H_o/R_s = 1.49$, $R_s'/R_s = 1.74$ and $R_s' = 1.74(6.7) = 11.7$ feet; use 11.75 feet. Points on the profile of the crest shape that conform to the lower nappe surface for $H_s'/R_s' = 0.30$ and $R_s' = 11.75$ are computed using values from table 9-7 and are plotted as shown on figure 9-65.

Computations for the required transition shape to pass 2,000 ft$^3$/s with a head of 10 feet on the crest are identical to those given in case 1. Figure 9-65 shows the plotted points and the crest and transition curves.

From an inspection of the transition and crest shape plots for case 2, it can be seen that the conduit diameter for case 1 is too large for case 2. If the 9.0-foot-diameter conduit used in case 1 were used in case 2, a smooth transition connecting the crest and conduit would be considerably outside the transition shape determined by equation (29). This means that for a head of 10 feet on the crest, the discharge would not longer be limited to 2,000 ft$^3$/s by the transition, but would increase because of the larger size transition. This discharge would require a larger uniform diameter conduit to pass the discharge and not flow more than 75 percent full. A still larger uniform diameter conduit with a still larger maximum discharge would finally be required for a satisfactory hydraulic design. However, a smaller uniform diameter conduit would flow more

Table 9-8.—Water surface profile computations for case 1. Conduit diameter = 9.0 feet; $Q = 2000$ ft$^3$/s, $n = 0.014$.

| Station | $\Delta L$ | Trial $d/D$ | $d$ | $a$ | $v$ | $h_v$ | $r$ | $r^{2/3}$ | $s$ | $\frac{s_1+s_2}{2}$ | $\Delta h_L$ | $\Sigma\Delta h_L$ | $d_2+h_{v_2}+\Sigma\Delta h_L$ | Invert elevation | Datum gradient | Remarks |
|---|---|---|---|---|---|---|---|---|---|---|---|---|---|---|---|---|
| 1+00 | – | 1.00 | – | 63.6 | 31.4 | 15.3 | 2.25 | 1.72 | 0.030 | – | – | – | – | 93.1 | 108.4 | – |
| 1+19 | 39 | 0.56 | 5.04 | 36.66 | 54.6 | 46.2 | 2.41 | 1.80 | .081 | 0.056 | 2.2 | 2.2 | 53.4 | 61.0 | 114.4 | Too high |
| | | .59 | 5.37 | 39.06 | 51.2 | 40.7 | 2.48 | 1.83 | .069 | .049 | 1.9 | 1.9 | 47.9 | – | 108.9 | OK |
| 2+30 | 111 | .63 | 5.67 | 42.2 | 47.4 | 34.8 | 2.54 | 1.86 | .057 | .063 | 7.0 | 8.9 | 49.4 | 60.5 | 109.9 | Too high |
| | | .64 | 5.76 | 42.99 | 46.5 | 33.6 | 2.58 | 1.88 | .054 | .062 | 6.8 | 8.7 | 48.0 | – | 108.5 | OK |
| 3+50 | 120 | .72 | 6.48 | 49.04 | 40.8 | 25.8 | 2.69 | 1.93 | .039 | .047 | 5.6 | 14.3 | 45.7 | 60.0 | 105.7 | Too low |
| | | .70 | 6.30 | 47.56 | 42.0 | 27.5 | 2.67 | 1.92 | .042 | .048 | 5.8 | 14.5 | 48.3 | – | 108.3 | OK |

Table 9-9.—Computations for discharge curve for case 1, $R_s$=7.0 feet.

| Head on crest, feet | Crest control | | | Throat control | |
|---|---|---|---|---|---|
| | $\frac{H_e}{R_s}$ | [1]$C$ | $Q = C(2\pi R_s)H_e^{3/2}$ | $H_a$ | $Q_a = \left(\frac{R}{0.204}\right)^2 H_a^{1/2}$ |
| 1 | 0.14 | 3.56 | 157 | – | – |
| 2 | .29 | 3.75 | 467 | – | – |
| 3 | .43 | 3.58 | 820 | – | – |
| 4 | – | – | – | 10.9 | 1,600 |
| 6 | – | – | – | 12.9 | 1,750 |
| 8 | – | – | – | 14.9 | 1,880 |
| 10 | – | – | – | 16.9 | 2,000 |

[1] Coefficient of 3.75 assumed for $H_e/R_s$=0.3 (from fig. 9.57). Coefficients for $H_e/R_s$ values other than 0.3 based on ratios shown on figure 9-58.

than 75 percent full at the downstream end.

The simplest solution to this problem is to vary the diameter of the conduit. An upstream diameter should be chosen based on the crest profile and transition where they converge. This procedure establishes the throat size necessary to limit the maximum discharge to 2,000 ft³/s. At some suitable location downstream from the throat, the conduit should be enlarged to prevent it from flowing more than 75 percent full. The location of this enlargement should be determined by economic or construction considerations to meet hydraulic requirements.

For this problem, an 8.25-foot-diameter conduit with its throat at elevation 86.0 is selected. It will be assumed that the most economical design is obtained by extending this conduit to the point where it flows 75 percent full. At this point the conduit is enlarged to the diameter needed to make it flow 75 percent full at the downstream portal. To determine the point at which the tunnel must be enlarged, water surface profiles are run downstream by the step method, as shown in table 9-10. A bend radius of 16.5 feet (2$D$) is used. The table shows that the conduit must increase in size starting at the P.T. (point of tangency) of the vertical bend, station 1+16.5. The size of the downstream conduit may be approximated by assuming a given size conduit flowing 75 percent full at the downstream portal and using the distance from the point of enlargement to the portal as one reach in the water surface profile computations. Although this method results in losses slightly larger than would be obtained by using shorter reaches, it is accurate enough to determine conduit size if the length of the conduit

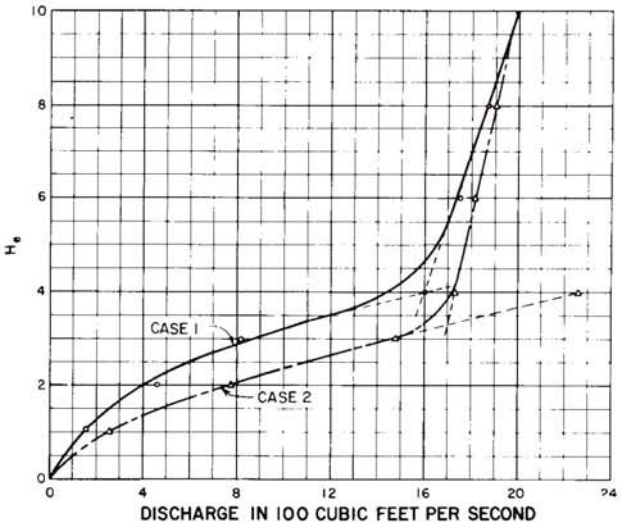


Figure 9-66.—Drop inlet spillway discharge curves. For design example in section 9.26(f). 288–D–2516.

downstream from the expansion is not excessively long. Use of shorter steps and an assumed minimum value of $n$ would be required to determine the depth and velocity at the downstream portal for use in designing an energy dissipator. The transition from the smaller to the larger diameter conduit should be proportioned as explained in section 9.19(b).

Discharge-head relationships for this case are computed similarly to those for case 1. The throat radius in this instance is 4.13 feet at elevation 86.0. Computations are shown in table 9-11, and the discharge curve is plotted on figure 9-66.

**9.27. *Culvert Spillways.*—**(a) *General.*—As described in section 9.8(j), a culvert spillway ordinarily consists of a simple culvert conduit placed through a dam or along an abutment, generally on a uniform grade, with its entrance placed vertically or inclined. The culvert cross section can be round if it is constructed of fabricated or precast pipe, or it may be square, rectangular, or of some other shape if cast in place. The culvert can freely discharge, or it can empty into an open channel so that the outflowing jet is supported along the channel floor.

The factors that combine to determine the nature of flow in a culvert spillway include such variables as the slope, size, shape, length, and roughness of the conduit barrel, and the inlet and outlet geometry. The combined effect of these factors determines the location of the control which,

Table 9-10.—Water surface profile computations for case 2. Varying diameter conduit, $Q$ = 2,000 ft$^3$/s, $n$ = 0.014.

| Station | $\Delta L$ | Trial $d/D$ | $d$ | $a$ | $v$ | $h_v$ | $r$ | $r^{2/3}$ | $s$ | $\frac{s_1+s_2}{2}$ | $\Delta h_L$ | $\Sigma\Delta h_L$ | $d_2+h_{v_2}+\Sigma\Delta h_L$ | Invert elevation | Datum gradient | Remarks |
|---|---|---|---|---|---|---|---|---|---|---|---|---|---|---|---|---|
| 1+00 | – | 1.000 | – | 53.5 | 37.4 | 21.7 | 2.06 | 1.62 | 0.047 | – | – | – | – | 86.0 | 107.7 | – |
| 1+16.5 | 30 | 0.650 | 5.36 | 36.9 | 54.4 | 45.9 | 2.38 | 1.78 | .082 | 0.065 | 1.9 | 1.9 | 53.2 | 61.0 | 114.2 | Too high |
| | | .690 | 5.69 | 39.3 | 50.8 | 40.1 | 2.43 | 1.81 | .070 | .058 | 1.8 | 1.8 | 47.6 | – | 107.6 | OK |
| *Try 9.0-foot-diameter conduit flowing 75 percent full at the portal* | | | | | | | | | | | | | | | | |
| 3+50 | 234 | .690 | 6.21 | 46.8 | 42.7 | 28.3 | 2.65 | 1.92 | .044 | .057 | 13.3 | 15.1 | 49.6 | 60.0 | 109.6 | Too high |
| *Try 9.25-foot-diameter conduit flowing 75 percent full at the portal* | | | | | | | | | | | | | | | | |
| 3+50 | 234 | .690 | 6.82 | 49.5 | 40.4 | 25.4 | 2.73 | 1.95 | .038 | .054 | 12.6 | 14.4 | 46.6 | 60.0 | 106.6 | OK |

Table 9-11.—Computations for discharge curve for case 2, $R_s'$ = 11.75 feet.

| Head on crest, feet | Crest control | | | Throat control | |
|---|---|---|---|---|---|
| | $\frac{H_e}{R_s'}$ | [1]$C$ | $Q = C(2\pi R_s')H_e^{3/2}$ | $H_a$ | $Q_a = \left(\frac{R}{0.204}\right)^2 H_a^{1/2}$ |
| 1 | 0.09 | 3.55 | 260 | – | – |
| 2 | .17 | 3.74 | 780 | – | – |
| 3 | .26 | 3.85 | 1,480 | 17 | 1,680 |
| 4 | .34 | 3.82 | 2,260 | 18 | 1,730 |
| 6 | – | – | – | 20 | 1,830 |
| 8 | – | – | – | 22 | 1,920 |
| 10 | – | – | – | 24 | 2,000 |

[1]Coefficient of 3.86 assumed for $H_e/R_s$ = 0.3 (from fig. 9-57). Coefficients for $H_e/R_s$ values other than 0.3 based on ratios shown on figure 9-58.

in turn, determines the discharge characteristics of the conduit. The location of the control dictates whether the conduit flows partly full or full, and thereby, establishes the head-discharge relationship.

The grade of the conduit might be mild or steep; that is, its slope may be flatter or steeper than one which for a given discharge will just support flow at the critical stage. For both the mild and steep slope conduit, the control may be either at the inlet or at the outlet, depending on the entrance geometry and head relationship and on the flow conditions at the outlet. The various conditions that may govern a particular flow are shown on figure 9-67.

If the inlet is not submerged, the control for a conduit on a mild slope flowing partly full will be at the outlet. If the outlet discharges freely, the flow at that point will pass through critical depth. This condition is shown as condition 1 on figure 9-67. If the tailwater is high enough to maintain a depth greater than critical, the tailwater level will control the flow in the upstream barrel. If the tailwater submerges the outlet, the conduit might flow full for its entire length and thus submerge the inlet. This flow condition is depicted as condition 6 on figure 9-67. Until the conduit flows full, the flow ordinarily will be at subcritical stage, and the discharge relationships will be determined according to Bernoulli's equation. Computations will start at the outlet where the reservoir level submerges the inlet and where $H/D$>1.2. The control at critical depth may be placed at the inlet if the culvert is relatively short so that a jump does not form within the barrel. This condition is shown as condition 4 on figure 9-67.

When the conduit is on a steep slope and the entrance is not submerged, the flow will be controlled by critical depth at the inlet, as indicated by condition 3 on figure 9-67. The water surface will drop rapidly to critical depth at the entrance, and open channel flow at supercritical velocities will exist throughout the conduit barrel. Discharge for a given reservoir level will be governed by channel or weir flow, assuming critical depth occurs at the culvert entrance.

After the inlet has been submerged or where $H$ exceeds about 1.2$D$, it is still possible to have open channel flow at supercritical stage in the conduit barrel, as depicted for condition 5, if the control remains at the entrance. In this case, flow at the inlet is analogous to orifice or sluice flow. This flow condition is contingent on the formation of a contraction at the top of the entrance so that an airspace is maintained along the top of the barrel to

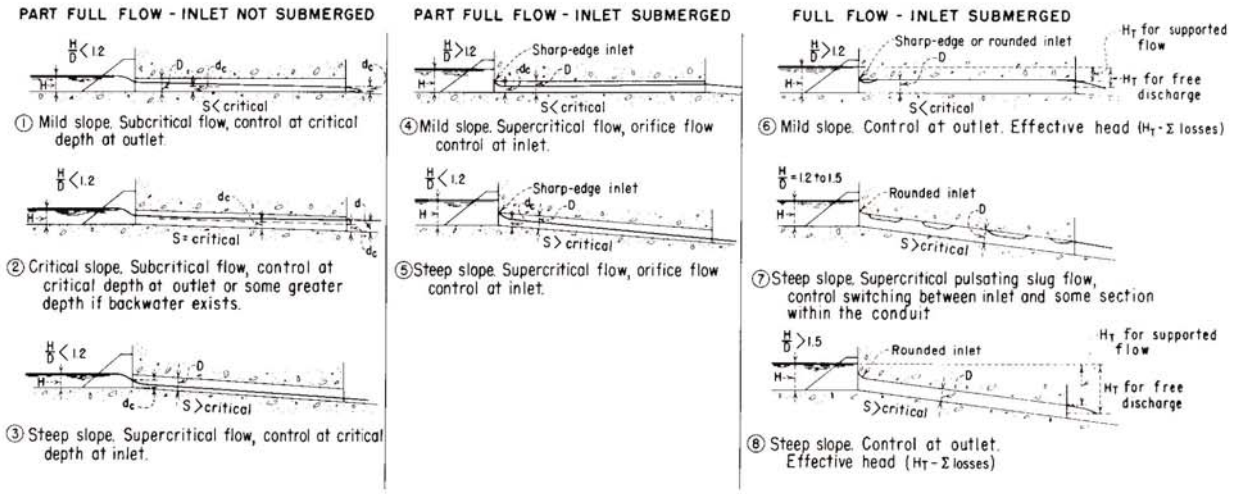


**Figure 9-67.—Typical flow conditions for culvert spillways on mild and steep slopes. 288–D–2517.**

permit partly full flow throughout the conduit length.

As the head at the entrance and the resulting discharge increase, channel friction or local disturbances may force the barrel to flow full near the outlet, sealing the conduit at the downstream end. The high-velocity flow in the culvert will carry away some of the air trapped at the top of the barrel, reducing the pressure in the conduit to less than atmospheric. Furthermore, if the entrance is shaped to eliminate the inlet contraction, the barrel will start to flow full near the inlet, after which the full-flow zone will extend rapidly down the conduit toward the outlet. The effect of the full-flow condition will be a draft-tube action (similar to siphonic action) that will increase the discharge. The increased discharge will cause a deeper drawdown just upstream from the inlet. A vortex will form, and the air that will be introduced into the culvert will break the draft-tube action. The reduction in discharge will result in the return to orifice control at the inlet. Immediately, the full-flow action will begin again, and the cycle will be repeated. This alternate priming and breaking action will cause a pulsating flow stage having the slug flow phenomenon indicated by condition 7 on figure 9-67. When the reservoir stage condition is such that $H/D>1.5$, the entrance drawdown may be insufficient to interface with the full-flow action, and a steady state of full pipe flow indicated by condition 8 will prevail.

If it is intended that the spillway conduit not flow full, the geometry of the inlet becomes an important consideration. The inlet must be shaped to obtain a maximum discharge efficiency and yet maintain a top contraction that will provide a freely aerated surface in the conduit barrel for all reservoir stages. The sharp-edged square inlet produces the desired contraction without materially reducing the discharge capacity. The inlet contraction can also be formed (but at reduced hydraulic capacity) by a projecting inlet, by a mitered inlet with a downstream sloping face, by an inlet orifice ring that is smaller than the remainder of the conduit, or by a curtain wall closing off the top of the conduit entrance.

If the conduit is permitted to flow full at the higher reservoir stages, the control will be at the outlet and the geometry of the inlet will have much less significance. For this case the inlet must be shaped to minimize the jet contraction to avoid separation of the incoming flow from the conduit barrel because full pipe flow is desired for all conditions except when the inlet is not submerged. The more streamlined shape will reduce entrance losses for the full pipe flow condition. The suppression of the contraction is achieved by rounding the inlet or by providing a gradually tapering transition to the conduit barrel.

Culvert inlets may have various approach conditions, cross-sectional shapes, and entrance arrangements. For example, an entrance may be

rounded, beveled, square or bellmouthed; it may be installed either flush with or protruding through a vertical or sloping headwall. The approach to the inlet may or may not be a well-defined channel. Wing walls or warped transition approaches may be used. In cross section, a culvert entrance may be round, square, rectangular, or arch-shaped. All such variations have a significant effect on the culvert performance because they affect orifice discharge, inlet contractions, and the entrance losses for full pipe flow.

A common arrangement for a circular pipe culvert installation involves a vertical headwall with the pipe end placed flush with the wall. Similarly, box culvert arrangements usually involve a trapezoidal approach channel with vertical or warped approach walls leading to the culvert entrance. The hydraulic designs of these two types of installation are discussed in detail below.

(b) *Circular Conduit with Vertical Headwall.*— Figure 9-68 shows a plot of head-discharge relationships for a circular conduit placed flush with a vertical headwall, for both square-edged and rounded inlets. This plot is based on an average of numerous experimental tests [25, 26, 27] of pipe culvert entrances with the conduit placed on steep slopes. The head-discharge relationships for the square-edged inlet are based on the control remaining at the inlet for all reservoir heads. Where $H/D<1.2$ (approx.), the flow characteristics are those of critical depth flow in a circular pipe, modified only by the effects of the jet contraction. For

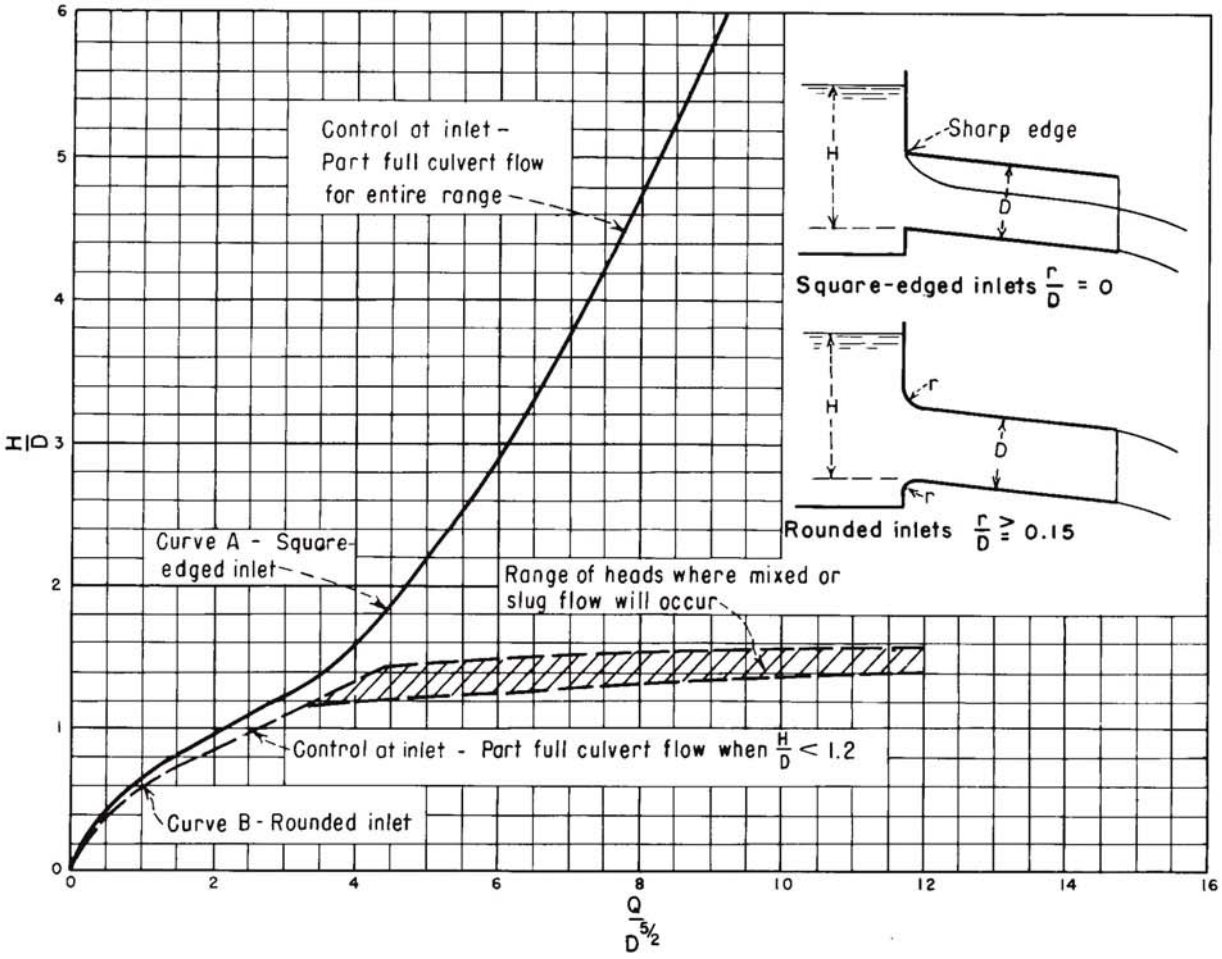


Figure 9-68.—Head-discharge curves for square-edged and rounded inlets for circular culverts on steep slopes. 288–D–2518.

$H/D>1.2$, the flow characteristics are those of orifice or sluice flow. Because the conduit is considered to be flowing partly full at supercritical stage for all $H/D$ ranges indicated, the downstream conditions have no influence on the discharge.

On figure 9-68, the head-discharge relationship for the rounded inlet for values of $H/D<1.2$ (approx.) lie to the right of those for the square-edged inlet. This indicates slightly greater discharges for equal size conduits. The increased discharge capacity through the critical-depth flow range is the result of improved streamlined flow brought about by the suppression of the inlet contractions. For $H/D>1.2$, the pulsating flow characteristics begin, and the discharge-head relationship in this range of flow is uncertain; it cannot be determined until the flow stabilizes at full flow stage. Because full pipe flow is governed by control at the outlet, the head-discharge relationship can be determined by the application of Bernoulli's theorem. Referring to figure 9-69:

$$H_T = H + L\sin\theta - \frac{D}{2} \qquad (30)$$

Similarly,

$$H_T = h_v + h_e + h_f$$

or

$$H_T = \left(1 + K_e + \frac{29.1n^2L}{r^{4/3}}\right)\frac{v^2}{2g} \qquad (31)$$

where:

$K_e$ = entrance loss coefficient, and
$n$ = friction factor in Mannings equation,
$h_f = (29.1\ n^2L/r^{4/3})(v^2/2g)$.

Combining equations (30) and (31), dividing by $D$, and stating the equation in terms of $Q$ instead of $v$ yields:

$$\frac{H}{D} + \frac{L}{D}\sin\theta - \frac{1}{2} =$$

$$0.0252\left(1 + K_e + \frac{29.1n^2L}{r^{4/3}}\right)\left(\frac{Q}{D^{5/2}}\right)^2 \qquad (32)$$

In equation (32), it is assumed that the culvert discharges freely at the outlet and that the pressure line at the outlet is approximately at the center of the pipe. If the outlet discharges into a channel so that the outflowing jet is supported, equation (32) becomes:

$$\frac{H}{D} + \frac{L}{D}\sin\theta - 1.0 =$$

$$0.0252\left(1 + K_e + \frac{29.1n^2L}{r^{4/3}}\right)\left(\frac{Q}{D^{5/2}}\right)^2 \qquad (33)$$

Equations (32) and (33) are for full-flow conditions. They are expressed in terms of $H/D$ and $Q/D^{5/2}$ so that by referring to figures 9-67 and 9-68, it can be determined whether or not the full-flow condition exists.

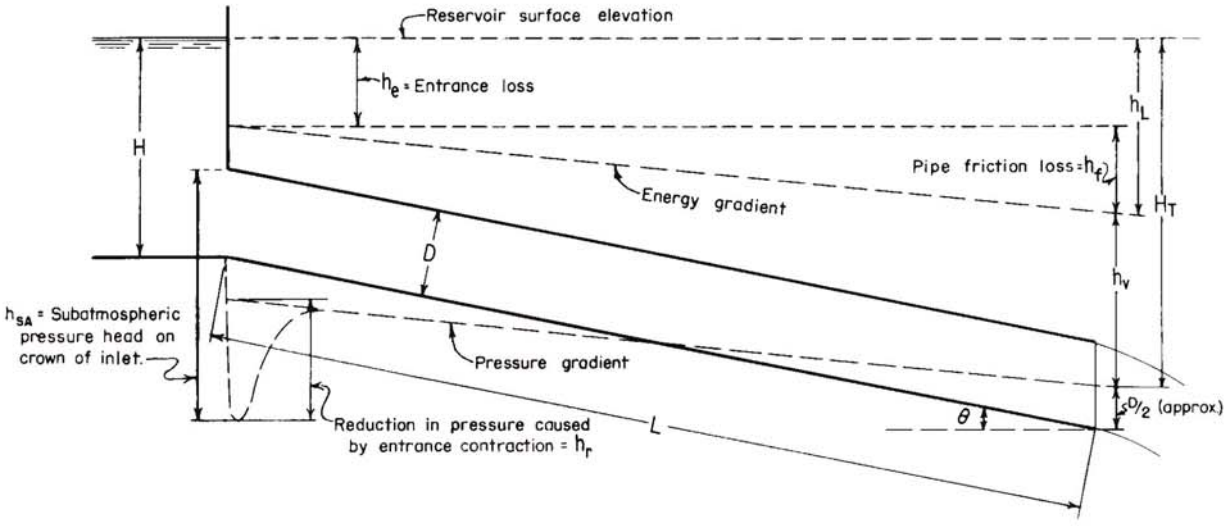


**Figure 9-69.—Hydraulic characteristics of full pipe flow for culvert spillways. 288-D-2519.**

Appropriate values of $n$ are given in section 10.15(b). Values of $K_e$ for various entrance conditions have been determined by different experimenters, as shown in the listing below:

| *Entrance condition* | *$K_e$ range* | *Average* |
|---|---|---|
| For square-edged inlets installed flush with vertical headwalls | 0.43 to 0.70 | 0.50 |
| For rounded inlets installed flush with vertical headwalls, $r/D \geq 0.15$ | 0.08 to 0.27 | .10 |
| For grooved or socket-ended concrete pipe installed flush with vertical headwall | 0.10 to 0.33 | .15 |
| For projecting concrete pipe with grooved or socket ends | — | .20 |
| For projecting steel or corrugated metal pipes | 0.5 to 0.9 | .85 |

Nomographs for determining flow in full-flowing circular pipes with entrance controls have been developed by the Federal Highway Administration. These nomographs, which are included in appendix B, can be used as design aids in determining flow in circular culvert spillways. Figure B-7 is for flow in concrete pipe culverts having entrance control and the following types of entrances: (1) headwall with square-edged entrance, (2) headwall with groove-end pipe, and (3) headwall with groove end of pipe projecting. Figure B-8 is for flow in corrugated metal pipe culverts having entrance control and the following types of entrances: (1) flush headwall, (2) end mitered to conform to slope, and (3) projecting pipe. Figure B-9 is for concrete pipe culverts flowing full, based on $n = 0.012$ and entrance loss coefficients of 0.1, 0.2, and 0.5. Figure B-10 is for corrugated metal pipe flowing full, based on $n = 0.024$ and entrance loss coefficients of 0.5 and 0.9.

(c) *Box Culvert with Vertical or Warping Inlet Walls.*—If the inlet is such that the bottom and side contractions will be suppressed, flow through a box culvert on a steep slope can alternately go through the three distinct phases of flow described previously, depending on submergence conditions and on the factors that dictate flow conditions within the conduit.

For conditions when the inlet is not submerged, critical flow will occur in the region of the inlet, in which case for a rectangular section, $d_c = \sqrt[3]{q^2/g}$ or $H = 1.5\sqrt[3]{q^2/g}$. Relating this equation of critical flow to the discharge $Q$:

$$Q = w\sqrt{g}\left(\frac{H}{1.5}\right)^{3/2} \tag{34}$$

where $w$ is the width at the culvert entrance.

When the conduit entrance is submerged, the flow may be considered analogous to that of a sluice if the entrance has a square edge at the top. For this condition, top contraction of the jet will occur, and flow can be computed according to orifice flow, or $Q = CA\sqrt{2gh}$. The coefficient, $C$, depends on whether the area, $A$, is defined as the area of the opening, the area of the contracted jet, or some similar referenced area. Similarly, $C$ will depend on the definition of the head, $h$: whether it is measured to the top, center, or bottom of the opening. Ordinarily, for a square-edged orifice in a vertical headwall, the area, $a$, is measured at the plane of the headwall face. If the head, $H$, is measured from the water surface to the bottom of the opening, the discharge can be computed by the equation:

$$Q = C_d a\sqrt{2gH}, \text{ or } Q = C_d wD\sqrt{2gH} \tag{35}$$

where $D$ is the height of the opening. Values of $C_d$ as determined from experiments [28] are plotted on figure 9-70.

As with circular culverts, full flow in box culverts depends on suppression of the top contraction. Full culvert flow will be governed by control at the outlet, and discharge-head relationships can be computed according to the equation:

$$Q = a\sqrt{2g(H_T - h_L)} \tag{36}$$

where $a$ is the area of the culvert barrel, and $H_T$ and $h_L$ are the heads indicated on figure 9-69.

Reducing the equation and expressing it in terms of the entrance loss coefficient, $K_e$, and of the friction loss coefficient, Manning's $n$:

$$Q = a\sqrt{2g}\left[\frac{H + L\sin\theta - \frac{D}{2}}{1 + K_e + \frac{29.1n^2L}{r^{4/3}}}\right]^{1/2} \tag{37}$$

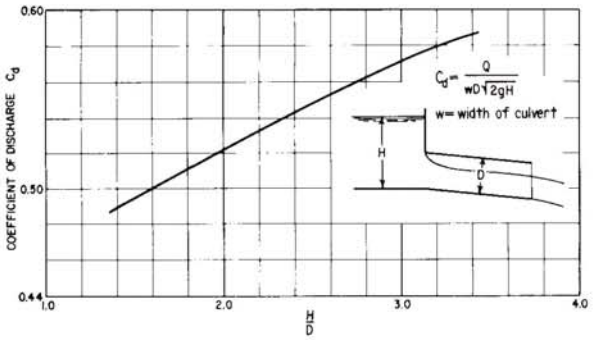


**Figure 9-70.—Discharge coefficient for submerged box culvert spillways with square-edged top opening. From [28]. 288–D–2520.**

where $r$ is the hydraulic radius of the culvert flowing full. Equation (37) is based on free discharge at the outlet. If the outflowing jet is supported, equation (37) will become:

$$Q = a\sqrt{2g}\left[\frac{H + L\sin\theta - D}{1 + K_e + \frac{29.1n^2L}{r^{4/3}}}\right]^{1/2} \qquad (38)$$

Federal Highway Administration nomographs for solution of flow in box culverts are also included in appendix B. Figure B-11 is for box culverts with entrance control for various positions of the wingwalls. The discharges are based on discharge coefficients that approximate those shown on figure 9-70. Figure B-12 is for concrete box culverts flowing full, based on $n = 0.0013$ and entrance loss coefficients of 0.1, 0.2, 0.5, and 0.7.

(d) *Conduit Pressures.*—When the grade of a culvert spillway is greater than the friction slope, for full pipe flow the pressure gradient will lie below the center of the pipe, as indicated on figure 9-69. The difference in head between this hydraulic gradient and any point on the pipe vertically above it will be the subatmospheric pressure at the point. Cavitation will occur whenever the subatmospheric pressure approaches 1 Atm (1 atmosphere), so that the residual absolute pressure is near vapor pressure. To avoid cavitation along the pipe surfaces, the minimum absolute pressure must be greater than the vapor pressure. The pressure reduction in the pipe will be greatest at the crown immediately downstream from the entrance. It can be reduced further by any pressure drop caused by an inlet contraction, such as a sharp-edged or constricted opening.

From figure 9-69 it can be seen that:

$$h_v + h_e + h_r = h_{SA} + (H - D) \qquad (39)$$

where:

$h_r$ = reduction of pressure head caused by contraction, and
$h_{SA}$ = resulting subatmospheric pressure head.

The vapor pressure of water varies with temperature. It is equivalent to about 0.2 foot of head at 32 °F and about 1.4 feet of head at 85 °F. To ensure that cavitation is avoided and to allow for other uncertainties, the residual pressure ordinarily should not be significantly less than 10 feet absolute. Based on probable maximum atmospheric pressures at different elevations above sea level, the limiting subatmospheric pressures indicated in table 9-12 are recommended.

**Table 9-12.—Allowable subatmospheric pressures for conduits flowing full.**

| Elevation above sea level | Allowable subatmospheric pressure, $h_{SA}$, feet of water |
|---|---|
| 0 | 22 |
| 2000 | 20 |
| 4000 | 18 |
| 6000 | 16 |
| 8000 | 14 |

The reduction in pressure head caused by jet contraction will depend on the geometry of the inlet. For streamlined entrances very little reduction will be effected, but for sharp-edged projecting inlets, the reduction can be almost equal to the velocity head. For sharp-edged square inlets the reduction in pressure may approach $0.7h_v$. Written in terms of loss coefficients (sec. 10.14), equation (39) becomes:

$$\frac{v^2}{2g}(K_v + K_e + K_r) = h_{SA} + (H - D) \qquad (40)$$

or

$$\frac{v^2}{2g} = h_v = \frac{h_{SA} + (H - D)}{K_v + K_e + K_r} \qquad (41)$$

where $K_r$ is the pressure reduction coefficient.

For a square-edged entrance where $K_e = 0.5$, $K_r = 0.7$, $K_v = 1.0$, $H = 1.5D$, and $h_{SA}$ (for an installation at 6,000 feet above sea level) = 16 feet, equation (41) can be written:

$$h_v = \frac{16 + 0.5D}{1.0 + 0.5 + 0.7} = \frac{16 + 0.5D}{2.2}$$

For a 4-foot-diameter conduit, $h_v = 8.2$ feet, and the volocity in the conduit would have to be limited to about $v = 23$ ft/s. From equation (31), the total drop from the reservoir water surface to the centerline of the downstream end of a 200-foot-long conduit for $D = 4$ and $n = 0.014$ is:

$$H_T = 8.2\left(1.5 + \frac{29.1n^2L}{r^{4/3}}\right)$$

or

$$H_T = 8.2\left(1.5 + \frac{29.1(0.014)^2200}{1^{4/3}}\right) = 21.7 \text{ feet}$$

(e) *Antivortex Devices.*—Although experiments have shown that for a properly rounded entrance the culvert begins to flow full after $H/D > 1.2$, the full pipe flow condition could not be stabilized until $H/D \geq 1.5$. This condition was caused by the "slug flow action," which resulted from the introduction of air into the conduit by entrance drawdown and by vortices immediately upstream from the inlet. To reduce the range where slug flow action prevails, antivortex devices have been used above conduit entrances. These devices not only stabilize the flow condition at a lower $H/D$, but they also help to start the priming action sooner. The devices have consisted of grillages, rafts, or fixed solid hoods placed so as to break up the vortices or to prevent their formation where they could feed air into the conduit [29]. To be effective, the hood or grillage must be placed immediately above the entrance and must extend at least two diameters in front of and to each side of the inlet.

(f) *Energy Dissipators.*—A culvert spillway may discharge freely, or it may empty into an open channel chute that conveys the flow to a downstream terminal structure. The flow from a freely discharging conduit may empty directly into the natural stream channel, into a trapezoidal plunge basin (described in sec. 9.24), or into an impact basin (sec. 10.17(b)). Where the discharge from the full-flowing culvert empties into an open chute, the hydraulics beyond the portal will be according to open channel flow, as discussed in section 9.19. Stilling devices such as those described in sections 9.18 through 9.24 can be used to dissipate the energy of flow before returning the discharge to the river channel.

(g) *Design Examples.*—To illustrate the procedures for a culvert spillway design, several typical examples are presented.

(1) *Example 1.*—The size of a culvert spillway required to discharge 100 ft$^3$/s at reservoir elevation 110.0 is to be determined. The normal sill level of the spillway entrance is at elevation 100.0. The culvert is to flow partly full for all heads. If a circular conduit is selected, the design procedure is as follows:

The head-discharge-diameter relationship for a circular conduit with entrance placed flush with a vertical headwall can be obtained from figure 9-68. Curve A is used because the conduit is to flow partly full. By assuming various sizes of conduit, a size can be found that meets the requirements, as follows:

Assume a conduit 3.5 feet in diameter, then $D^{5/2} = 23$ and $Q/D^{5/2} = 4.35$. For $Q/D^{5/2} = 4.35$, $H/D = 1.75$ and $H = 6.1$. Because $H = 10$ feet is allowable, the culvert can be made smaller.

As a second trial, assume a 3-foot-diameter conduit. Then $D^{5/2} = 15.6$ and $Q/D^{5/2} = 6.41$. From curve A, $H/D = 3.2$ and $H = 9.6$, which approximates the 10 feet available.

If a box culvert is selected, the design procedure is as follows:

$$Q = C_d wD\sqrt{2gH} \quad \text{(eq. (35))}$$

$$wD = \frac{Q}{C_d\sqrt{2gH}}$$

Assuming a 2.5-foot-high culvert, $H/D = 10/2.5 = 4.0$, and $C_d$ from figure 9-70 is approximately 0.6. Then,

$$2.5w = \frac{100}{0.6\ (8.02)\ \sqrt{10}} = 6.6,$$

and $w = 2.6$ feet.

(2) *Example 2.*—Find the discharge through the conduits in the previous example if the entrances are shaped to provide full conduit flow. The conduit length is 200 feet, and the invert grade at the outlet

is elevation 80.0. The conduit discharges freely at the outlet end. The procedure is as follows:

Equation (32) may be written:

$$\left(\frac{Q}{D^{5/2}}\right)^2 = \frac{1}{0.0252}\left[\frac{\frac{H}{D} + \frac{L}{D}\sin\theta - \frac{1}{2}}{1 + K_e + \frac{29.1n^2L}{r^{4/3}}}\right]$$

For a 3-foot circular conduit with $K_e = 0.10$ and $n = 0.014$:

$$\left(\frac{Q}{15.6}\right)^2 = \frac{1}{0.0252}\left[\frac{\frac{10}{3} + \frac{200}{3}\left(\frac{20}{200}\right) - \frac{1}{2}}{1 + 0.10 + \frac{29.1(0.014)^2 200}{(0.75)^{4/3}}}\right]$$

$= 136$, therefore

$$Q = 182 \text{ ft}^3/\text{s}$$

This flow will provide a velocity of 25.7 ft/s in the conduit.

Equation (40) may be written:

$$h_{SA} = \frac{v^2}{2g}(K_v + K_e + K_r) - (H - D)$$

The subatmospheric pressure in the conduit, based on a pressure reduction coefficient $K_r = 0.1$ and $K_e = 0.1$ for a rounded entrance is equal to:

$$\frac{(25.7)^2}{64.4}(1.0 + 0.1 + 0.1) - (10.0 - 3.0) = 5.3 \text{ feet}$$

This subatmospheric pressure is less than the limit allowed in table 9-12; therefore, the design is satisfactory.

For the box culvert spillway, from equation (37), assuming $K_e = 0.1$ and $n = 0.014$:

$$Q = 2.5(2.6)8.02\left[\frac{10 + 200\left(\frac{20}{200}\right) - 1.25}{1 + 0.1 + \frac{29.1(200)0.014^2}{0.64^{4/3}}}\right]^{1/2}$$

$= 157 \text{ ft}^3/\text{s}$.